NASw-4435

Straight Out of

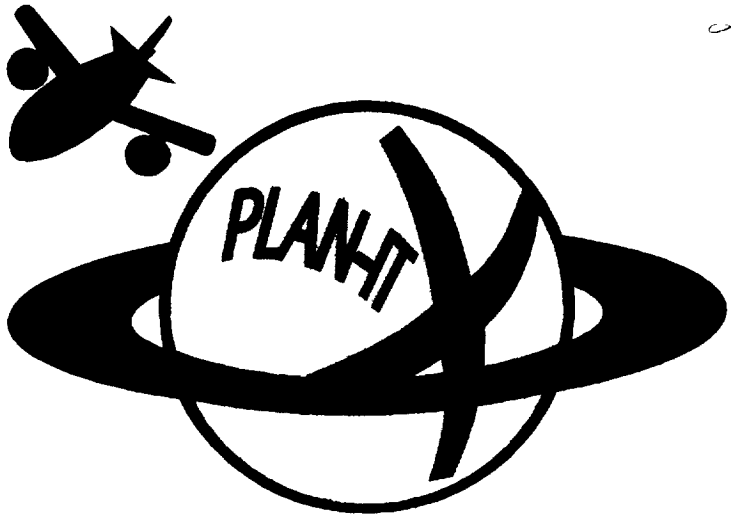

The OFP-6M Transport Jet

We're fat like that

By

Kelly Alexander
Brian Heneghan
Joules Holmes
Bret Hughes
Mark Kettering
Jennifer Wells
Todd Whelan

Presented To

Professor: **Robert van't Riet**
Assistants: **Jae Lee**
Dani Soban
Date: **June 3, 1994**

California Polytechnic State University, San Luis Obispo

FOLDER NAME

Plan-It X

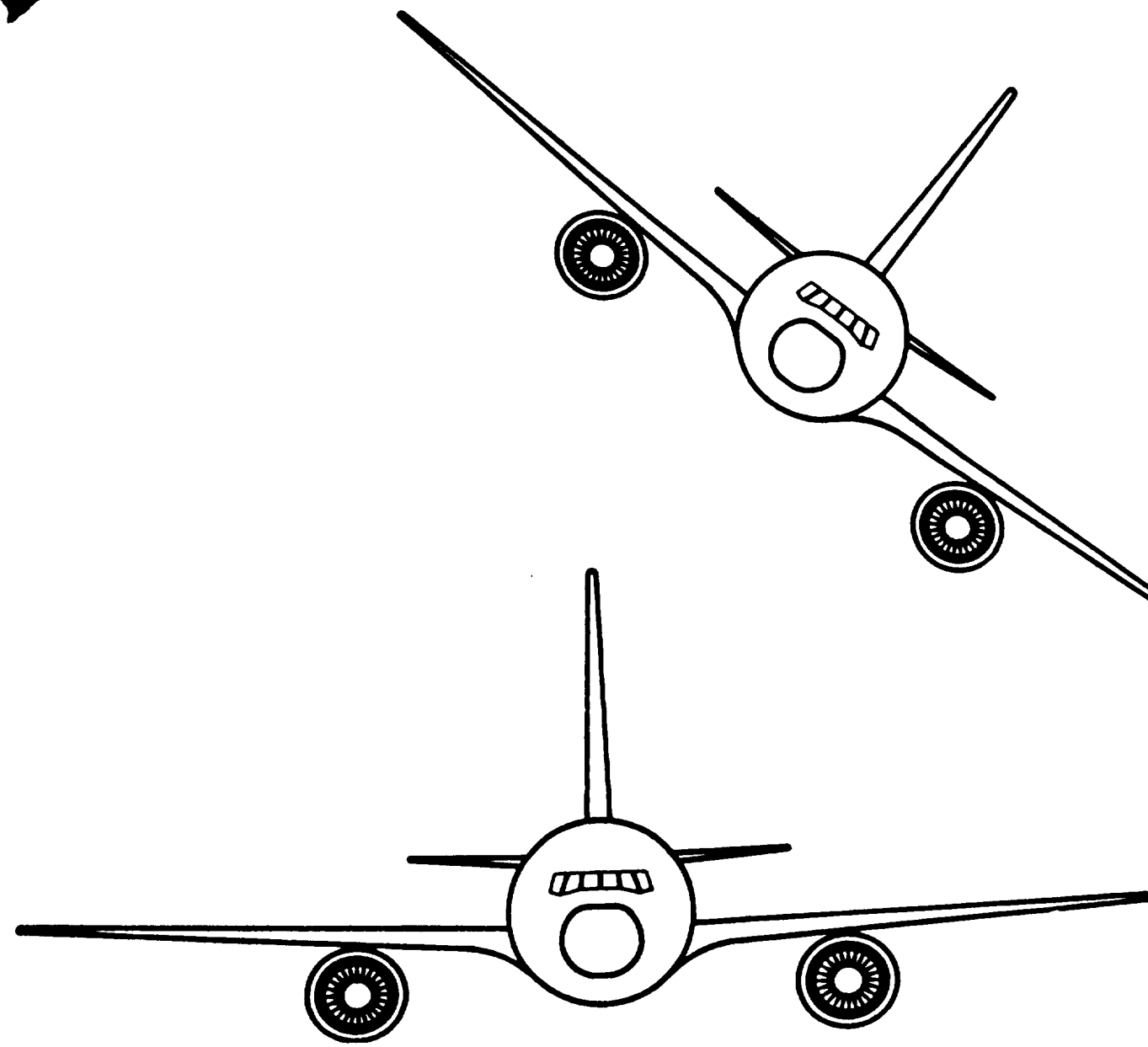

FOLDOUT FRAME 2

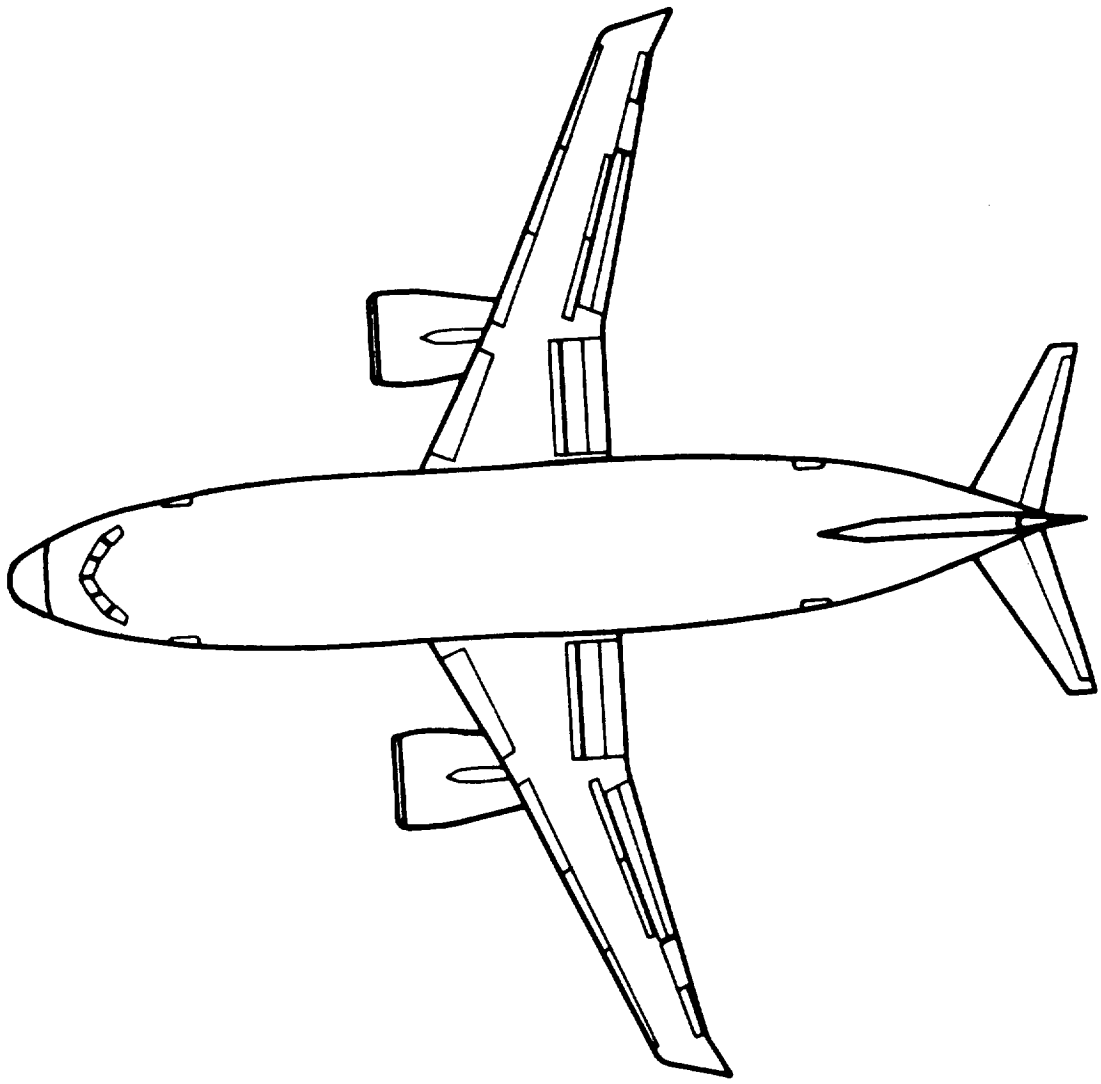

OF

FOLDOUT FRAME 3

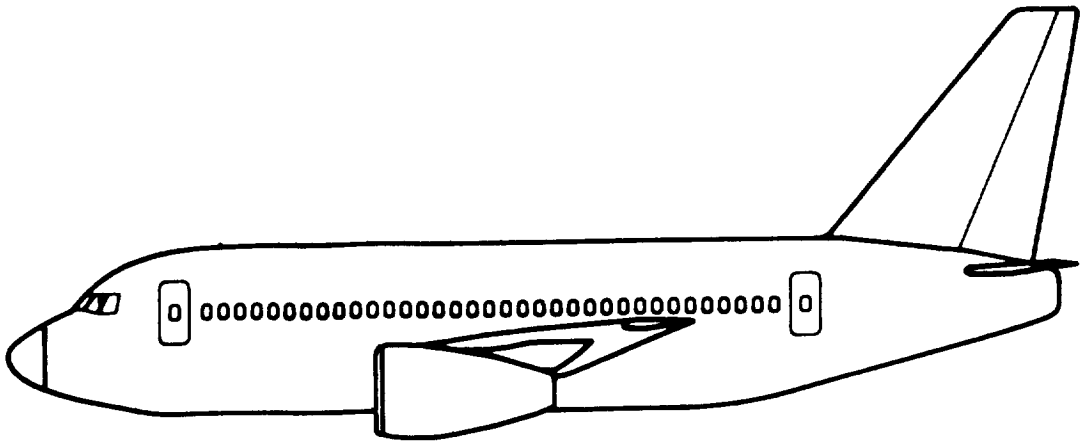

P-6M

Abstract

This report shows the development of a preliminary design of a commercial jet transport that meets the criteria of the Request For Proposal (RFP), presented by the American Institute of Aeronautics and Astronauts (AIAA). The proposal requires an innovative design of a low cost domestic commercial transport that will reduce operating costs for airline companies while still meeting present and future requirements of the Federal Aviation Regulations (FAR) for this type of aircraft. Specifications for the design include a mixed class, 153 passenger aircraft, traveling a range of 3000 nm. The intent of the project is to identify factors that reduce cost and to design within the limits of these constraints. The project includes techniques or options that incorporate new technologies but do not override practicality, alternative design approaches, and a comparison between the new design and current aircraft in its class. The OFP-6M is an alternative design approach to the conventional commercial transport jet and is geared towards customer satisfaction through efficiency and reliability. The goals of the OFP-6M transport are to provide an original but sensible, and practical solution to the RFP, by combining important, essential preliminary design factors with growing technology.

The design focus of the OFP-6M is to reduce costs by simplifying systems where significant weight or maintenance savings can be achieved, and integrate advanced technology to improve performance. Key aspects of the OFP-6M design are the efficient use of materials like composites, and efficient advanced ducted high bypass turbofan engines. The high bypass engines result in a lower fuel consumption which aid in reducing costs and meeting future noise emission restrictions. Composite are used for most structural components, including flooring and wing box. Although composites are an emerging technology and presently, a high maintenance material, they can be cost-effective and an alternative to aluminum structures when correct manufacturing and

design strategies are applied (Ref. 10). Since, composites are lighter in weight and require less manufacturing of complex parts, they can significantly reduce the structural weight.

Because of the large diameter of 17 ft, sophisticated aerodynamic considerations were implemented to significantly lower the drag. Supercritical airfoils were chosen with simple control surface design which allows for less maintenance and manufacturing costs. The interior configuration accommodates either all passenger, dual and single class flights or complete cargo. Also, a relaxed conventional stability is integrated with a Stability Augmentation System (SAS). As a result of these design implementations, the OFP-6M bottom line direct operating cost (DOC), compares favorably with the Boeing 737 and 757, at 3.49 cents per Available Seat Mile (ASM) and costs are expected to reduce when improved manufacturing and maintenance methods are implemented (see Section 13).

Table of Contents

List of Figures

List of Tables

Nomenclature

b	Wing Span
C_D	Total Drag of Aircraft
C_{Dq}	Variation of Drag Coefficient with Pitch Rate
C_{Du}	Variation of Drag Coefficient with Speed
$C_{D\alpha}$	Variation of Drag Coefficient with Angle of Attack
$C_{D\alpha.dot}$	Variation of Drag Coefficient with Rate of Change of Angle of Attack
C_{DB}	Fuselage Drag Coefficient
C_d	Coefficient of Drag for Wing
C_L	Coefficient of Lift for Aircraft
C_{Lq}	Variation of Lift Coefficient with Pitch Rate
C_{Lu}	Variation of Lift Coefficient with Speed
$C_{L\alpha}$	Aircraft Lift Curve Slope
$C_{L\alpha.dot}$	Variation of Lift Coefficient with Rate of Change of Angle of Attack
C_l	Coefficient of Lift for Wing
C_{lp}	Variation of Rolling Moment with Roll Rate
C_{lr}	Variation of Rolling Moment with Yaw Rate
$C_{l\beta}$	Variation of Rolling Moment with Sideslip Angle
$C_{l\beta.dot}$	Variation Rolling Moment with Rate of Change of Sideslip Angle
C_{mq}	Variation of Pitching Moment with Pitch Rate
C_{mu}	Variation of Pitching Moment with Speed
$C_{m\alpha}$	Variation of Pitching Moment with Angle of Attack
$C_{m\alpha.dot}$	Variation of Pitching Moment with Rate of Change of Angle of Attack
C_{np}	Variation of Yawing Moment Coefficient with Roll Rate
C_{nr}	Variation of Yawing Moment Coefficient with Yaw Rate

$C_{n\beta}$	Variation of Yawing Moment Coefficient with Sideslip Angle
$C_{n\beta.dot}$	Variation of Yawing Moment with Rate of Change of Sideslip Angle
C_r	Root Chord
C_t	Tip Chord
C_{yp}	Variation of Side-Force Coefficient with Roll Rate
C_{yr}	Variation of Side-Force Coefficient with Yaw Rate
$C_{y\beta}$	Variation of Side-Force Coefficient with Side-Slip Angle
$C_{y\beta.dot}$	Variation of Side-Force Coefficient with Rate of Change of Sideslip Angle
c	Average Chord
c_d	Coefficient of Drag for Airfoil
c_l	Coefficient of Lift for Airfoil
d_f	Exterior Diameter of Aircraft
e	Oswald's Efficiency Factor
I	Moment of Inertia
l_f	Total Length of Aircraft
M	Mach Number
P	Design Point For Aircraft Operation
S	Surface Area of Aircraft Wings
T	Thrust of Aircraft
W	Weight of Aircraft

Greek

α	Angle of Attack
α.dot	Rate of Change of Angle of Attack
β	Sideslip Angle
β.dot	Rate of Change of Sideslip Angle
ϕ	Bank Angle

Λ	Angle of Sweep
λ	Taper Ratio
ν	Kinematic Viscosity
Θ	Turn Over Angle
ρ	Density

Subscripts

D	Drag for Wing
d	Drag for Airfoil
FL	Field Length
L	At Landing, Landing Distance
L	Lift for Wing
LG	Landing Ground Roll
l	Lift for Airfoil
l	Rolling Moment
m	Pitching Moment
max	Maximum
n	Yawing Moment
TO	At Take-Off
TOFL	Take-Off Field Length

Acronyms and Abbreviations

AC	Aerodynamic Center
ADF	Advanced Ducted Fan
AIAA	American Institute of Aeronautics and Astronautics
ASM	Available Seat Mile
BPR	Bypass Ratio; mass ratio of cold fan flow to engine core flow

CG	Center of Gravity
CMU	Central Maintenance Computer
DFMA	Design for Manufacturing and Assembly
DOC	Direct Operating Cost
DPP	Design Point Program
EICAS	Engine Indication and Crew Alerting System
FAA	Federal Aviation Administration
FADEC	Full-Authority Digital Engine Controls
FAR	Federal Aviation Regulations
FBL	Fly-By-Light
FBW	Fly-By-Wire
FOD	Foreign Object Damage
IPD	Integrated Product Development
KEAS	Knots Equivalent Airspeed
KCAS	Knots Calibrated Airspeed; the airspeed indicated to the pilot
LCN	Load Classification Number
MAC	Mean Aerodynamic Chord
ND	Navigational Display
OEI	One Engine Inoperative
OFP-6M	One Fat Plane Worked on by Six Group Members and Then There is Mark
PFD	Primary Flight Display
RFP	Request For Proposal
SAS	Stability Augmentation System
SFC	Specific Fuel Consumption; fuel flow rate per pound of thrust (lb/lb/hr)
TQM	Total Quality Management

1 Introduction

In recent years, deregulation has been a major source of the heavy competition between airline companies (Ref. 2). Deregulation can effect the economic growth and stability of airlines. As shown in Figure 1.1, under deregulation there are less nonstop flights per day than those with regulation. With less non-stop flights, operating costs continue to rise because of the increasing need for maintenance, more airport accessibility is required, and slower service, resulting in customer dissatisfaction.

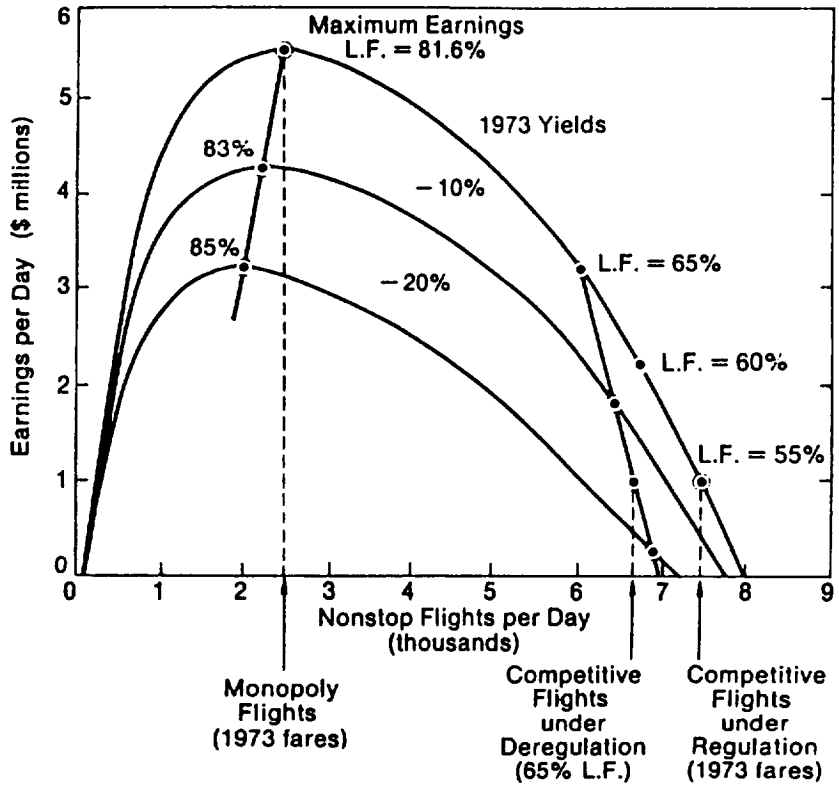

(Source: Ref. 2)

Figure 1.1 Effects of Airline Deregulation for OFP-6M

Because of the continuing deregulation, airlines have been forced to decrease their fares due to the heavy competition. In addition, operational and maintenance costs

continue to escalate. Therefore, airlines have experienced higher expenditures and lower revenues teaming to produce lower profits. However, the outlook for sales of new commercial jet transports is expected to improve steadily throughout the next decade, as airline companies continue to recover financially and begin to replace aging aircraft (Ref. 23). The current transport jets that are in competition within the mid-size class, including the relatively new A320, Boeing 737 and the MD-80, are derivatives of older designs and the industry is ready for new design concepts. Although these designs are successful, maintenance costs for older aircraft are escalating and exceed the amortization costs of new aircraft. This fuels the current demand for more efficient air transportation at the lowest possible cost (Ref. 23).

Another problem that the world's airline industry is facing is the unsuccessful trends of the traditional hub and spoke system (Ref. 46). In the past, by having all flights land at one large hub, airlines could retain the business from the lucrative long distance flights. Hub and spoke routes, however, have resulted in increased competition and staggering losses, especially in the United States (Ref. 46). Direct routes and lower fares are now being considered for more efficient flight time and to compensate for losses. Shorter more direct flying times can result in lower operational costs which will increase profitability for airlines.

The need for more direct flights is the growing trend in airline companies around the world, both domestically and internationally especially the Asian and Eastern block countries (Ref. 27). Although Japan is experiencing a recession, they expect an end in 1995, and purchases of 100-200 seat transports will increase as well as scheduling more international non-stop flights (Ref. 20). The smaller, direct flight transport will help earn more return on investment for domestic and international routes. Also, Germany is scheduled to begin long-range direct service to overseas holiday resorts (Ref. 27). This shows the demand for smaller, more efficient aircraft with longer ranges and emphasizes the need for a new design of a low cost, high efficient commercial transport.

The preliminary design project is intended to propose a possible solution to the problems that the airline companies are facing. The RFP, requires a low cost commercial transport that will carry 153 passengers and travel a range of 3000 nm. The specifications of the proposal impose difficult parameters on the design process and creates a challenging problem. These parameters include an unusually long range compared to similar aircraft of this size, low DOC, and technology advances up to the year 2000. Figure 1.2 shows a comparison of aircraft with similar payloads and their ranges on medium haul.

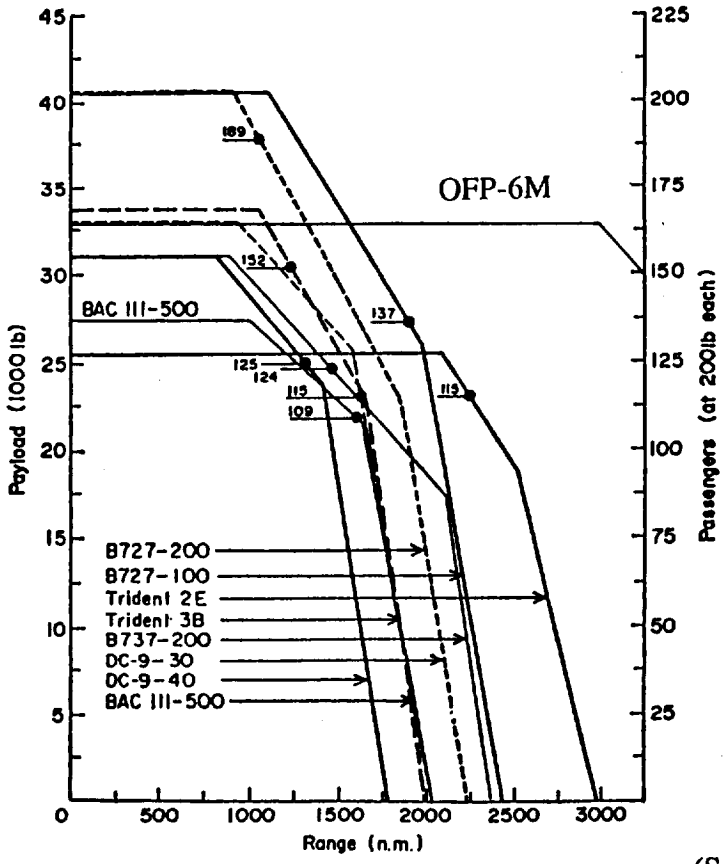

(Source: Ref. 43)

Figure 1.2 OFP-6M Payload Range Comparison on Medium Haul

The OFP-6M compared to the Boeing 727-100, which was one of the first transport jets to provide an increased payload while maintaining a low thrust required,

travels a much longer range with approximately the same payload (see Section 6.8 and Ref. 43). Although the MD-80/90, similar to the DC-9-30 shown in Fig.. 1.2, has a large payload, its range does not match the extended range of the OFP-6M. Since current aircraft are based on these older designs with outdated technology, the RFP's request for a new design with current technology is necessary.

Due to the airlines cutting back on capacity in order to trim costs and minimize losses, the RFP also requests that the project identify all factors that drive operating costs high and develop design concepts to help reduce these costs. An example is American Airlines planning to reduce system capacity and concentrate on cargo and non-aviation business to reduce costs and improve earnings (Ref. 23). The use of new manufacturing and design processes at Boeing are being used to lower production time and cost (Ref. 30). Therefore, it is clear that airlines as well as manufacturers are devising solutions to reduce costs in all possible ways and in the current market, the need for lower DOC is essential and a key factor in gaining a competitive edge.

To meet the proposed specifications and optimize the design, the OFP-6M has integrated newer design concepts that will improve quality and customer satisfaction. Composite construction is used along with sophisticated airfoil concepts. Composites are used to take advantage of the higher strength to weight ratio which result in a lighter structure. This in turn will yield reduced operating costs because of the lower fuel consumption that can be obtained with a lighter aircraft. Supercritical airfoils will be used to generate higher drag-divergence Mach numbers which allow for higher speeds at a lower wing sweep. Because of the low sweep angle, wing structure can be manufactured more easily, which reduces manufacturing time and costs. Also, supercritical airfoils have good performance characteristics at cruise and will accommodate a generous amount of fuel due to their increased thickness. In addition, a double-slotted flap design is used which has fewer parts than a triple-slotted flap and is lighter and simpler to maintain. This design is similar to the Boeing 737-X flap design

and reduces manufacturing time and cost (Ref. 25). A wider body is used for maximum passenger comfort, increased interior volume for a given wetted area, and quick turnarounds due to the twin aisle configuration (see Section 3). By integrating technology and satisfying customer needs, a balance between efficiency and customer comfort can be obtained to result in a more profitable commercial transport.

1.1 Market Study

The introduction of a new design requires a tremendous investment that could ruin the company if the design fails to satisfy the buyer. A study is required to determine what is necessary to create a design that is better than the competition in the particular market segment.

Similar aircraft to the OFP-6M are shown in Table 1.1. The OFP-6M exceeds the competition in range, speed. The OFP-6M is slightly lighter at maximum take-off weight than comparable competition with the same number of passengers. This weight savings is due to the extended use of composites in the interior, wing, empennage, and a reduced tail size made possible by use of a SAS. The engines of the competing aircraft are similar to each other. In contrast, the OFP-6M will utilize the Advanced Ducted Fan (ADF) technology which will achieve the needed thrust per engine at lower SFC (see Section 6). Unlike the Boeing 737 and other competition, high by-pass engines will be fitted to the OFP-6M's original design so there will be no drag penalties due to engine retrofit design compromises.

Table 1.1 Comparison of the OFP-6M and its Competition

Aircraft	PAX	Range (nm)	Mach	Wmax at Take-Off	Engine	Engine Number	Thrust (lb)	Econ. Pitch (in)	Wing Span (ft)	Aspect Ratio	Wing Loading (psf)	Diameter (ft)
Airbus												
A320-200	150	2900	NA	162,000	V2500-A1	2	25,000	32	111	9.4	123	13
A321-100	186	2400	NA	181,000	V2500	2	30,000	32	112	9.4	123	13
McDonnell Douglas												
MD90-30	153	2400	0.76	156,000	V2500-D5	2	25,000	32	108	9.2	128	11
Boeing												
737-200	120	2300	0.73	125,000	JT8D-17A	2	26,000	32	93	8.8	127	13
757	186	2800	0.80	230,000	RR 535C	2	37,400	32	124	7.8	110	13
OFP	**153**	**3000**	**0.80**	**148,500**	**P & W ADP**	**2**	**25,000**	**30**	**107**	**10.0**	**130**	**17**

The current average seat width and pitch of similar aircraft in the economy class is about 17.5 in. and 31 in., respectively. The OFP-6M has a seat width of 17 in. and a seat pitch of 30 in. Although the OFP-6M does not seem comparable to the competition in this area, the large diameter and twin aisle allow for a roomy feeling and more aisle seats. Table 1.1 shows the design specifications of the OFP-6M and competing aircraft. The actual dimensions of the cabin configuration that the airlines implement may be different from the Table 1.1. For example, the seat pitch on a United Airlines Boeing 737 was measured and found to be 29 in. The OFP-6M seat pitch is comparable with the way the airline actually configures the seating. With the twin aisle, access to lavatories and storage compartments are easier and allows quick passenger loading and unloading, which can be money saving for the airlines due to the faster arrivals and departures. With the longer range of the OFP-6M, additional focus on passenger comfort is the key to staying competitive.

The OFP-6M is able to grow in its configuration and technology The relatively low wing loading of the OFP-6M allows for growth in the number of passengers by approximately 30%. This is an advantage since it gives the airlines the possibility of future fleet commonalty when purchasing a new aircraft. Recent technological advances in the fields of materials and engineering strategies that are implemented into new designs like the OFP-6M will make the new designs more compatible with future technological advances. The objective of these future changes in engines, materials, controls, systems, aerodynamics and other areas of design will still be to reduce the cost and increase efficiency without sacrificing performance. One past example was McDonnell-Douglas Aircraft Company implementing new aerodynamic technology to reduce the drag on the MD-11. As in the past, continued improvements of existing designs will be necessary to stay competitive. The design of the OFP-6M will most likely follow this historical trend and the OFP-6M takes this into consideration.

2 Concept Evolution

The OFP-6M is the result of an aggregate of the ideas presented in the preliminary design of eight different aircraft. Three representative preliminary designs are shown in Figure 2.1. Only the evolution is presented in this section. The reasons for each of the design decisions are presented in there appropriate sections. The lifting surface configuration of the preliminary designs included conventional wing with aft vertical and horizontal stabilizers; conventional wing with lifting body, dual aft vertical stabilizers, and trailing edge pitch control; and canard with forward swept foreplane. The engine placements were wing mounted twin turbo fan, aft mounted twin turbo fan, and aft mounted triple turbo fan. The fineness ratio varied from 5:1 to 9:1 due to the variation in interior layout. The interior layouts all seated the required 153 passengers but the number of seats in a row were three plus three, two plus four plus two, and three plus four plus three. The wing loading had a range from 90 lb./ft^2 to 120 lb./ft^2. Airfoil sections of conventional, supercritical design, and advanced supercritical design were employed. The wing aspect ratios had a range of 8:1 to 12:1. Wing taper ratios were all near 3 to 1. Straight, sheared, drooped, and winglets were employed. Conventional, Fly-By-Wire (FBW), and Fly-By-Light (FBL) control systems were specified. All of the preliminary designs had conventionally sized control surfaces and positive static margin to provide stability. Construction methods included conventional riveted aluminum, mixed conventional riveted aluminum and riveted composite, riveted aluminum and bonded composite, and full bonded composite.

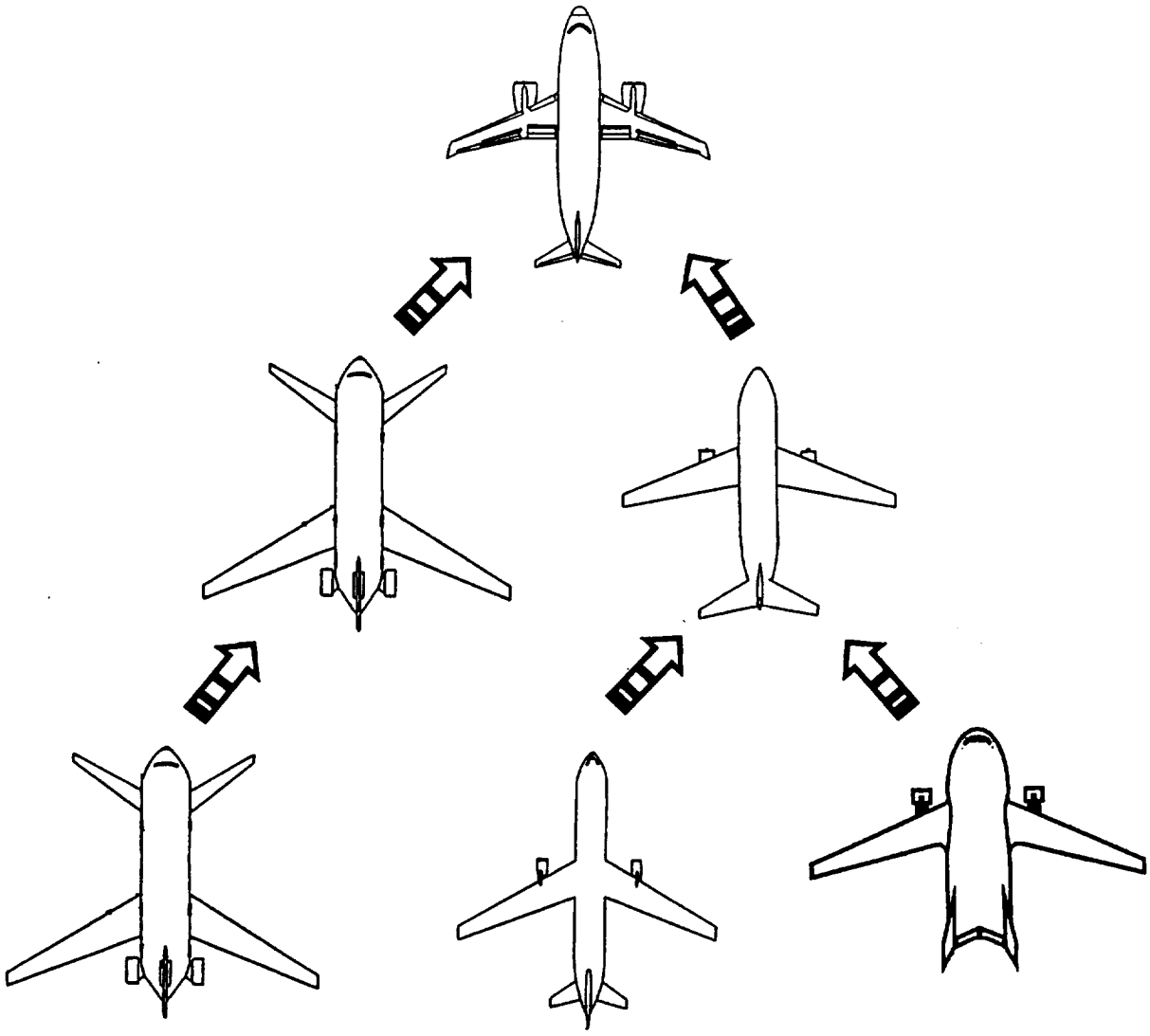

Figure 2.1 Preliminary Designs of OFP-6M

The major design elements of each of the eight preliminary designs were considered and a new concept, the OFP-8, emerged with most of the preferred and compatible features as shown at the top of Figure 2.1. The OFP-8 had conventional wing/tail configuration with twin wing mounted turbo-fan engines. The seating was two-four-two and a fineness ratio of 6:1 was achieved. The wing loading was 100 lb/ft^2. FBW, a positive static margin and conventionally sized tail were employed. Bonded composite wing and tail with a conventionally riveted aluminum fuselage were used. The OFP-8 was over weight, over winged, and too copious for the RFP.

The OFP-8 evolved into the OFP-7 due to down sizing of the aircraft and the design team. The weight was reduced, the wing size decreased, the engine size decreased, the over-wing exits eliminated, the landing gear type changed, the wing loading increased, and the aerodynamics improved on the new design.

The OFP-7 evolved to the final configuration, the OFP-6M. The new name reflects the further trimming of the aircraft and a new improved design team organization. The major changes are the incorporation of an advanced SAS, the elimination of all conventional stability, the use of electrohydrostatic actuators, and the use of bonding to eliminate rivets. The changes have produced a design that will be viable well into the next century and currently able to manufacture with today's state-of-the-art technology.

2.1 Other Design Philosophies Considered

In the design of the OFP-6M Plan-It X considered not only the above configurations but numerous others, including practical, impractical, not proven, and unworkable for the given RFP. The practical included, but were not limited to, tri-surface, unducted fan, advanced unducted geared fan, and span loading. The not practical designs for the RFP included canard, tandem wing, forward swept wing, and forced laminar flow. The not proven designs included spiroid wing tips, and riblits. For example, the spiroid wing tips have less then 5 flight hours of flight test on an aircraft with an aspect ratio of only 6 and wind tunnel tests were inconclusive according to the inventor. The unworkable included single engine, M wing, no tail, and highly oval cross-section fuselage. Not practical or not proven configurations were not incorporated to prevent escalating development costs. Escalating costs are not conducive to the RFP. Unworkable configurations were not used since they were unworkable. A practical configuration was not incorporated if trade studies were not positive due to prohibitive costs, performance degradation or high technology development risk. The trade studies

were mainly based on performance, due to the limits of the analysis tools that were available. The ability to manufacture, technology availability, and most importantly, costs were the limiting factors for inclusion of a feature. The unworkable are not impossible. The unworkable are not compatible with the RFP, the FARs or the level of current technology.

2.2 Historical Effect on the Design of the OFP-6M

The OFP-6M is of the same size as the original aircraft that pioneered the Jet age(Ref.45). The first commercially successful jet transport was the Boeing 707, a four engine turbo-jet. Douglas followed with the larger DC-8 four engine transport. The use of four engines was required for safety, due to the relatively poor reliability of the engines; the FARs; and the level of thrust the engines produced. Soon the reliability and thrust improved to the point that a tri-jet was acceptable for all flights and a twin-jet for over-land flights. The Boeing 727 and 737 along with the Douglas DC-9 were designed in this time period. The twin-jets have since been improved to the point that extended twin operations over water are allowed. The use of two engines is highly desirable from a cost and maintenance perspective and have effectively eliminated tri-jets and quad-jets from this size range. The newer Boeing 737s, the McDonnell Douglas MD80/MD90 and the Airbus A320 are of this time period and are of similar size to the OFP-6M and were an inspiration and design starting point for the OFP-6M.

2.3 Market Strategy Synopsis

The OFP-6M is designed for low DOC along with realistic manufacturing technology to provide maximum return on investment for the manufacturer and the

operator. The design is at the minimum point of the trade off between amortization of the cost to purchase and the DOC, using available technology. This point is the maximum potential profit point for Plan-it X, the airframe manufacturer. The goal of the OFP-6M is to provide the maximum profit for Plan-it X and the greatest return on investment to the stock holders. This may not be stated in the RFP but is the goal of every corporation and is implied since corporations build the aircraft in the United States of America and most other nations on this planet. Pricing will be determined by the maximum that the market can bear. Given the same total cost of operation for the airline as the competition, including amortization of the cost of the aircraft, the selling price to the airline can be larger then the competition since the DOC is smaller. Production costs will be lower due to the elimination of superannuated technology, a lean organization, and streamlined management. The lower costs to produce the OFP-6M and the higher selling price that the market will support (due to the lower cost of operation) will combine to produce the highest return on investment in the industry.

2.4 Mission Profile

As outlined in the RFP, the mission profile for the OFP-6M is shown in Figure 2.2. The profile begins with takeoff from a 5,000 ft field, carrying a payload of 153 passengers and their bags. After takeoff, the OFP-6M accelerates to 242 Knots Calibrated Airspeed (KCAS) and climbs at constant indicated airspeed to arrive at a cruising altitude of 38,000 ft at Mach 0.8. The cruise range with a full complement of passengers is 3,000 nm, as required. The final portion of a normal mission is a descent to land on a 7,000 ft runway, with fuel reserve provisions for loiter, a missed approach, and a flight to an alternate airport.

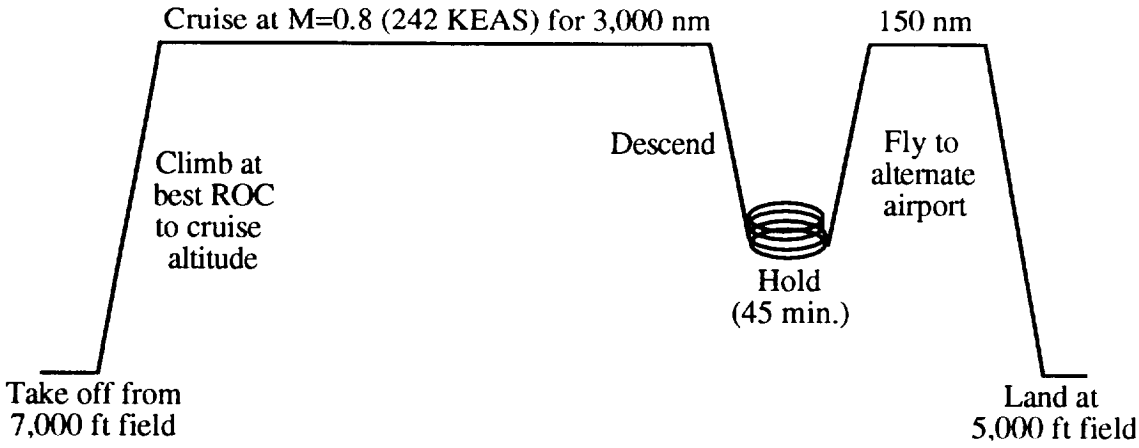

Figure 2.2 OFP-6M Mission Profile

2.5 Weight Sizing

The first step in designing a transport jet meeting this mission profile was to get a working system to estimate the weight size of the aircraft. The system that was produced to accomplish this weight sizing is called the Design Point Program (DPP).

2.5.1. Design Point Program

The DPP needed to combine specific mission requirements, aircraft performance characteristics and assumptions to quickly give other dependent and related results (Ref. 33). To do this a computerized spreadsheet was used incorporating performance and jet transport restrictions in conjunction with principles of flight and FAR restrictions (Ref. 42, 17). Since the OFP-6M is in a standard configuration for its class many values were assumed from standard aircraft examples (Ref. 33).

2.5.2. Design Point Plot

In order to put the information from the DPP in a usable form a design point plot was used efficiently condensing and displaying important restrictions and options. This design point plot is shown in Figure 2.3. Major restrictions in the design point plot are the FAR 25.121 One Engine Inoperative (OEI) balked landing and cruise speed requirements (Ref. 17). Major design considerations were implicating practicality, cost of production, DOC, etc.

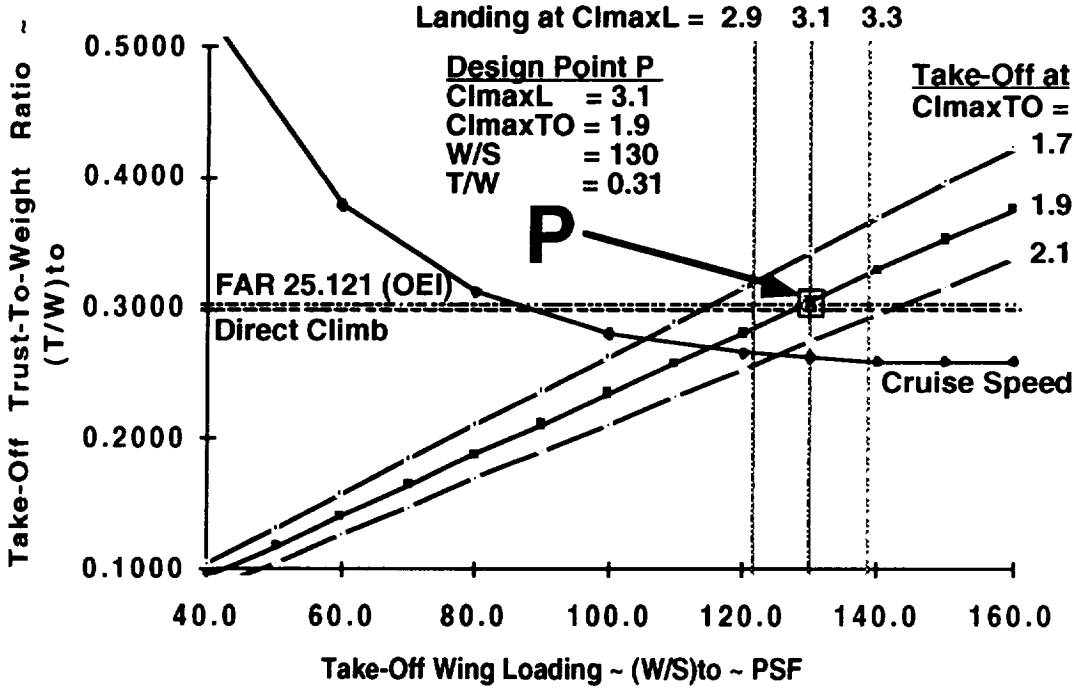

Figure 2.3 Design Point Plot Showing OFP-6M Limitations

Once the restrictions from the design point plot were found, the actual operating point of aircraft operation needed to be chosen from available options. This would identify the wing loading, thrust-to-weight ratio, and the maximum lift coefficients

required for take-off and landing. This designation is identified in Figure 2.3 as design point P. The vertical axis in the design point plot corresponds to the take-off thrust-to-weight ratio of the OFP-6M which was minimized for the following reasons:

- **Reduced weight from smaller engines (Ref. 32).**
- **Fuel saved from a lower required thrust (Ref. 44).**
- **Reduced maintenance costs from smaller engines (Ref. 32).**

The horizontal axis in Figure 2.3 corresponds to the take-off wing loading of the OFP-6M which was maximized while keeping the lift coefficients for take-off and landing reasonable for the following reasons:

- **Reduced aircraft weight from a smaller wing area (Ref. 44).**
- **Better maneuverability (Ref. 18).**
- **Load structure remains small from use of composites (Ref. 14).**
- **Fuel tank capacity remains large enough for its mission.**
- **Reduced production costs from a smaller wing area (Ref. 44).**
- **Reduced wing span for better airport compatibility (Ref. 17).**

Table 2.1 gives the results from the DPP for the optimized design point P. Other information correlating to the design point P is given in Figure 2.3.

Table 2.1 OFP-6M Weight Sizing Summary

	Payload (lb)	Mission Fuel (lb)	Empty (lb)	Take-Off (lb)
Max Weight	30,600	36,000	79,700	148,700

2.6 Exterior Layout

The round shape of the fuselage was chosen for its simple structural design, low structural weight, large overhead space and good pressurization characteristics. The circular diameter does, however, result in a larger cross-sectional area. This larger cross-sectional area is partially offset by a lower drag coefficient (see Section 4.5).

The height of the wing on the fuselage affects drag, dihedral, and operational cost. As shown in Figure 3.5, a near mid-wing was chosen. This is done by placing the wing directly under the floor. Since the fuselage is so large, this places the wing almost at the center of the fuselage. This is done because the body-wing joint of a mid-wing does not have a high interference drag as does a usual low or high wing. In addition, less filler would be needed for the near mid-wing. This would result in less wetted area decreasing drag. As compared with a standard low wing, the near mid-wing does not need a large dihedral thus stability is better. The near mid-wing also allows a more comfortable margin of ground clearance for the engines. Another advantage of the near mid-wing is less moment on the body because of a shorter moment arm than a low wing.

Two engines are placed underneath the wings for better stability, easier access for maintenance, and to reduce noise. The disadvantage of placing the engines under the wing is the increase probability of Foreign Object Damage (FOD) and less stability in the case of when there is only one engine operating (see Section 2.7).

FOLDOUT FRAME

CHARACTERISTIC DATA			
ITEM	WING	HORIZONTAL STABILIZER	VERTICAL
AREA (sqft)	1144	200	368
ASPECT RATIO	10	6.1	2
TAPER RATIO	0.3	0.3	0.3
SWEEP (deg)	20	25	30
DIHEDRAL (deg)	4	3	NA

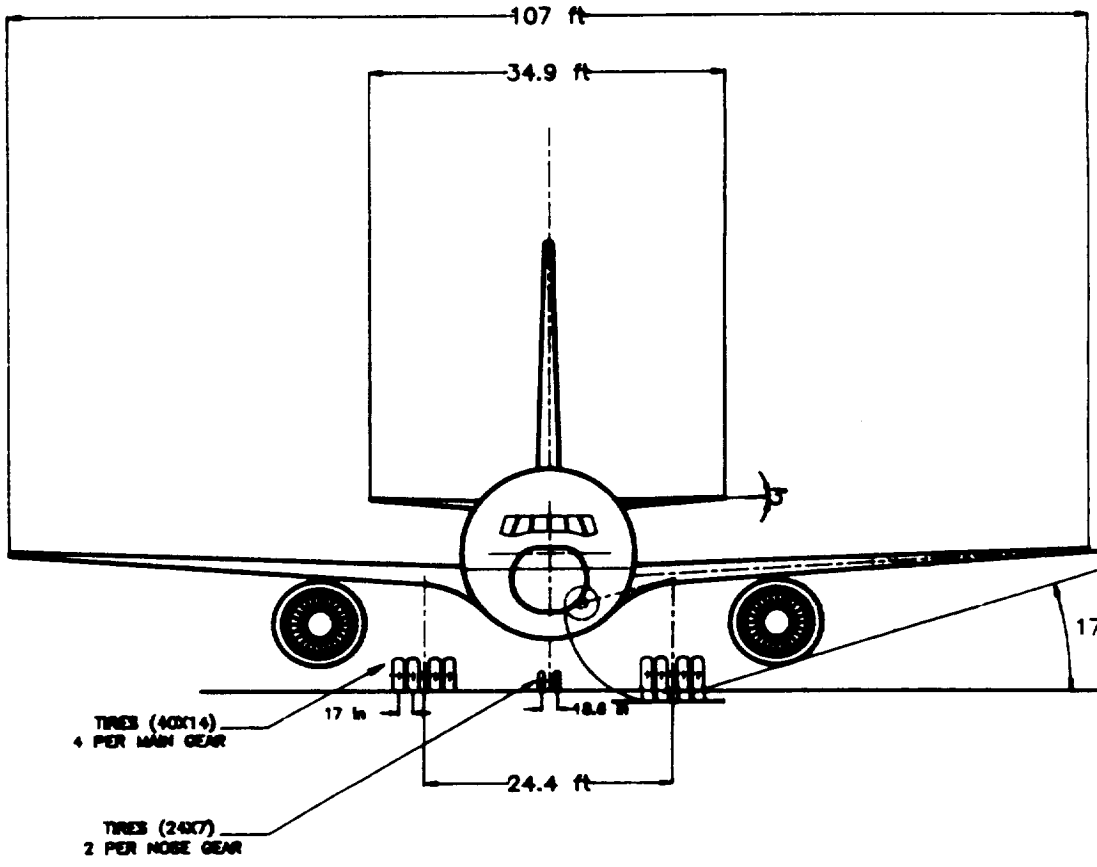

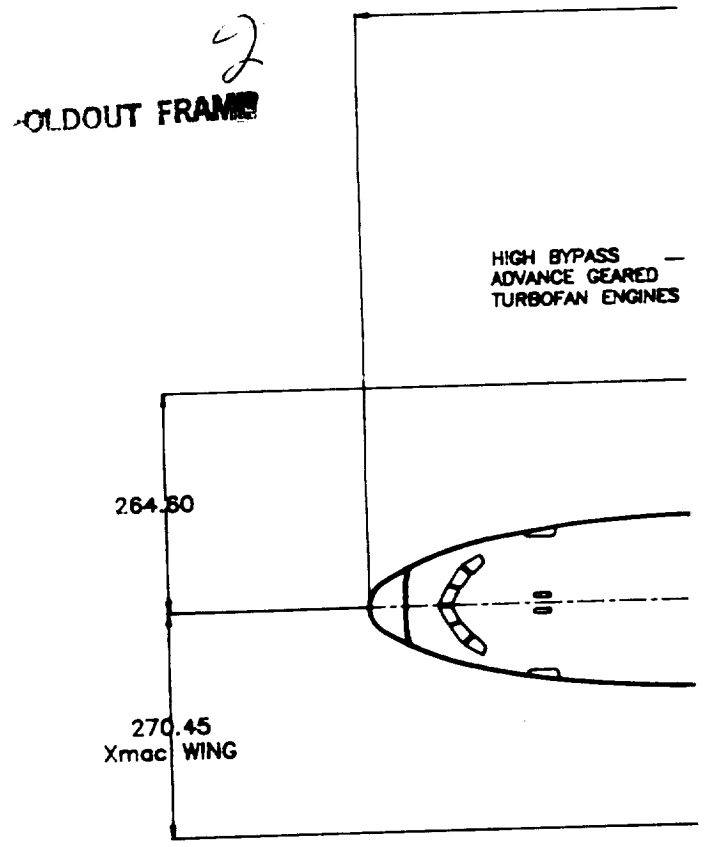

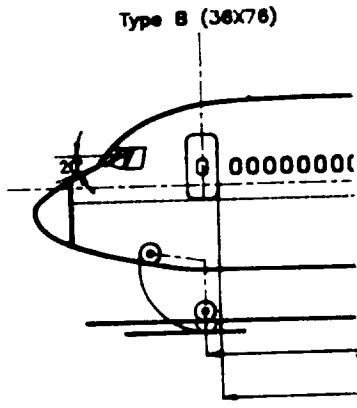

Figure 2.4 OFP-6M Three-View Layout

FOLDOUT FRAME 3

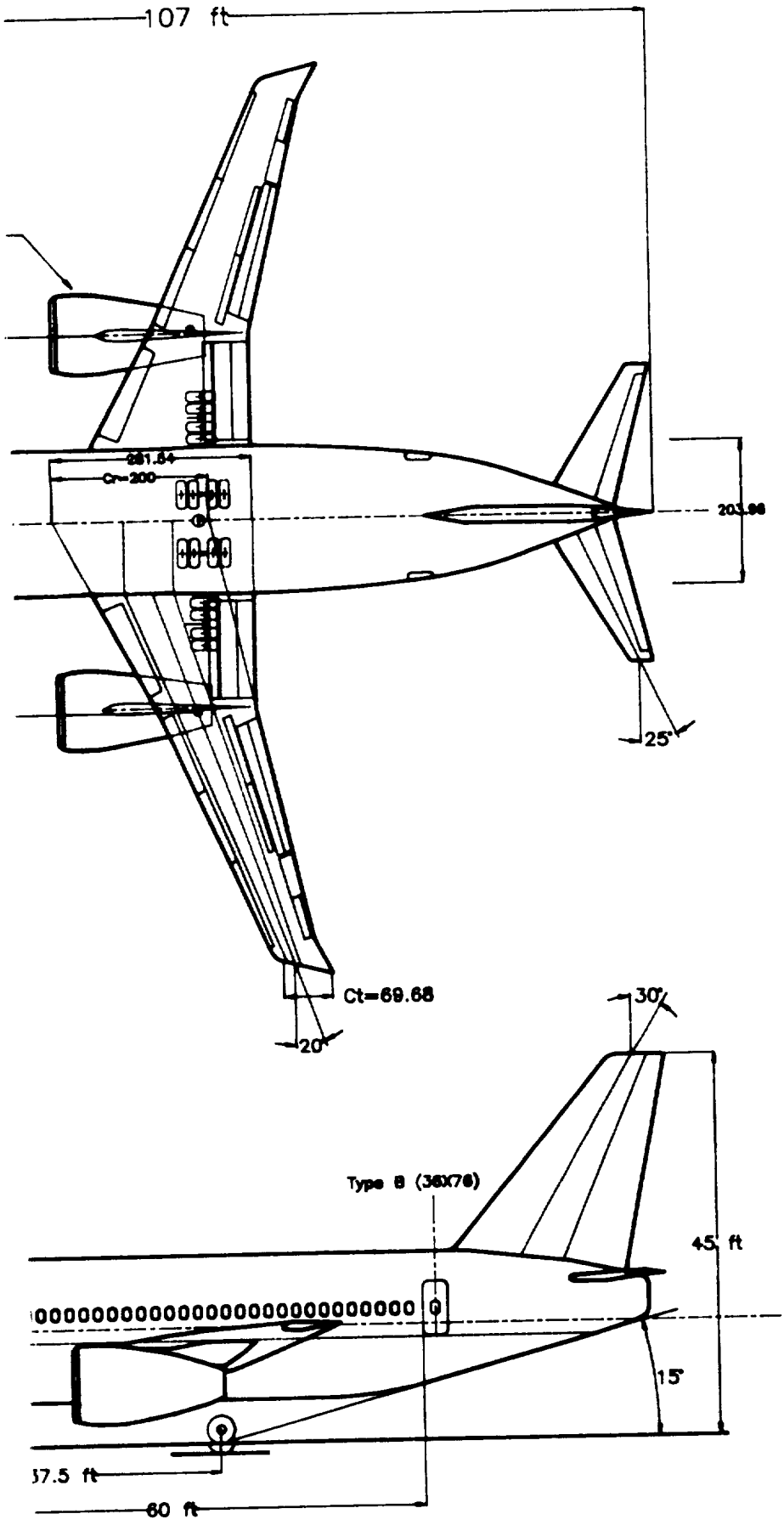

2.7 Engine Placement and Integration

During the preliminary design of the OFP-6M, two engine installation configurations were considered viable: under the wings or in fuselage pods on the tail. As a result of the advantages and disadvantages outlined in Table 3.3, the engines are placed under the wings.

Table 2.2 Comparing Engine Placement under Wings for OFP-6M

Advantages	Disadvantages
Reduced Center of Gravity (CG). Excursion = Reduced Trim Drag	Larger Yaw Moment for OEI = Larger Vertical Stabilizer
Eliminate FOD from Wing Ice Ingestion	Increased Chance of FOD from Ground Debris
Better Accessibility for Maintenance	Longer Landing Gear
Wing Load Alleviation	Interference With Wing Flow Field
Simpler Systems Integration	
Reduced Noise and Vibration Transmission to Fuselage and Cabin	

3 OFP-6M Interior Layout

3.1 Main Cabin

The interior layout of this aircraft was designed with concern for low cost, while still catering to passenger comfort. As shown in Figure 3.1, the interior is a dual class configuration with first class and an extensive tourist class. The large circular diameter gives a spacious feeling and ample room for overhead compartments (2.8 ft^3 per passenger).

The twin aisle will help reduce the turn around time for the cabin. Each aisle gives enough space for a food cart to pass freely. A twin aisle configuration was chosen not just for passenger comfort, but also to shorten the fuselage. This allows compliance with the 60-ft rule without having a door above the wing. This was done to save the weight of the doors and to reduce the complexity of the overall design. Another advantage of the twin aisle is the availability of aisle seats. It is commonly known that a number of travelers prefer aisle seats and window seats. This design provides accommodations for those passengers who have this preference (Table 3.1). Though the seating accommodations of the OFP-6M are comparable to its competition, the larger interior volume gives the passenger a feeling of more room. This in turn makes the passenger perceive that the plane is more comfortable. See Table 3.2 for seating accommodations of the OFP-6M. Research is also being done on seat materials. By using a high energy absorbent material in the seat backings, the OFP-6M can reduce the seat pitch to only 30 in, yet still maintain the leg room of a 32 in pitch.

FOLDOUT FRAME

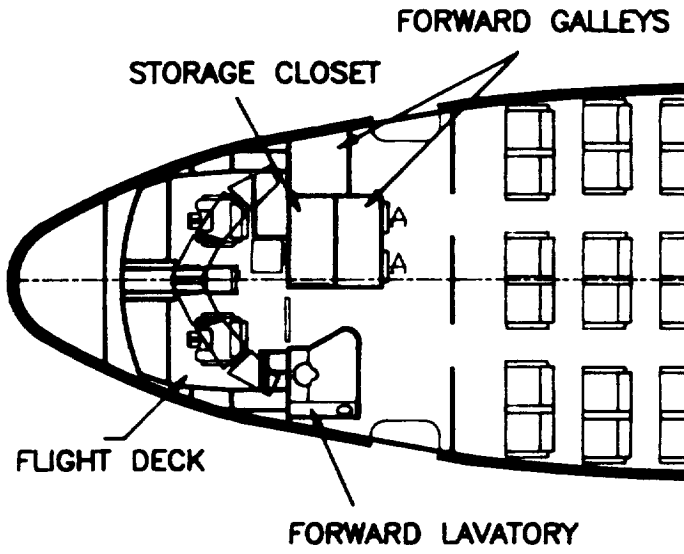

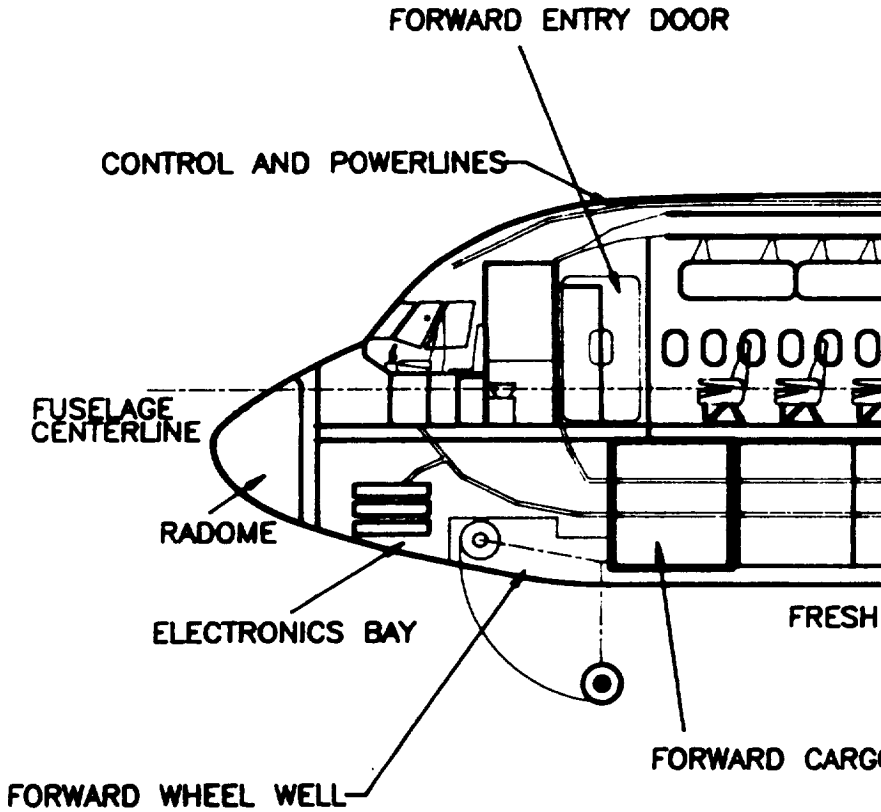

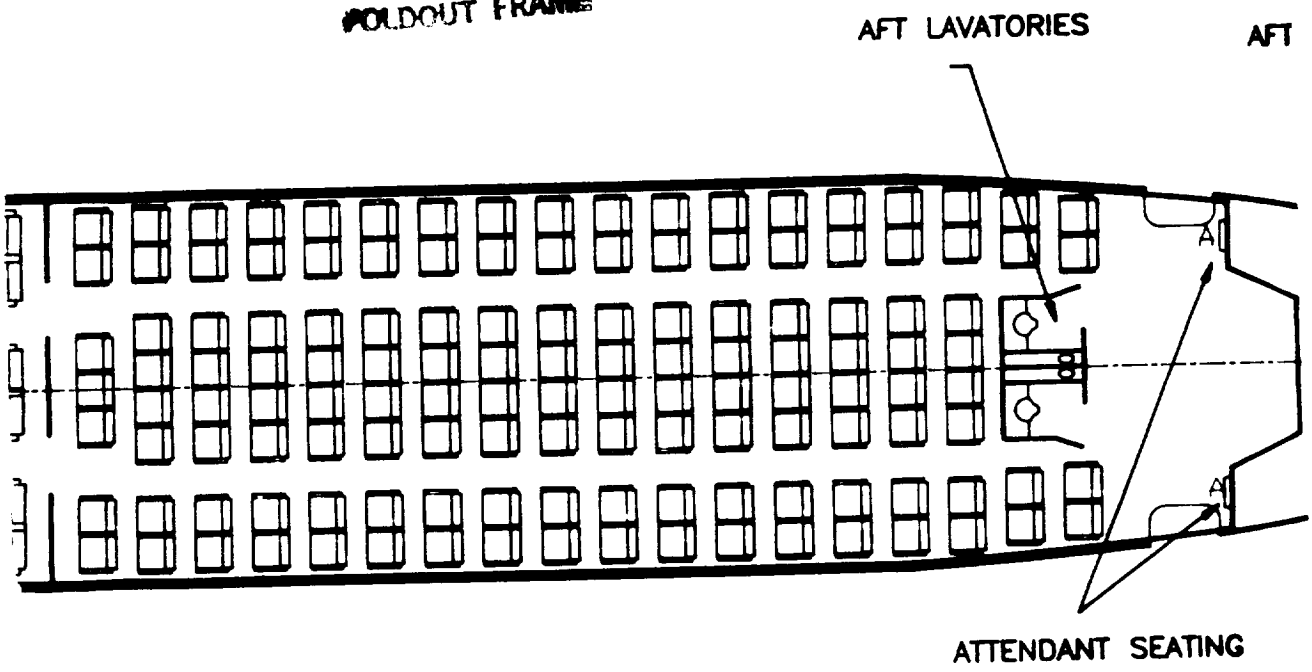

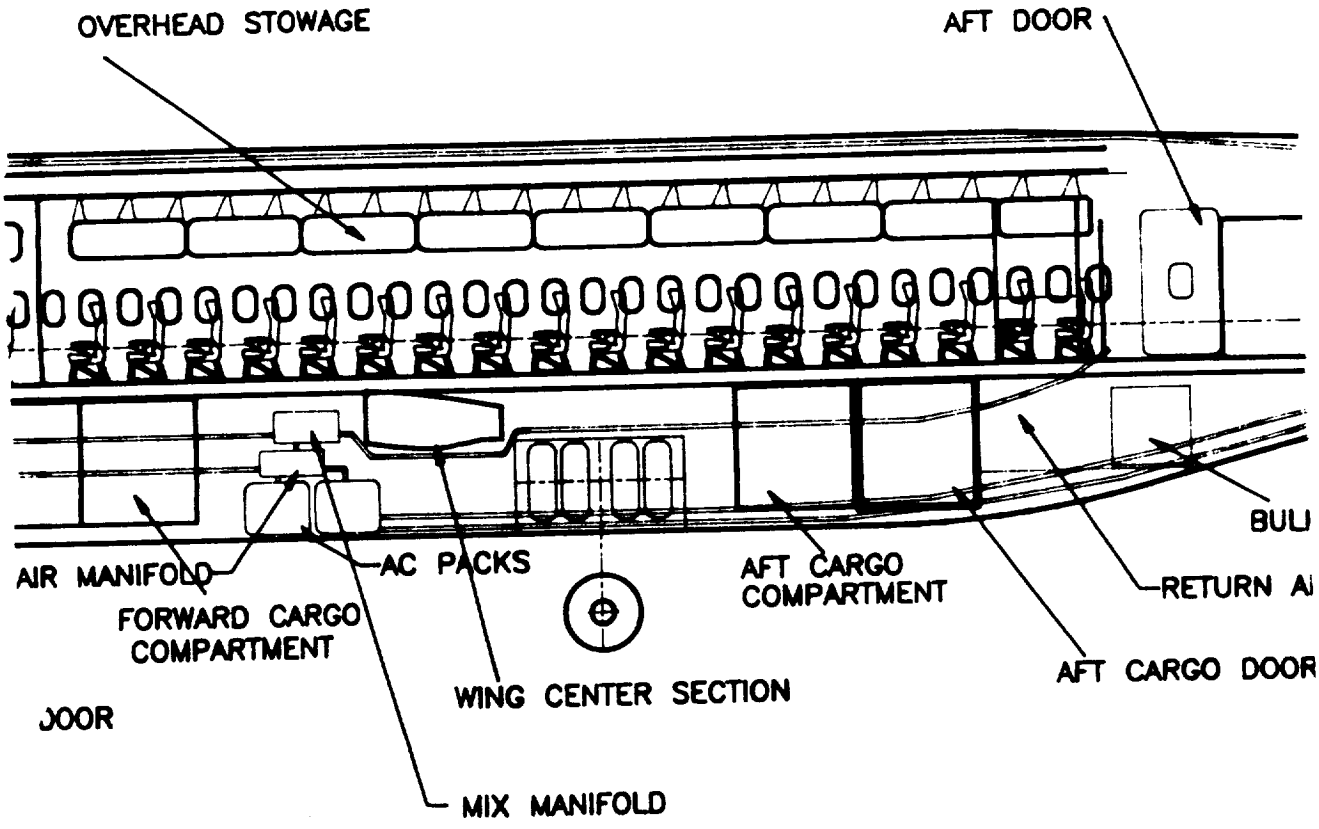

Figure 3.1 Interior Layout and Inboard Profile of OFP- 6M

3.

FOLDOUT FRAME

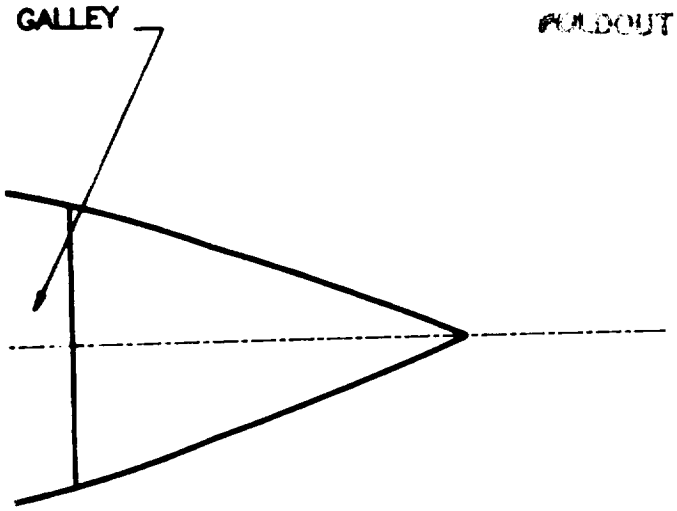

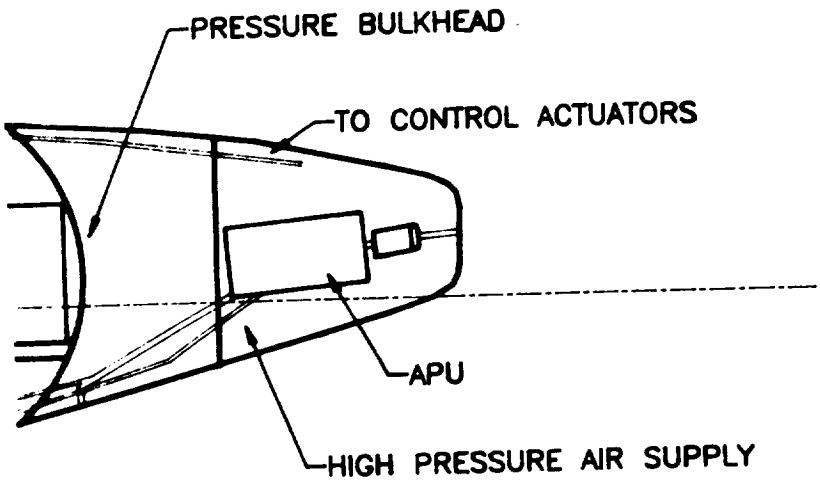

< CARGO DOOR

R

Table 3.1 Seat Breakdown of OFP-6M

	Window Seats	Aisle Seats	Center Seats
Number of Seats	42	80	31
Percentage of Seats	28%	52%	20%

Table 3.2 OFP-6M Seating Accommodations

	Pax	Rows	Abreast	Seat Width	Armrest	Seat Pitch	Aisle
First Class	18	3	6	20"	3 - 4 - 3"	40"	20" min
Economy	128	16	8	17"	2.5"	30"	17"
	7	1	7	17"	2.5"	30"	23"

Lavatories, galleys, and storage were placed forward and aft where they can easily accommodate all passengers completely and comfortably. There are 3 lavatories; one in the front with first class travelers and cabin crew, and two in the rear with the economy class. This will provide one lavatory for approximately every 51 passengers. There is a small galley in the front to service first class, and a large galley in the back to provide service for the tourist class. Lavatories and galleys are placed apart from each other to avoid interference. Closets are located in the front of the cabin with two small storage spaces in the back. Attendants were placed in both the front and the back with an near 100% passenger view when the first class cabin partitions are opened. Figure 3.2 shows the cross-sections of the OFP-6M. As can be seen from the cross sectional views, the OFP-6M can easily be transformed to a total cargo plane. This increases the market for the OFP-6M.

Plan-It X

FOLDOUT FRAME 1

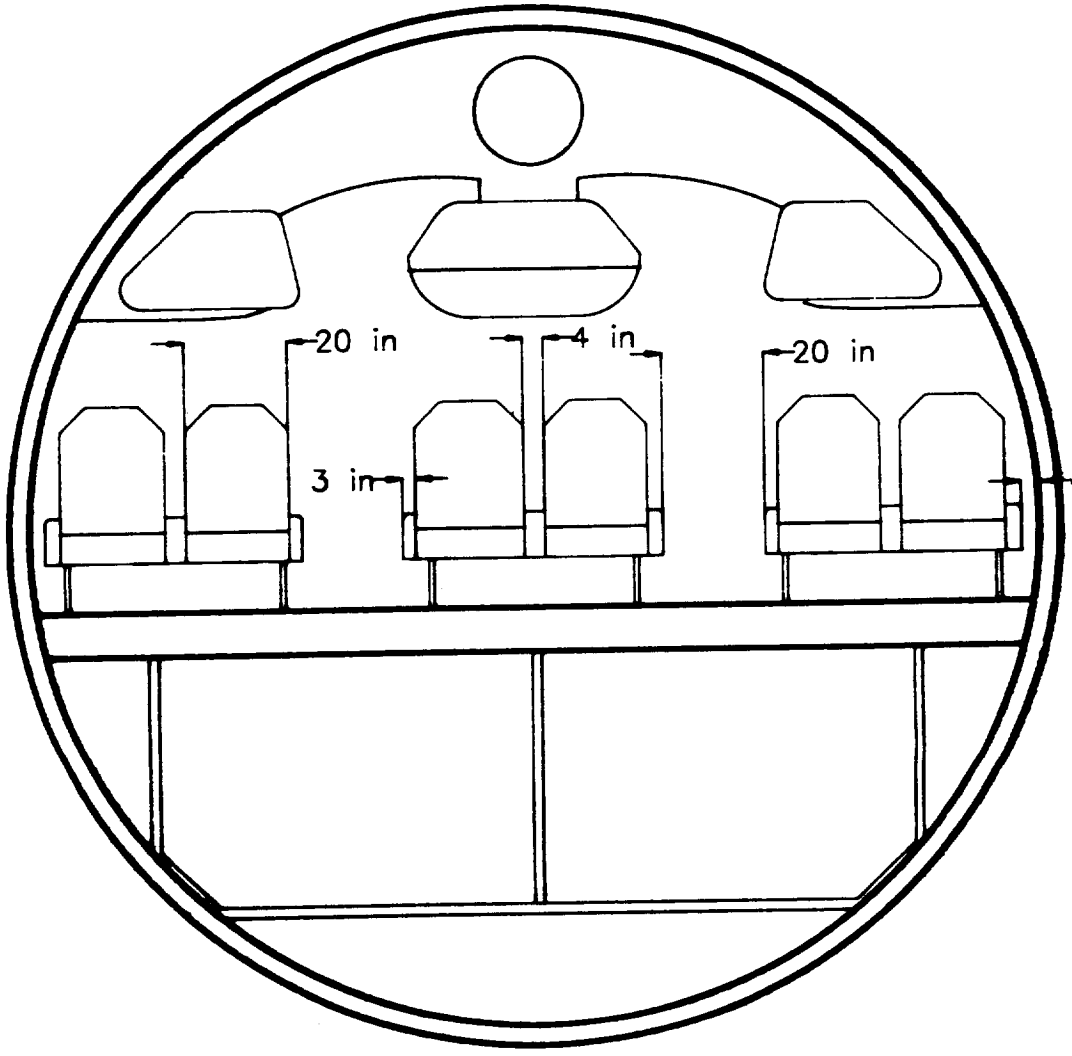

FIRST CLASS

AVERAGE VOL
PER SEAT
2.8 CUBIC FT

LD-3
VOLUME-
(4.5 CUB
GW - 3

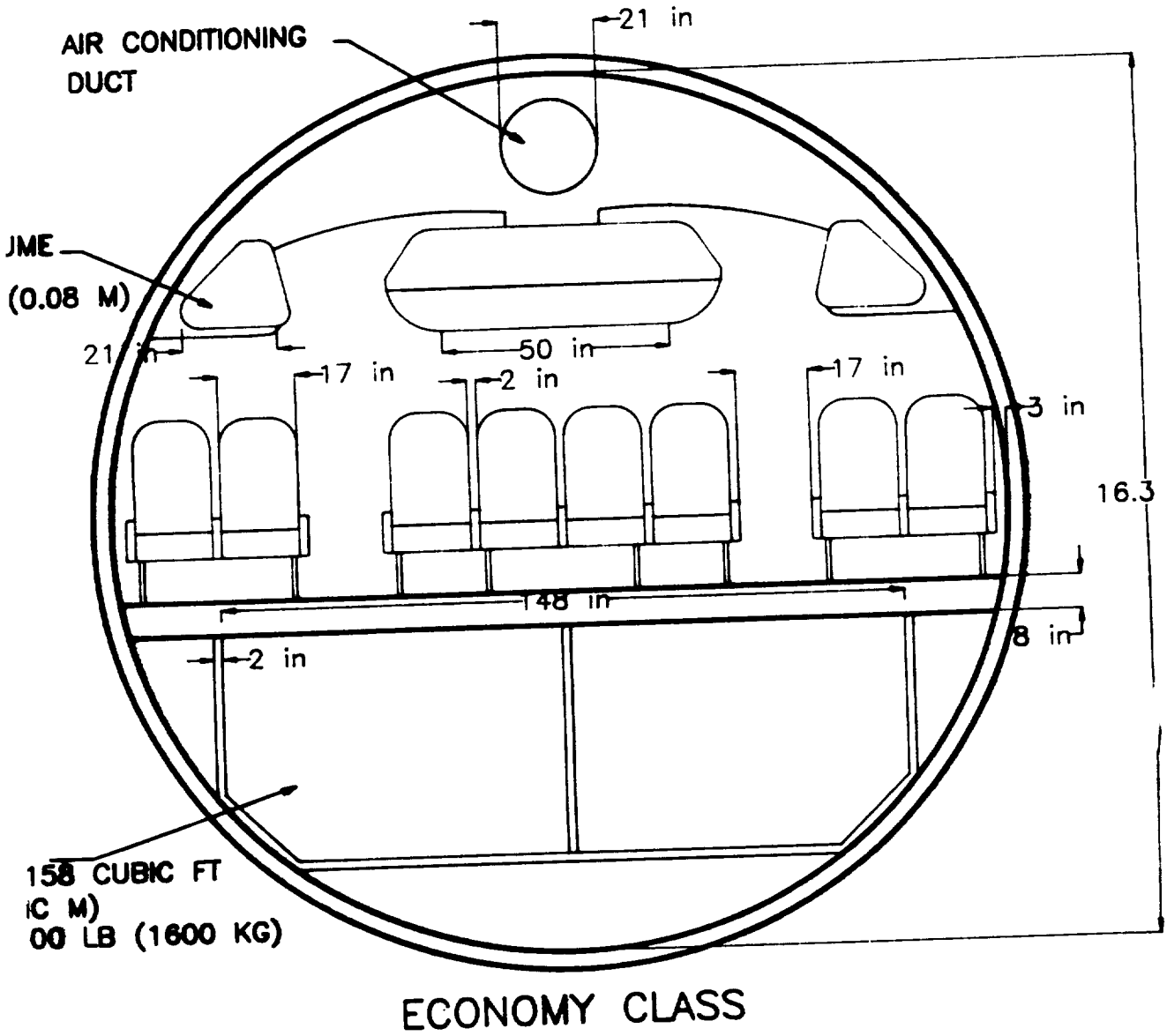

Figure 3.2 Cross-Sections of OFP-6M

PALLET OUT FRAME 3

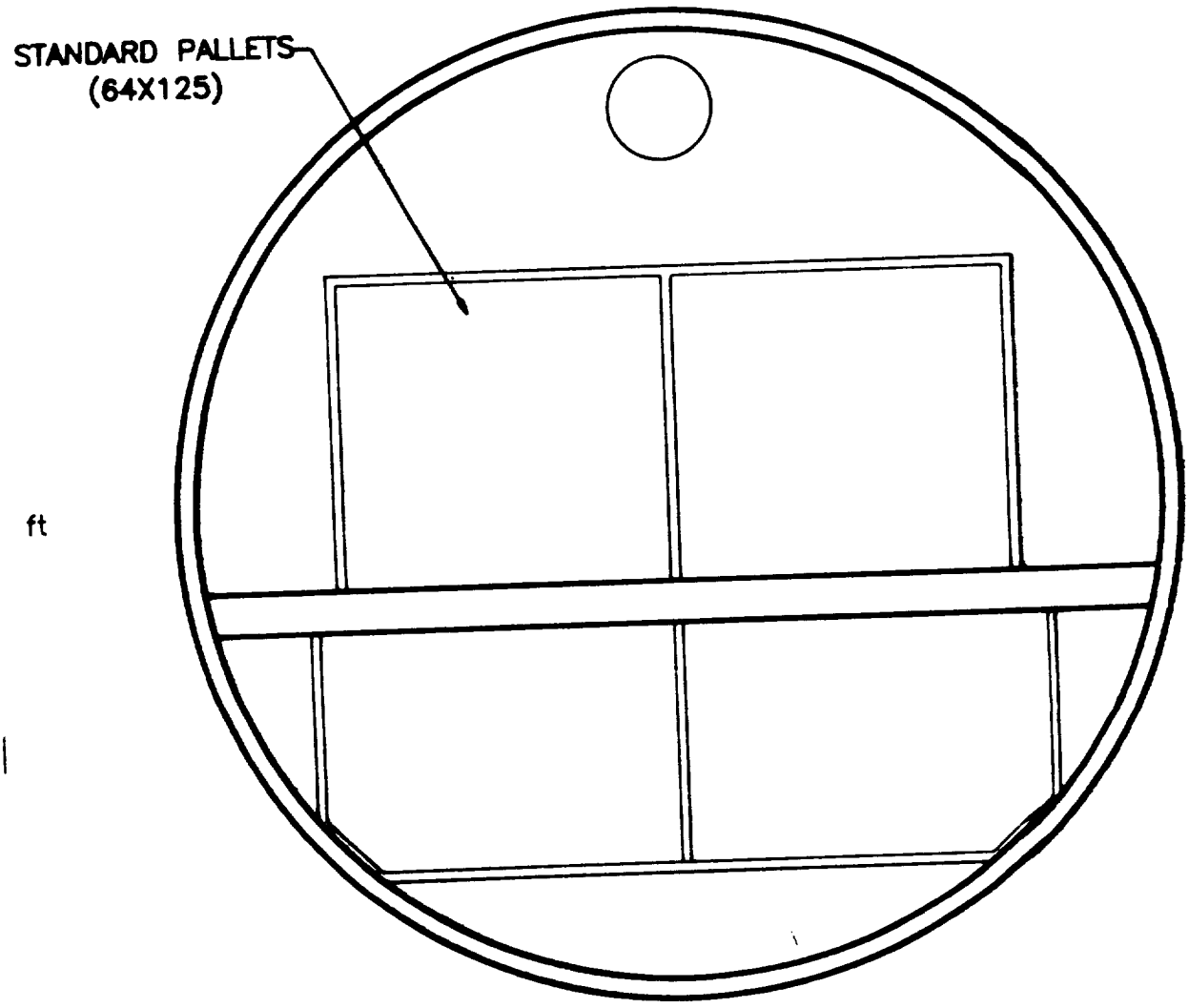

ALL CARGO

The location and type of exits and doors is important when considering loading, unloading, and emergency evacuation of the aircraft. Type B doors were selected because of their large size. This will aid in loading and unloading quickly. They are located two in the front and two in the rear one on each side of the aircraft. This layout is best for symmetry and offers easy access for the service trucks.

3.2 Flight Deck

The overall design philosophy for the flight deck was to make the environment as comfortable and easy to use as possible, while still providing support and protection during emergencies. The flight deck was designed to meet the needs of a two man crew, with an observer present as required by the FAA. A full six display 'glass cockpit' was used for the most efficient transfer of needed information to the pilot. The main instrument panel has six flat panel integrated display units which show Primary Flight Display (PFD), Navigational Display (ND), Engine Indication and Crew Alerting System (EICAS), and Central Maintenance Computer (CMU) displays. The PFD changes depending on what mode of flight the plane is in, i.e. climb, cruise, descent, etc. It will also display extra information such as best rate of turn, and deviation along the flight path. It is capable of high or low speed warnings, speed predictions for set flight conditions, and potentially dangerous flight conditions and/or flight path warnings by using a flight management control system.

The main instrument panels for the OFP-6M are shown in Figure 3.3. The ND gives compass information and includes a map of the area with radio beacons, holding patterns, restricted airspace, airports, and recommended flight paths. Superimposed on this map is a weather radar picture. This information helps the pilot avoid potentially dangerous turbulence situations and find favorable winds. All systems of the aircraft can be shown on the maintenance screen if there is a malfunction (see Section 11). This

indicates when there is a problem or malfunction with a system. It lets the pilot know what and where the failure is so he can take the appropriate action, and can contact the computer at the next stop to send for the correct part before landing and reduce maintenance time and cost. The screens that are most important for a safe landing are backed up by the mechanical displays located around them. Among these are the altimeter, compass, airspeed, clock, turn and bank, attitude indicator and CDI with glide slope.

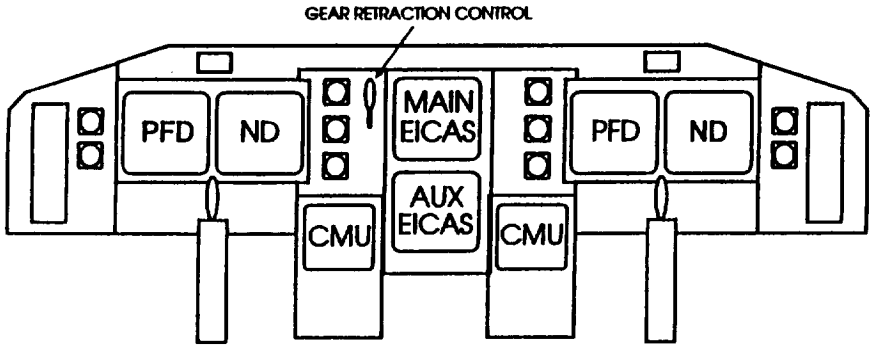

Figure 3.3 OFP-6M Main Instrument Panels

The PFD, ND and CMU displays discussed above are shown on both the pilot's and the first officer's sides, while the EICAS is placed in the center panel for equal access. The center panel as shown in Figure 3.3 also contains auto brake, standby engine instruments, thrust management mode selection, landing gear controls, alternate flaps, and alternate gear extension. The glare shield panel contains both left and right controls for the master caution, warning lights, the VOR and DME controls, while in the center is the auto pilot/auto throttle/flight director controls.

The forward overhead panel is centered so that either pilot can reach the controls. It includes such systems as the inertial reference mode, yaw damper with anti skid option, electric engine control module, hydraulic system control, standby power, electrical power system, auxiliary power, fuel system, wing and engine anti-ice control, cabin pressure control, and much more. These systems controls are also indicative of different states by

color coding, green for working, amber for caution and red for danger. This panel allows the pilots to deal with the problems quickly and effectively. The aft overhead panel is for circuit breakers .

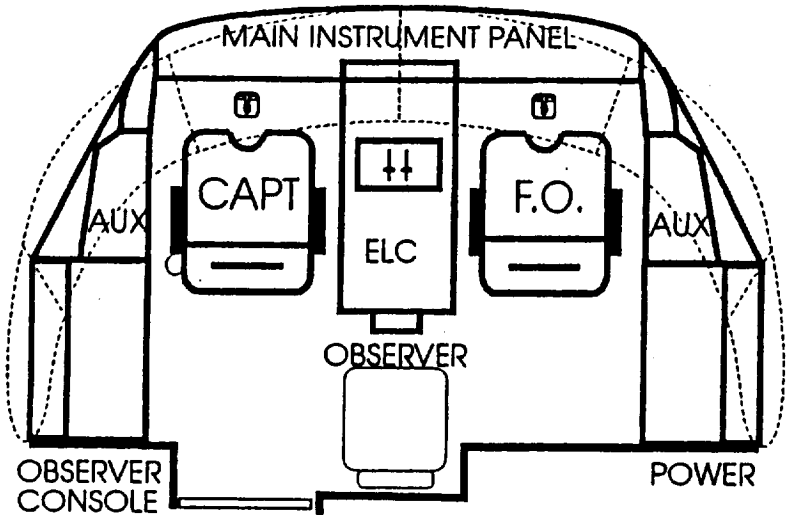

Figure 3.4 OFP-6M Fight Deck Layout

Figure 3.4 shows the flight deck layout. The crew chairs are designed to give comfort, support, and protection during emergencies, while still allowing the pilots full mobility to do their jobs. The center stick locks in place during normal flight and has a joystick on top which controls the plane. Both joysticks move together when in operation.

4 Aerodynamics

4.1 Airfoil Selection

The majority of the time spent in flight for the 3000 nm mission is in cruise. A supercritical airfoil was chosen over a classical profile because a supercritical airfoil would be the most beneficial for this mission. Supercritical airfoils, in general, significantly extend drag divergence Mach numbers beyond those of conventional airfoils. This in turn reduces the sweep angle needed, which reduces induced drag for the aircraft (Ref. 1, 12). This is also a structural advantage which helps in reducing the weight of the aircraft because less support was needed for the sweep. Supercritical airfoils result in lower cruise drag, high lift over drag ratios, and have good stall characteristics (Ref. 12, 44). Also, because of the large thickness, supercritical airfoils can hold greater amounts of fuel. The larger fuel capacity will allow the OFP-6M to travel farther without refueling or adding additional fuel tanks. The lower cruise drag and high lift to drag ratios conserve fuel which also allows further travel and lowers fuel cost.

The airfoil chosen for the OFP-6M aircraft was the NASA supercritical airfoil SC-9 2, with a Mach divergence for the SC-9 2 is M = 0.78. The disadvantage to choosing this airfoil was that supercritical airfoils also have lower lift coefficients, therefore significant high lift devices will be needed. The SC-9 2 is shown with some of its characteristics in Figures 4.1, 4.2 and 4.3 (Ref. 11). This data was then analyzed for the wing and can be seen in section 4.3.

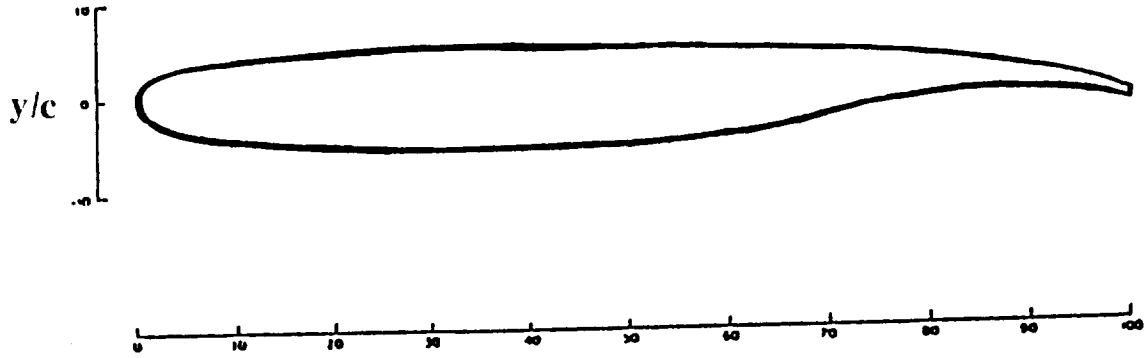

(Source: Ref. 12)

Figure 4.1 SC 9-2 Airfoil Section for OFP-6M

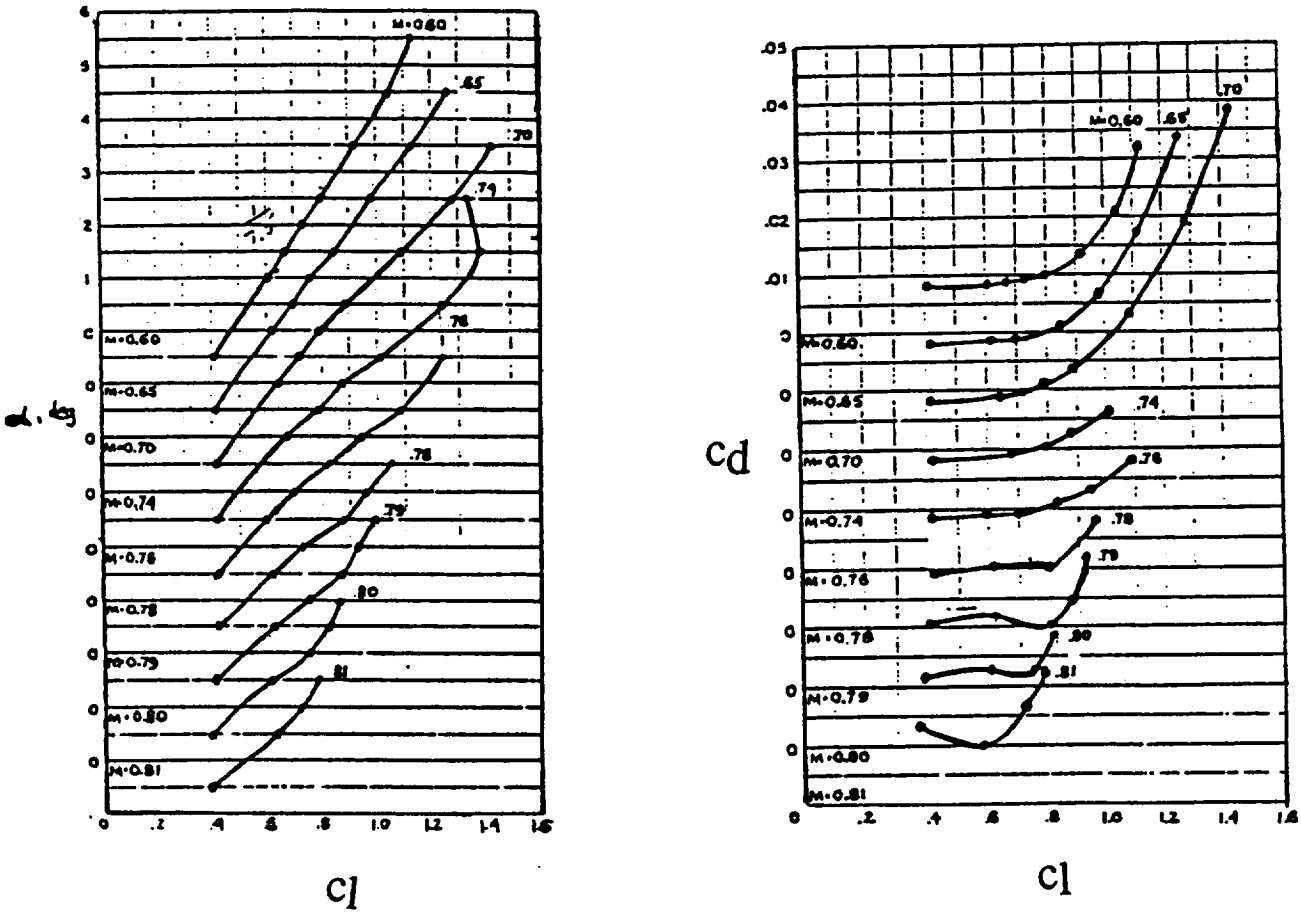

(Source: Ref. 12)

Figure 4.2 SC-9 2 Airfoil Data for OFP-6M

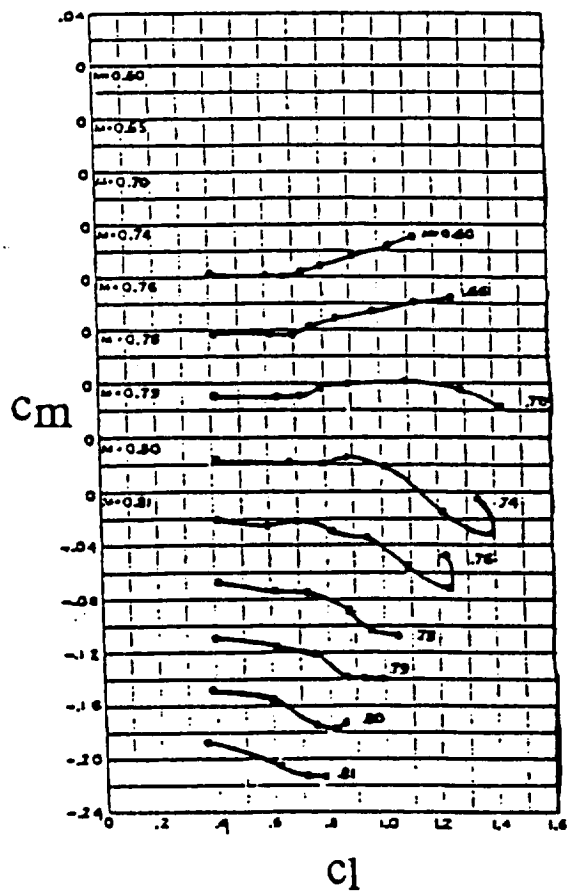

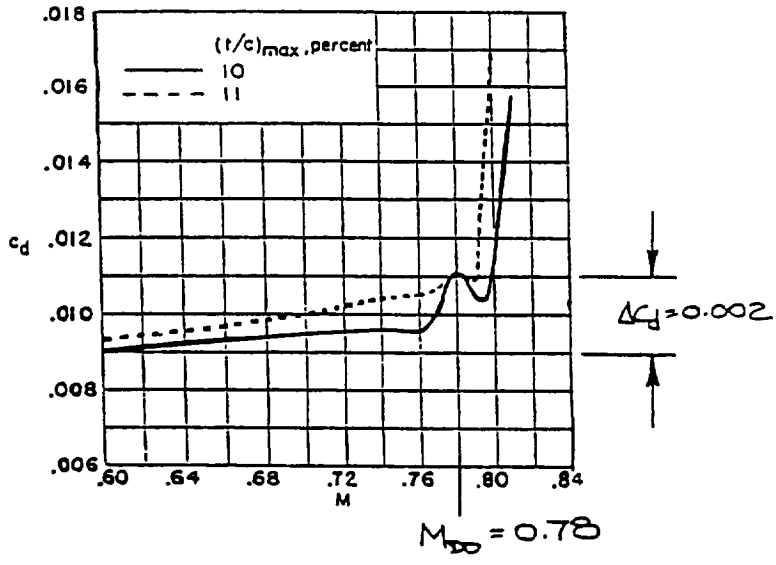

(Source: Ref. 12)

Figure 4.3 SC-9 2 Airfoil Data for OFP-6M (Continued)

4.2 Wing Geometry

The OFP-6M has a conventional wing design as shown in Figure 4.4. This planform was decided upon because of proven performance and based on the technology of existing aircraft (Ref. 4, 5, 6, 7, 8, 42, 44). After analysis, the wing area resulted in 1144 ft^2 which was calculated from the design point wing loading of 130 psf.

An aspect ratio of 10 was chosen to reduce induced drag effects and increase structural simplicity, therefore making the aircraft more efficient. Since the aspect ratio of 10 is less then the ideal ratio of infinity, wing tip design is extremely important. A sheared aft angled shark fin tip was chosen to reduce induced drag. The shark fin helps to reduce the tip vortex, relieving the induced drag, while a shearing angle of 20 degrees is

chosen for the most efficient induced drag reduction at an aspect ratio of 10 (Ref. 18, 44, 45).

The taper ratio is essential for good lift distribution and an elliptical wing is the most efficient. A taper ratio of 0.3 is chosen because it is the closest approximation to an elliptical wing, providing the most efficient lift distribution (Ref. 17). From this data, a root and tip chord of 16.5 and 4.94 ft, were calculated, respectively (Ref. 42). Lastly the sweep angle was found to be 20 degrees at quarter chord by using the critical Mach number of 0.78 and taking flow acceleration around the fuselage into account. The wing planform is shown in the Figure 4.4 (Ref. 12). A flaperon was chosen instead of a simple aileron to help in high lift situations, such as takeoff and landing (see Section 4.4). The flaperon was split for better response in high speed maneuvering. During cruise, the outer section is locked down and only the inside section is used for maneuvering to avoid reverse handling at high speeds (Ref. 44).

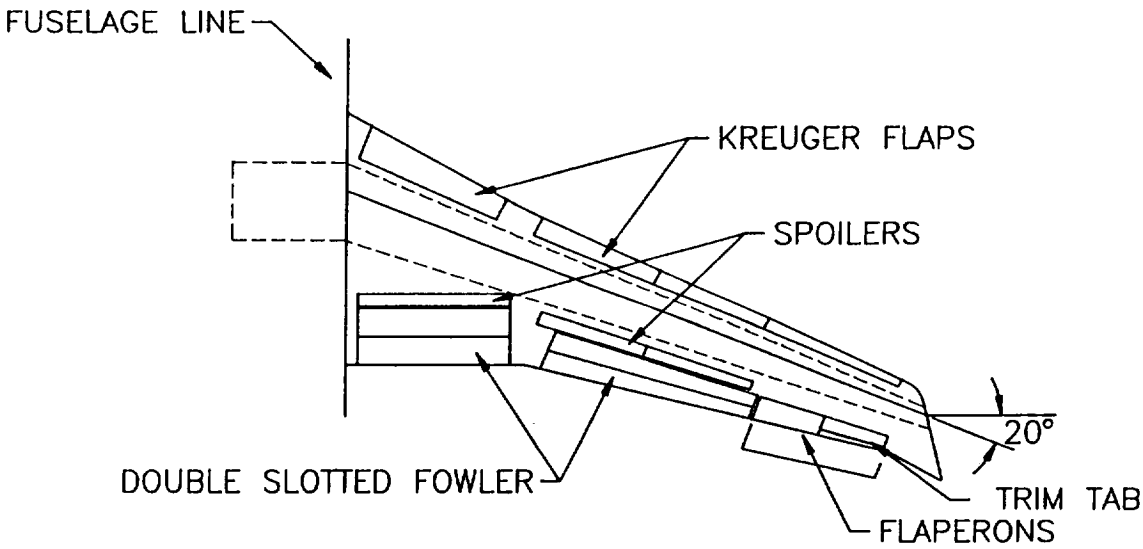

Figure 4.4 OFP-6M Wing Planform

4.3 Wing Data

Once the basic wing geometry was chosen, the airfoil data was transformed to wing data to determine if this airfoil would produce the required lift coefficients (Ref. 39). The results are presented in Figures 4.5, 4.6 and 4.7. As can be seen, the SC-9 2 meets the design point criteria of a C_L cruise of 0.58 (see Section 2.5). Also, the take off C_L of 1.9 and landing C_L of 3.1 are obtainable with high lift devices.

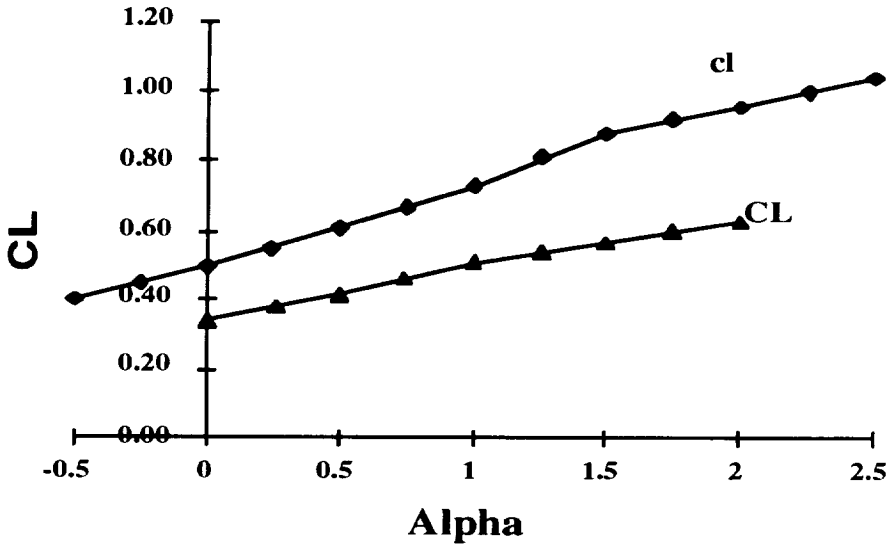

Figure 4.5 CL vs. Alpha for Wing and Airfoil Curve of OFP-6M

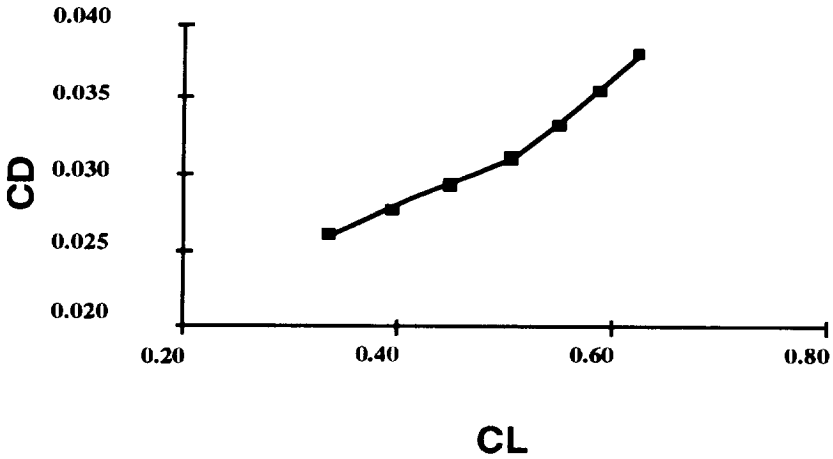

Figure 4.6 C_L vs. C_D for Wing of OFP-6M

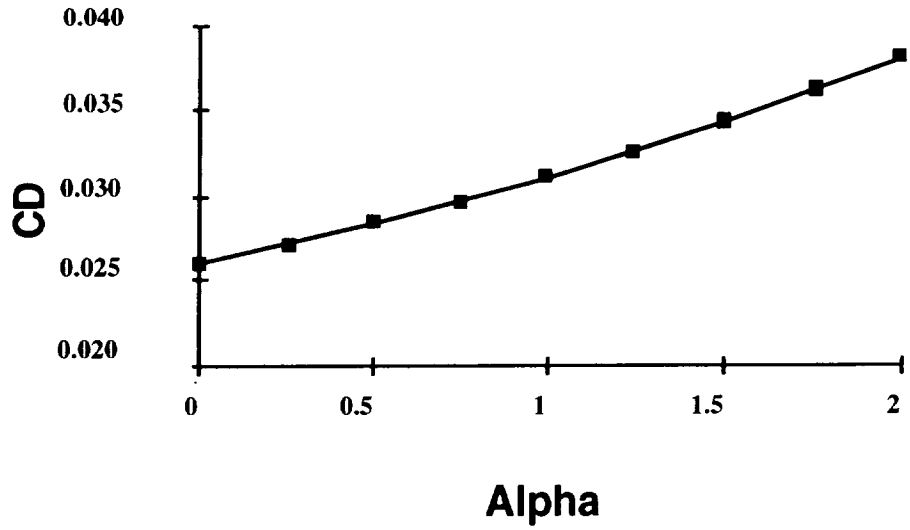

Figure 4.7 C_D vs. Alpha Curve for OFP-6M

Supercritical airfoils are designed to be the most efficient at cruise. Though the data for the SC-9 2 is limited at the moment, more research is planned to tailor the airfoil to the needs of the OFP-6M.

4.4 High Lift Devices

After careful analysis and comparisons to empirical data, the lift coefficient of 1.2 at low speeds requires a double Fowler flap with a leading edge Kreuger flap (Ref. 4, 5, 6, 7, 8, 12, 18, 25, 31). This configuration is shown in Figure 4.8. With these high lift devices, the OFP-6M reaches the required C_L of 1.9 at take off with a flap deflection angle of 10 degrees, and a C_L of 3.1 at landing with a deflection angle of 25 degrees.

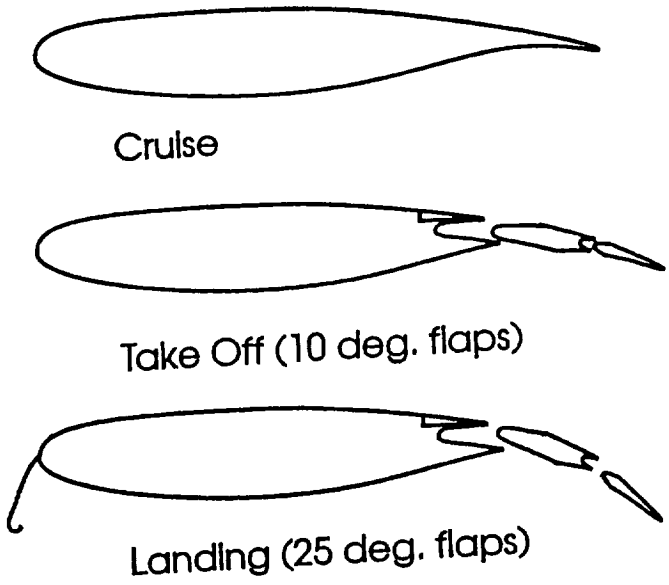

Figure 4.8 High Lift Devices for OFP-6M

This flap configuration was chosen for the simplest design possible, while still producing maximum effect and meeting the required lift necessary from the DPP. The Leading edge Kreuger flap increases lift coefficient by creating an air dam and forcing the flow up and over the wing. Kreuger flaps also have the advantage of being lighter in weight than leading edge slats (Ref. 31). The disadvantage is that they increase drag at small angles of attack. The Fowler flap extends the wing area and increases camber, thereby improving lift. Though the Fowler flap can be complicated, through careful design for manufacturing, this can be simplified and parts reduced with help from the manufacturer.

4.5 Drag Analysis

Having a large fuselage diameter, intensive analysis and design implementations were used to keep the parasite, trim and induced drag of the OFP-6M low. The results of the drag analysis are compared to other aircraft to appraise the effectiveness of the OFP-6M design.

4.5.1. Parasite Drag

Parasite drag was very important to reduce for the OFP-6M because of its large fuselage diameter. To keep this drag down the OFP-6M utilized an optimum fineness ratio, smooth exterior lines and reduced its wetted surface area. Wetted surface area from the vertical and horizontal stabilizers were reduced by using SAS in combination with a relaxed static stability (see Section 9.1).

As shown in Figure 4.9 the fuselage friction drag is a minimum at a fineness ratio of 6.0 (Ref. 35). If static stability is incorporated the optimum fineness ratio changes to 8.0 in order to increase the lever arm and decrease the tail size (Ref. 35). Since the OFP-6M was designed with negative static stability by using a SAS, the tail size is reduced and the fuselage was designed to the correct optimum finess ratio of 6.0 (Ref. 35). While the diameter of the OFP-6M is generally larger than other aircraft with the same passenger capacity, this lower fuselage drag coefficient provides a much lower drag to internal volume ratio.

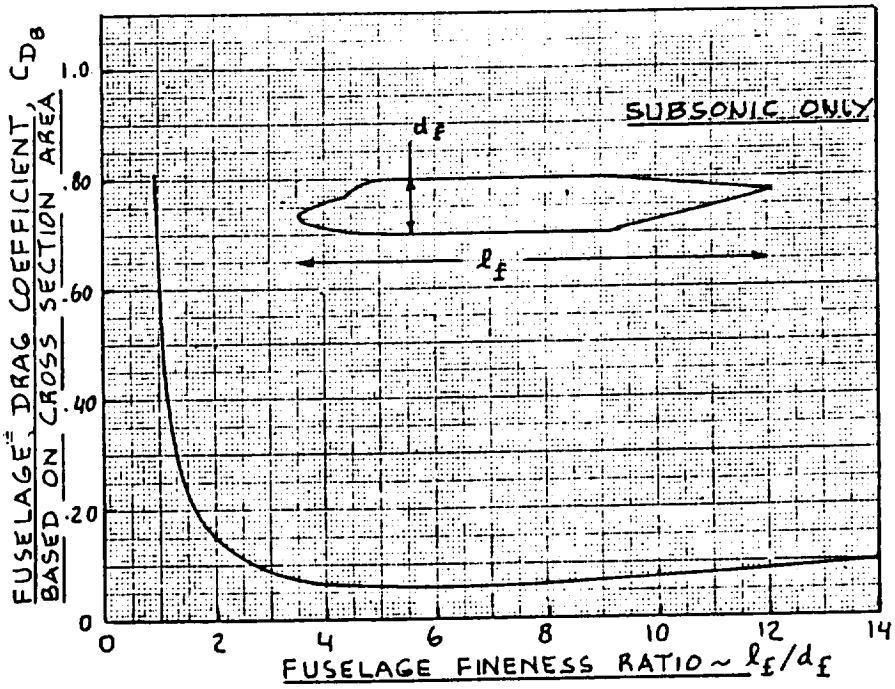

(Source: Ref. 35)

Figure 4.9 Fineness Ratio vs. OFP-6M Fuselage Drag

In order to correctly assess the parasite drag of the OFP-6M a highly accurate method of multiplying the wetted surface area by a common parasite drag coefficient was used assuming mostly attached flow (Ref. 18). To keep the flow attached the OFP-6M was designed with smooth exterior lines minimizing airflow perturbations. This same parasite drag analysis was used on similar aircraft (Ref. 18, 47). Table 4.1 shows the results from this analysis as well as a useful volume comparison estimated from basic aircraft dimensions and compared to the A320 (Ref. 47). The lower parasite drag to volume ratio shows that OFP-6M is a highly efficient design for its volume. The resulting larger fuselage diameter also creates numerous advantages for the OFP-6M passengers and cargo capabilities (see Section 3.1).

Table 4.1 Estimated Parasite Drag and Volume Comparison to the A320

Fuselage	OFP-6M	A320	737-300	MD-80
Parasite Drag	112%	100%	91%	89%
Volume	135%	100%	83%	78%
Parasite Drag / Volume	**83%**	**100%**	**110%**	**128%**

4.5.2. Induced and Trim Drag

To lower the trim and induced drag, the OFP-6M combined supercritical airfoils, a high aspect ratio, SAS, raked tips and shark fins (Ref. 35, 44). To reduce induced drag from wing tip vortices, the raked tips were sized and angled to an optimized condition for the OFP-6M (Ref. 44). These tips are easier and lighter to implement structurally than vertical winglets. These raked tips in conjunction with shark fins create more efficient wings and weaken the tip vortices. This reduces the separation required for smaller aircraft on landing or take-off (Ref. 44). The operational benefits in using these components were determined well worth the production costs.

4.5.3. Total Drag Polars

Using the drag analysis above, the total drag polars were determined. Figure 4.10 gives the total drag polars for Mach values at and around the OFP-6M's cruise Mach of 0.80 (Ref. 17). They show that the OFP-6M is most efficient when cruising at its lowest drag polar, which corresponds to Mach 0.80.

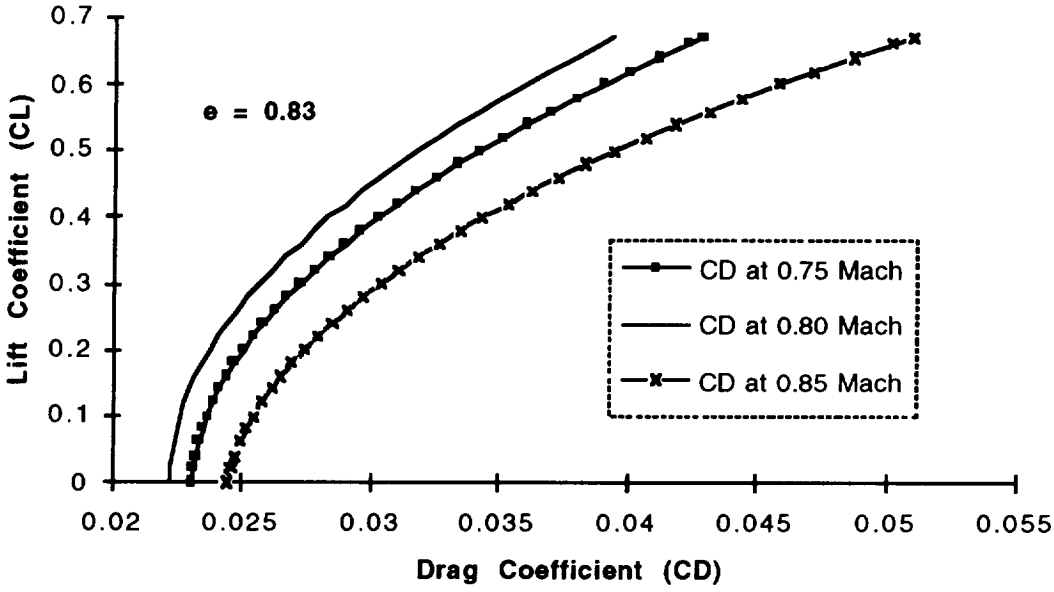

Figure 4.10 OFP-6M Total Drag Polars

Figure 4.11 shows how the OFP-6M compares with its total drag polars during cruise conditions with other aircraft (Ref. 47). This shows that the OFP-6M has a larger drag coefficient at a given lift coefficient than other aircraft close to its passenger capacity. However, as shown previously in Table 4.1, the configuration of the OFP-6M yields greater volume per drag point, in addition to other benefits such as passenger comfort and reduced c.g. travel.

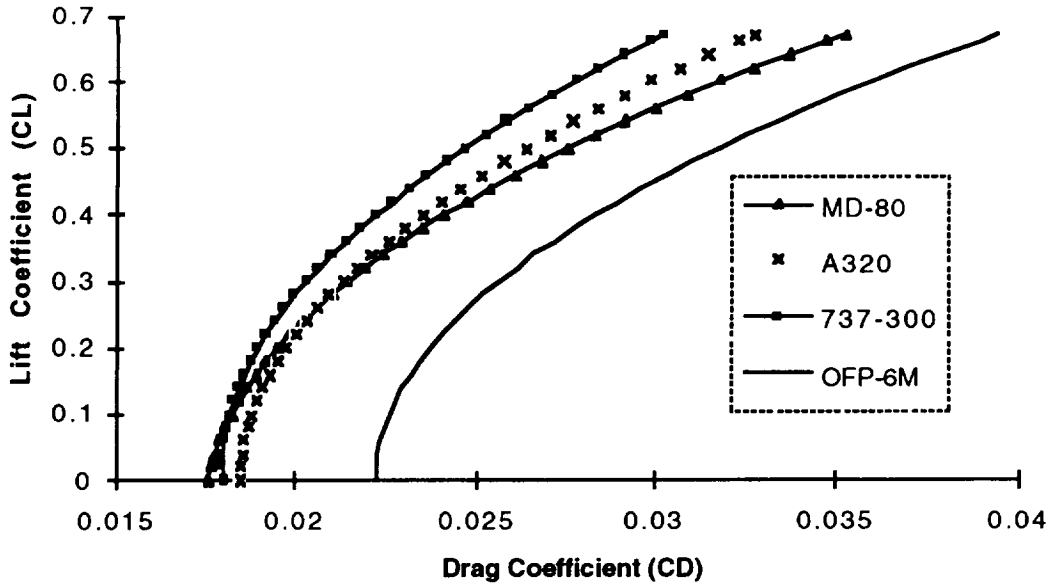

(Source: see Section 4.5.1 and Ref. 47)

Figure 4.11 OFP-6M Total Drag Polars and Competition Estimation

4.5.4. Total Drag Build-Up

The total drag build-up is important to confirm the optimum cruising speed and to find the dive limitation of the aircraft (Ref. 17). In Figure 4.12 the total drag build-up for the OFP-6M is shown. The sharp drag rise at about Mach 0.88 provides sufficient resistance to acceleration to keep the OFP-6M from obtaining damaging speeds in a twenty degree dive at full power (Ref. 17). Also, the total drag is at a minimum at Mach of 0.80, which confirms the optimum cruising speed of the OFP-6M (see Section 6.7).

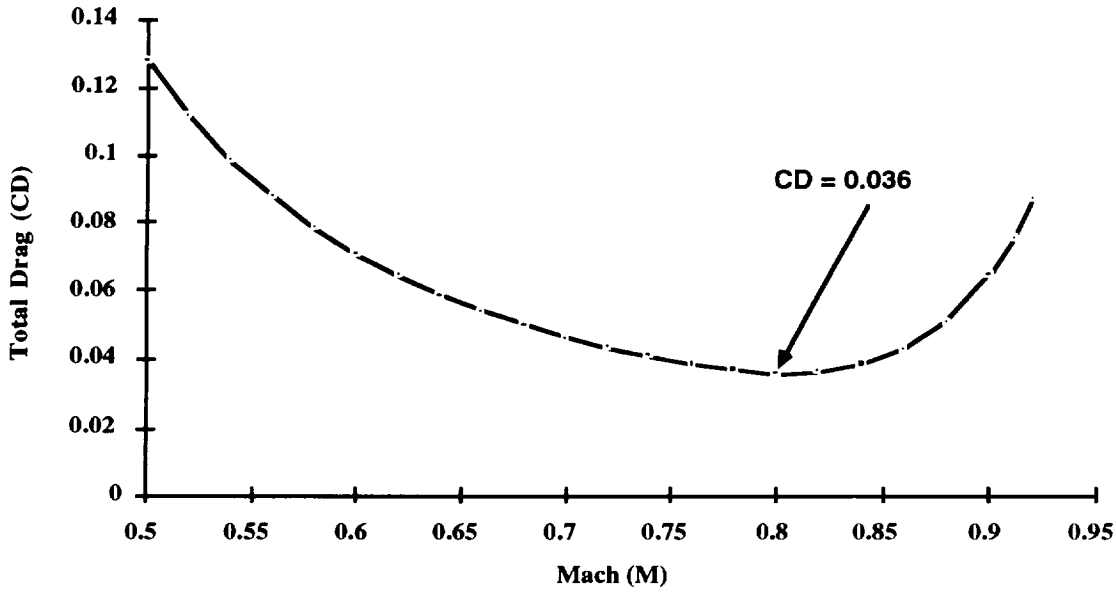

Figure 4.12 OFP-6M Total Drag Build-Up

4.6 Fuselage Justification

The fuselage shape was determined mostly by the interior configuration. Once it was decided to consider the twin aisle, it was a matter of fitting the exterior around the interior and analyzing the drag penalties to make sure this was a viable solution. As the Mach of the aircraft increases the induced drag decreases. This is due to the lower CL_{max} that is obtained at higher speeds which is directly proportional to the square root of the induced drag. The OFP-6M does not pay a drag penalty for its shape (Section 4.5 and Ref. 17, 18, 35). The optimum finess ratio with a SAS in operation is 6:1 (see Section 4.5.1). Also, the large diameter, allows the landing gear inside the fuselage during flight without local fairing, thus reducing drag. The wing was placed near the middle of the fuselage, underneath the floor, reducing drag (refer to Section 9). The nose was determined by empirical data for the most aerodynamic shape and the tail was

determined by rotation angle (refer to Section 9). It was determined that the large fuselage had many benefits and would set the OFP-6M apart from its competition.

4.7 Empennage Geometry

The horizontal tail uses the same supercritical airfoil section as the wing with double slotted elevators and a maximum lift coefficient of 2.5. The area of the horizontal tail area was determined to be 200 ft^2 and the elevator area was determined to be 76 ft^2. Horizontal tail geometry is shown in Figure 4.13.

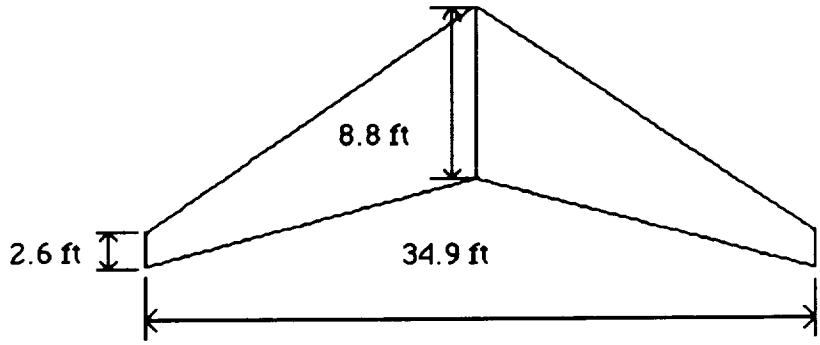

Area	200 ft^2	Taper Ratio	0.3
Airfoil Type	Supercritical	Span	34.9 ft
Λ at 0.4c	25°	Average Chord	5.73 ft
Aspect Ratio	6.1	Elevator Area	76 ft^2

Figure 4.13 Horizontal Tail Geometry for OFP-6M

The vertical tail is a conventional symmetrical airfoil with a maximum lift coefficient of approximately 2.0. With 20% maneuverability during the OEI condition, the required vertical tail area was calculated to be 319 ft^2. Additionally , the rudder area was determined to be 131 ft^2. Vertical tail geometry is shown in Figure 4.14 .

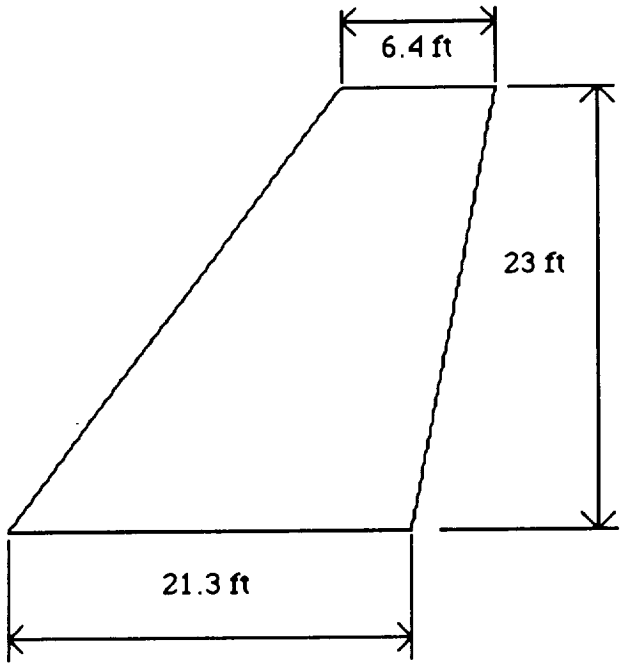

Area	319 ft^2	Taper Ratio	0.3
Λ at 0.4c	30°	Average Chord	13.8 ft
Aspect Ratio	2.0	Span	23.0 ft
Airfoil Type	Conventional Symmetrical	Rudder Area	131 ft^2

Figure 4.14 Vertical Tail Geometry for OFP-6M

5 Propulsion

5.1 Engine Selection

From the outset of the analysis toward fulfilling the mission requirements for the OFP-6M, it has been evident that minimizing the SFC at cruise conditions was crucial. With the 3,000 nautical mile cruise segment, the SFC has an extreme impact on the weight sizing of the structure and on the fuel required. The first engines considered for integration on the OFP-6M were the industry standards in high-bypass turbofans in the 30,000 lbf thrust class: the CFM-56 and V-2500, produced by CFM International and International Aero Engines, respectively. These engines were used to provide baseline values for thrust and fuel consumption. A generic turbofan engine deck provided by AIAA was scaled to estimate performance envelopes according to altitude and Mach number for the engine concept implemented on the OFP-6M, the Pratt and Whitney Advanced Ducted Prop (ADP).

Because of the dominance of SFC on the weight of the airframe and the fuel required to meet the RFP, the more sophisticated ADP engine option has been implemented based on future projections of engine trends in configuration and performance. As shown in Figure 5.1, SFC has been steadily improving over time. Another significant step will be in place by the year 2000 as engines with much higher bypass ratios come into service. For the purpose of analysis, the SFC of the engines on the OFP-6M was chosen to reflect a 10% improvement over the V-2500, which currently has the best fuel efficiency in its thrust class. As indicated by Figure 5.1, this is actually a conservative estimate.

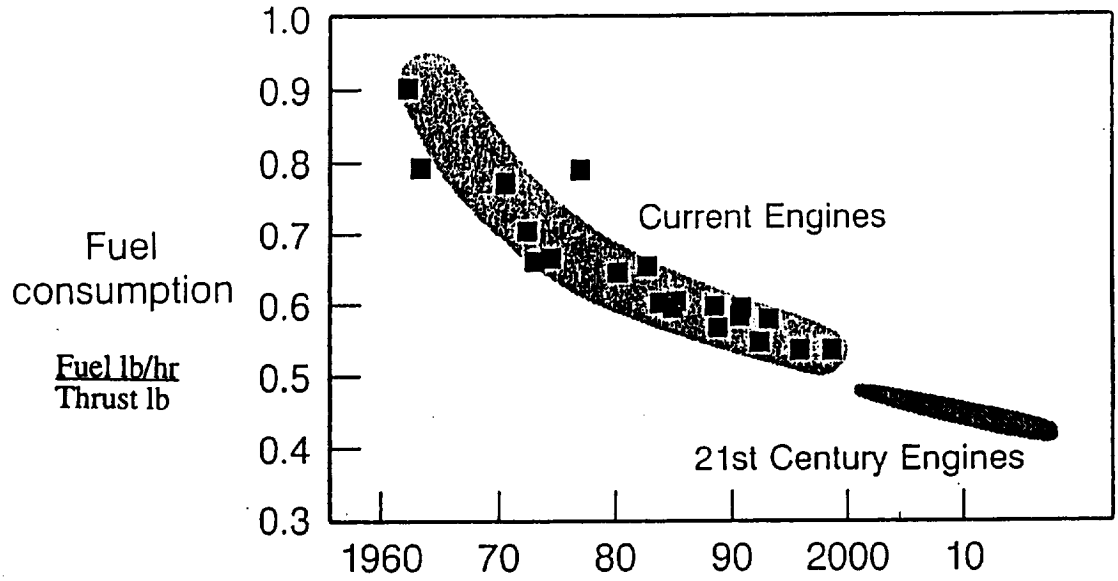

(Source: Ref. 14)

Figure 5.1 OFP-6M Historical Trends of Specific Fuel Consumption

Critical technologies which have contributed to the improved efficiencies include advanced materials such as superior alloys and ceramics to withstand higher turbine temperatures, and composite blades for large, high-bypass fans. Engine efficiencies have also been improving with the implementation of Full-Authority Digital Engine Controls (FADEC), which optimize performance for the current flight condition, and active clearance control to minimize leakage around the ends of the spinning blades. As shown in Figure 5.2, although the higher bypass engines yield decreasing specific thrust through increasing proportions of slower cold flow, the new engines are achieving higher thermal and overall efficiencies for lower fuel consumption.

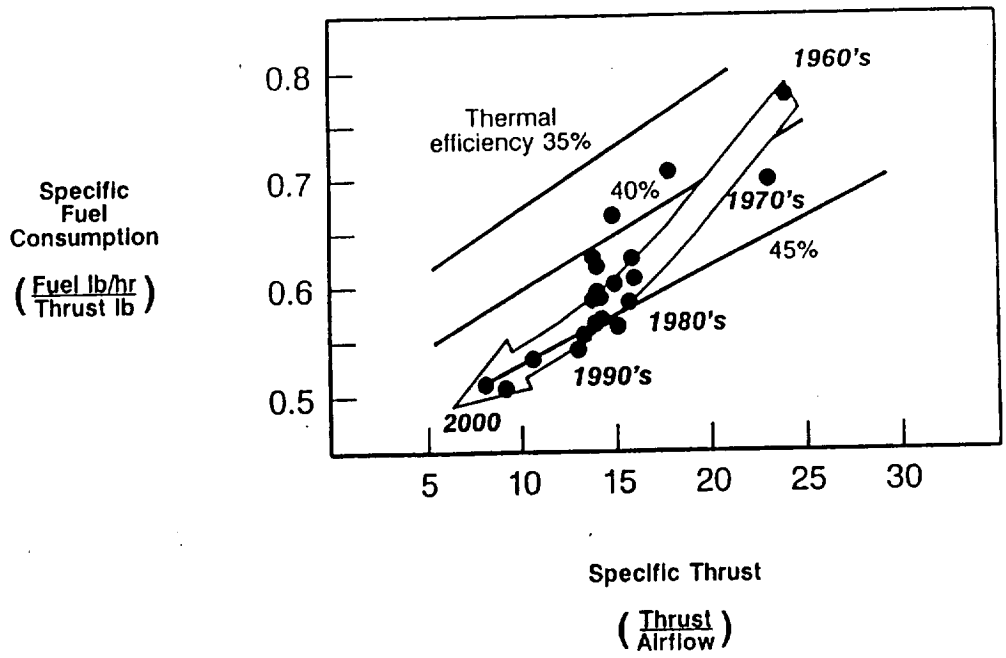

(Source: Ref. 14)

Figure 5.2 Trends in Thermal and Propulsive Efficiencies for OFP-6M

Another advantage of the higher bypass-ratio engines is lower noise emissions, as shown in Figure 5.3. The larger mass of airflow exits the engine at a slower velocity than in a turbojet or low-bypass engine, which reduces the noise producing shear forces between the exit flow and the free stream air. The quieting effects can be further enhanced by mixing the hot and cold flows within the engine nacelle. As noise restrictions continue to become more strict, it is crucial to implement quiet engines to power future aircraft.

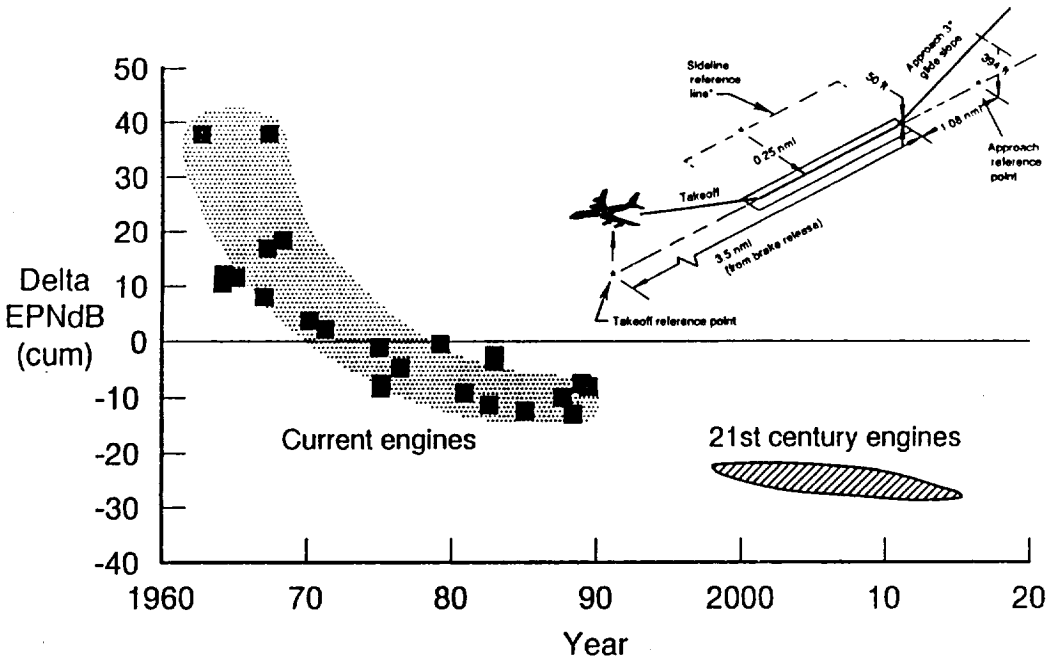

(Source: Ref. 14)

Figure 5.3 Historical Trends of Noise Emissions for OFP-6M

Therefore, in order to minimize fuel consumption and noise emissions, the OFP-6M will utilize a turbofan with a bypass-ratio on the order of 10, and implement an internal flow mixing nacelle. One concept for achieving a Bypass Ratio (BPR) up to 10 or 15 is the Rolls-Royce counter-rotating aft ducted fan, shown in Figure 5.4. This configuration has the advantage of simplicity, in that the fans are driven directly by the low pressure turbine blades with no gearbox or concentric drive shaft running the length of the engine. By spinning the fans in opposite directions, swirl energy is removed from the flow and converted to thrust. However, while Rolls-Royce may push the concept to production in order to engine a fleet of 800 OFP-6M's, there are no current indications that the engine will be in operation by the year 2000.

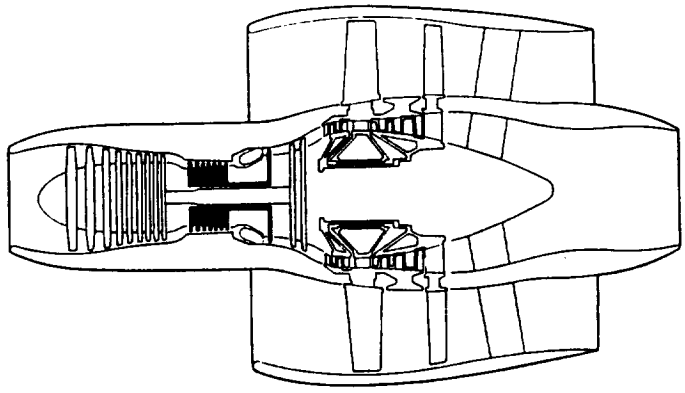

(Source: Ref. 30)

Figure 5.4 Rolls-Royce Counter-Rotating Aft Ducted Fan for OFP-6M

The Pratt and Whitney ADP is a high bypass engine option that will soon be entering service in a higher thrust class, with plans to produce smaller versions in the near future. As shown in Figure 5.5, the Pratt and Whitney ADP utilizes existing engine cores to drive a large, variable-pitch fan through a gearbox that allows the turbine and fan to run at different speeds for better efficiency.

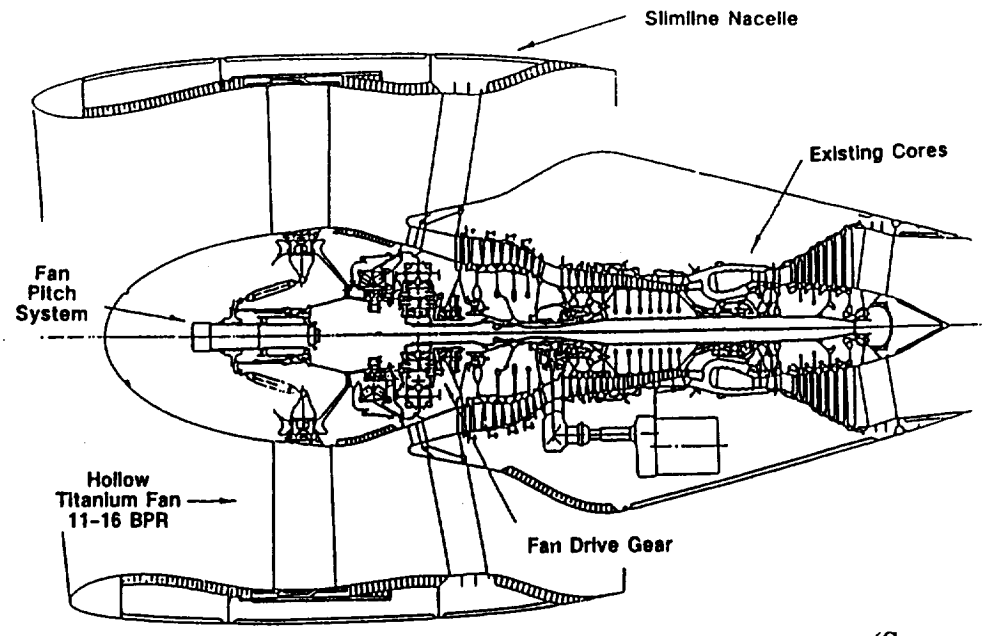

(Source: Ref. 14)

Figure 5.5 Pratt and Whitney Advanced Ducted Prop for OFP-6M

The increased weight and maintenance costs of the gearing system will offset some of the gains achieved by this concept, but the conservative estimate of a 10% improvement in SFC reduced the OFP-6M's weight by thousands of pounds of structure and fuel necessary for its intended mission.

In conclusion, fuel efficiency and engine availability were the two factors driving power plant selection for the OFP-6M. The future trends for improvements in SFC are due in part to advances in materials, blade design, and integrated engine control, but most of the savings come from higher BPRs. Until the noise and vibration fatigue problems are solved on the unducted fan concept, turbofans or ducted propfan engines will continue to power transport aircraft. The Rolls-Royce aft-ducted fan is mechanically the simplest design for achieving high BPRs, and most likely the least expensive to maintain, but there is no indication that the engine will be ready for production by the year 2000. Therefore,

the geared turbofan concept, pioneered by Pratt and Whitney and near entry into service, is the engine design of choice for the OFP-6M.

5.2 Engine Integration

The engine that has been selected for the OFP-6M, a high-bypass geared turbofan with a BPR of 10, is shown integrated with the wing, nacelle, and pylon in Figure 5.6.

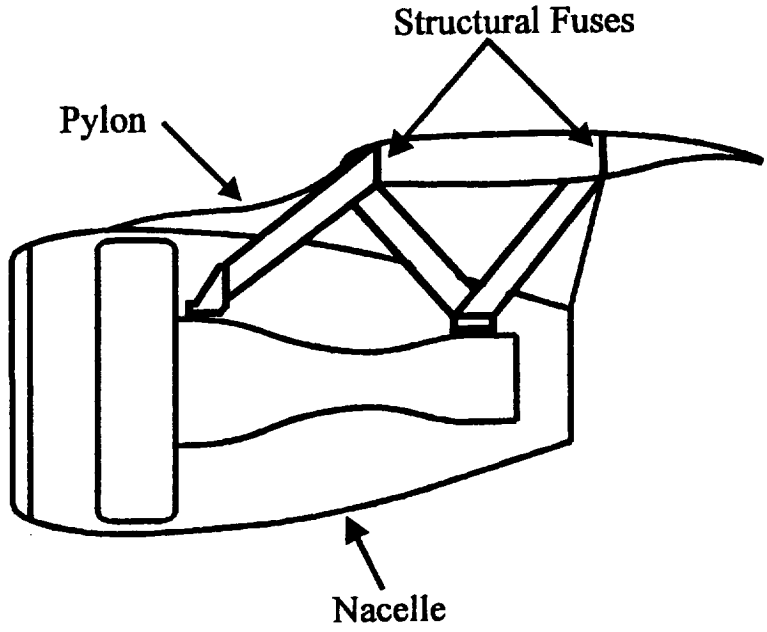

Figure 5.6 High Bypass ADP Integrated with OFP-6M

The large size of the engine relative to the wing section where it is attached creates a structural challenge, a problem which is solved by using a composite truss mated to the wing spars. The wing spars have been strengthened both in the vicinity of and inboard of the engine. To facilitate engine break-away in an emergency, structural fuse pins are incorporated in the fittings where the support truss joins the wing spars.

The leading edge of the nacelle incorporates an electric anti-ice system rather than a pneumatic de-icing system to avoid FOD to the engine by ice ingestion. As shown in Figure 5.7, the inlet, nacelle, and core housing all incorporate noise absorbing materials to quiet engine noise. The nacelle also extends past the turbine nozzle to mix the hot and cold flows internally for lower discharge noise emissions.

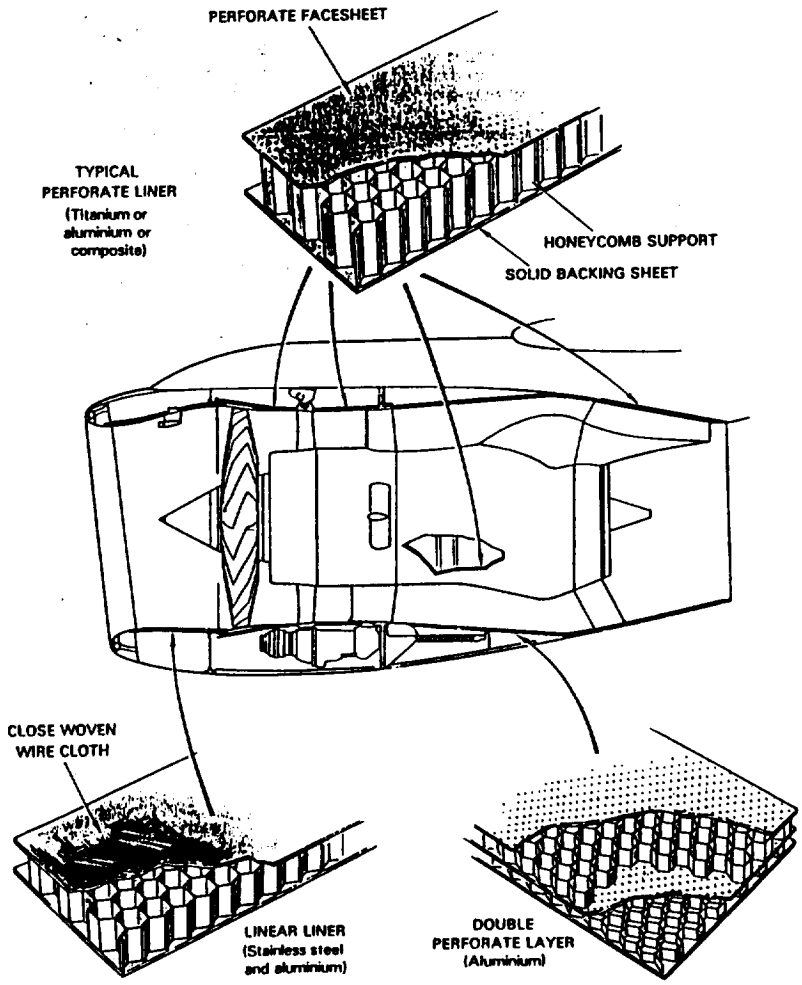

(Source: Ref. 15)

Figure 5.7 Noise Absorbing Materials Within the OFP-6M Nacelle

6 Performance

6.1 Rate of Climb

The true airspeed for an aircraft's best rate of climb varies with altitude, and has been shown in practice to be very close to a constant calibrated airspeed (Ref 15). Assuming no instrument or static port position errors, the airspeed indicator shows calibrated airspeed. The flight control computer could be programmed to follow a more complex climb profile to further optimize for minimum time or fuel consumed as a function of ambient conditions and winds aloft, but for simplified analysis and to simulate a task that could be carried out easily by an unaided pilot, the constant indicated airspeed was utilized. This airspeed schedule is usually followed up to the initial cruise Mach number (Ref. 15).

The rates of climb for the OFP-6M at maximum power, starting at maximum gross takeoff weight, are shown in Figure 6.1. As shown in Figures 6.2 and 6.3, the minimum time and fuel required to climb to cruise altitude are achieved at 242 KCAS, which will place the aircraft at Mach 0.8 at 38,000 ft.

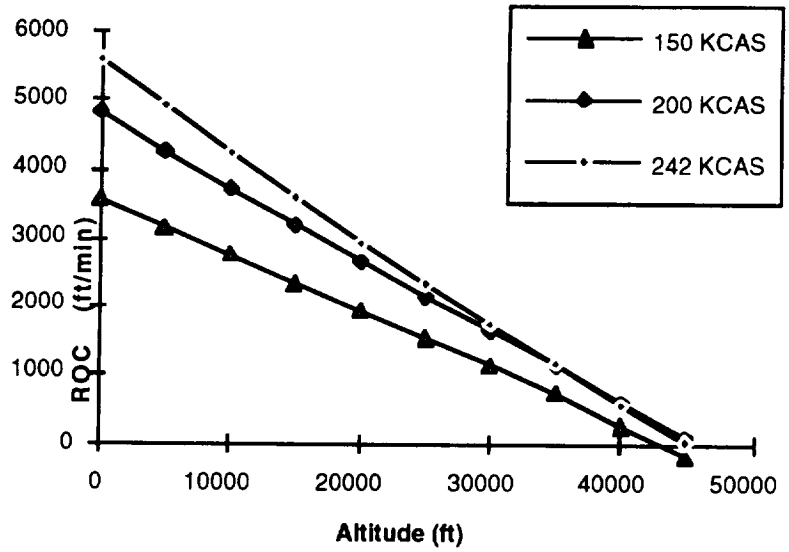

Figure 6.1 Maximum Rate of Climb for the OFP-6M

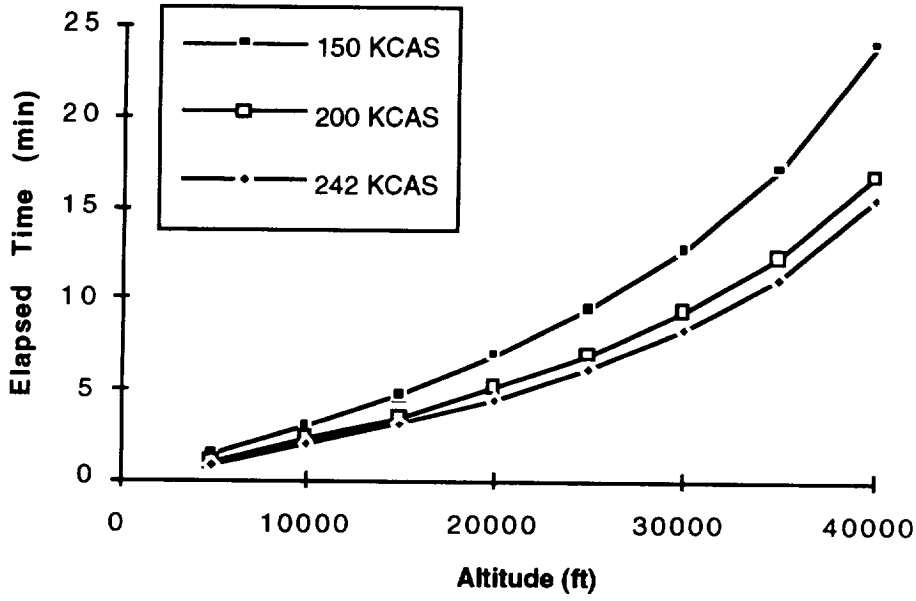

Figure 6.2 Time to Climb for the OFP-6M

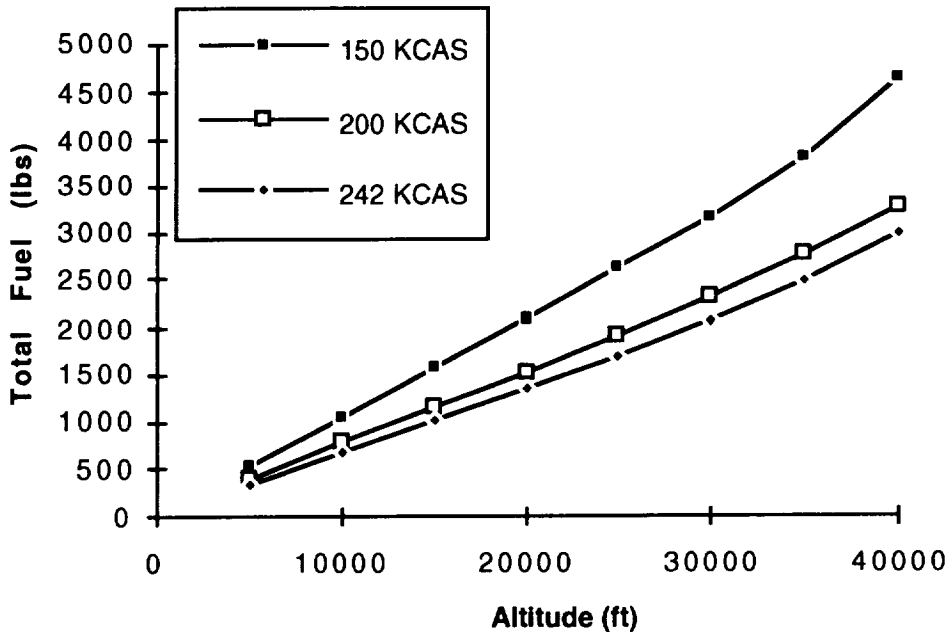

Figure 6.3 Fuel Required to Climb for the OFP-6M

The results of the previous analysis for time and fuel required to climb to cruise altitude are shown in Table 6.1. The conclusion is that the most efficient climb at constant calibrated airspeed occurs at 242 KCAS. This is below the FAA imposed maximum speed of 250 kts below 10,000 ft, and will result in the aircraft arriving at cruise altitude at cruise Mach.

Table 6.1 Time and Fuel to Climb to Cruise Altitude for OFP-6M

Airspeed (KCAS)	Time (min)	Fuel (lb)
150	21	4,300
200	15	3,100
242	14	2,800

6.2 Takeoff and Landing Distance

The OFP-6M's wing loading, maximum lift coefficient in takeoff configuration, and thrust-to-weight ratio were chosen to meet the 7,000 ft balanced field length required by the RFP (Ref. 31). The definition of this field length is shown in Figure 6.4, in which the total distance from brake release to 35 ft of altitude, with an engine failure just before rotation speed, is the same as the distance from brake release to stopping the aborted takeoff, with the engine failure at the same speed.

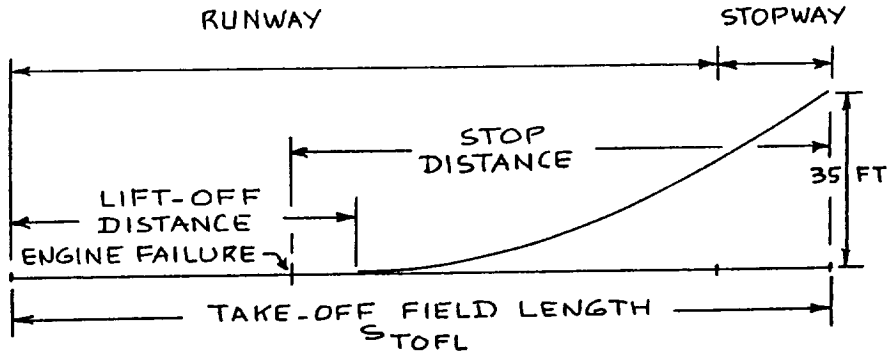

(Source: Ref. 31)

Figure 6.4 Definition of FAR 25 Balanced Field Length for OFP-6M

The maximum lift coefficient in the landing configuration allows an approach speed that is slow enough to meet the landing distance requirement of 5,000 ft set forth by the RFP without the use of thrust reversers (Ref. 31). The definition of landing distance, in accordance with FAR 25, is shown in Figure 6.5. The approach speed, obstacle height, and safety factor are included in this figure.

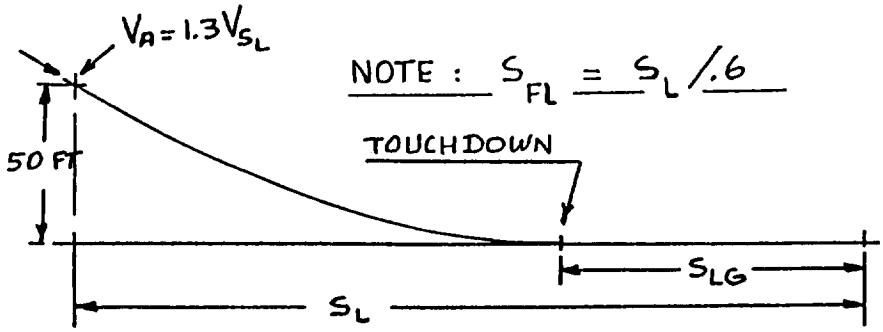

(Source: Ref. 31)

Figure 6.5 Definition of FAR 25 Landing Length for OFP-6M

To improve the OFP-6M's operational landing ground roll, especially on wet or icy runways, cascade thrust reversers are implemented in the cold flow, as shown in Figure 6.6. Cascade reversers were chosen because they are the quietest and best suited for high bypass turbofan engines. In this configuration, high pressure bleed air is used to actuate doors that block the bypass flow from its normal passage, and divert it outward through cascade vanes. The vanes turn the flow forward, generating thrust that will slow the aircraft faster than using the brakes alone. The thrust reversers also reduce the load on the brakes, extending their life and reducing maintenance costs.

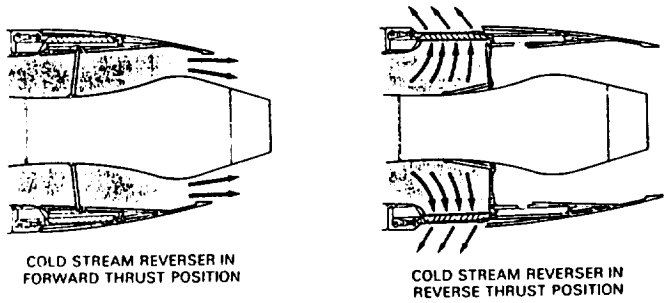

(Source: Ref. 30)

Figure 6.6 Cascade Thrust Reversers on the OFP-6M

6.3 Installed Thrust

The engine data provided by AIAA for the design competition does not account for installation losses due to bleed air and electric power extraction. The uninstalled thrust rating of the engines for the OFP-6M are therefore based on 103% of the thrust required to account for the installation losses (Ref. 33).

6.4 Completion of RFP Requirements

The OFP-6M is unequaled in its combination of takeoff and landing field performance, cruise speed, range, and passenger comfort. As shown in Table 6.2, the OFP-6M meets all of the requirements put forth by the RFP, a claim which none of the competitors can make.

Table 6.2 OFP-6M Completion of RFP Requirements

Requirement	OFP-6M	737	MD-90	A320
Take off within FAA field length of 7,000 ft	X			
Climb at best rate of climb	X	X	X	X
Cruise at .99 Vbr for 3,000 nm (M > 0.7)	X			
Land, with domestic fuel reserves, within FAA field length of 5,000 ft	X			
Passenger capacity--mixed class, 153	X	X	X	X
Meet proposed noise regulations	X			
Overhead storage space provided	X	X	X	X
Front and rear galleys required	X	X	X	

6.5 Accessories

By implementing electrohydrostatic actuators for the flight controls and landing gear, each actuator has its own electric hydraulic pump and pressure accumulator. In this configuration, the need for a centralized hydraulic system is eliminated (see Section 11).

Therefore, large hydraulic pumps are not needed on the OFP-6M's engines. The power generation task is achieved with engine-driven electric generators, and the pneumatic system is fed with bleed air from the low pressure and high pressure compressor stages. The power required by these systems accounts for a 3% decrease in thrust (Ref. 33).

6.6 Engine Performance and Analysis

The engine performance data provided by AIAA for the design competition is representative of a generic modern technology, separated flow, high BPR (BPR=6) turbofan engine in the 25,000 lbf thrust class. This data was scaled for thrust and SFC values indicative of the engine installed on the OFP-6M. The results of the design point analysis for the OFP-6M mission profile required an installed thrust-to-weight ratio of 0.3 at sea level and maximum gross takeoff weight, which corresponds to 22,300 lb of thrust per engine. This value is increased by 3%, to account for bleed air and power generation, to 23,000 lb per engine. The SFC values were scaled to reflect a 10% improvement over the IAE V-2500 turbofan engine at cruise conditions (see Section 5). The fuel consumption and thrust performance of the OFP-6M's engines, as functions of altitude and Mach number, are shown in Figures 6.7 and 6.8, respectively.

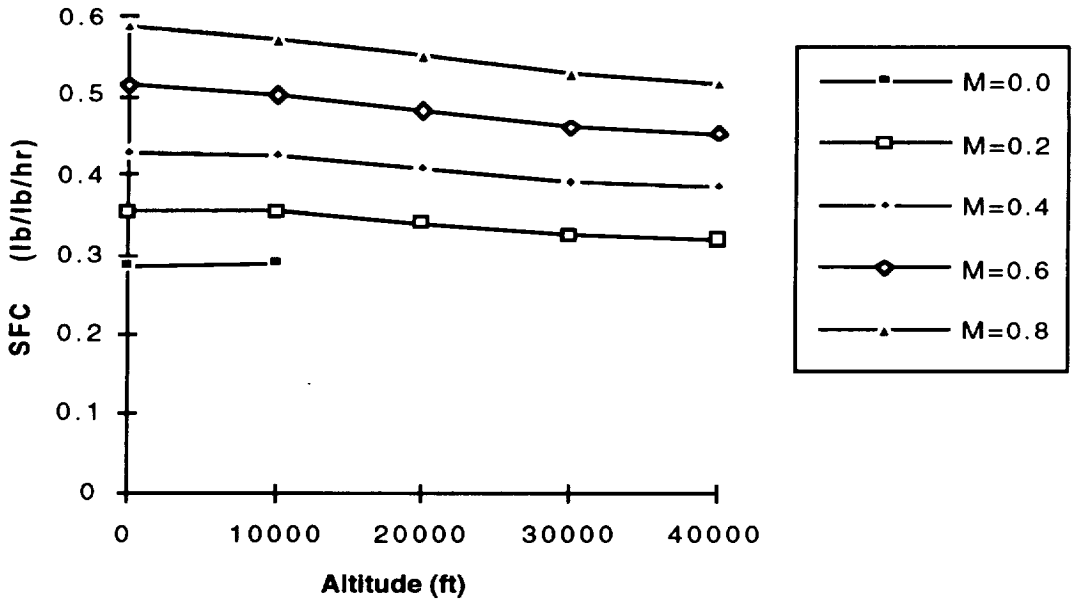

Figure 6.7 SFC vs. Altitude and Mach at Cruise Power for the OFP-6M

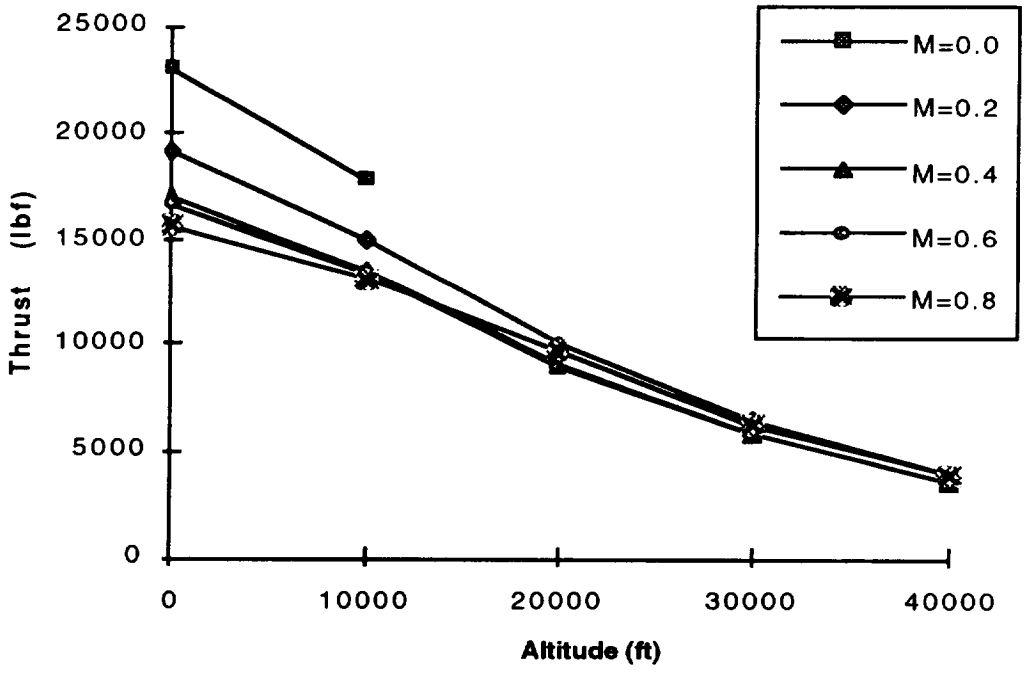

Figure 6.8 Thrust vs. Altitude and Mach (Per Engine) for the OFP-6M

6.7 Velocity for Best Range

The velocity for best range is shown in Figure 6.9. The velocity for best range is where the Mach number corresponds to a maximum of (Cl)^0.5/Cd (Ref. 17). For each discrete value of Mach from 0.5 to 0.94 numerous calculations were made to find (Cl)^0.5/Cd. This is due to the numerous Mach dependent values and required reiterative processes which affect the (Cl)^0.5/Cd value. Using a macro in the DPP for these operations, the best velocity for range was found to be just above 0.8 Mach.

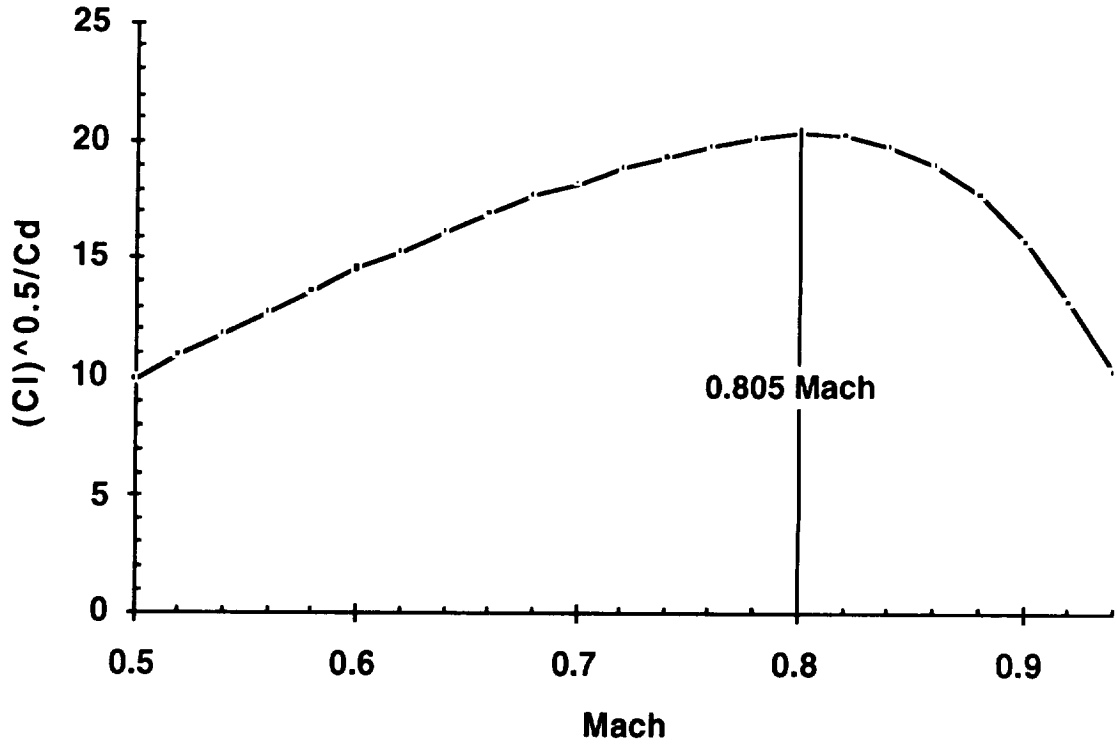

Figure 6.9 OFP-6M Velocity for Best Range

6.8 Payload-Range Diagram

In Figure 6.10 the payload-range diagram shows the OFP-6M capabilities with respect to range and payload (Ref. 17). This aircraft is designed to carry 153 passengers 3000 nm. With the fuel tanks completely filled, the aircraft can reach a range of over 3420 nm holding 133 passengers and their baggage. The ferrying range of about 3850 nm is not much more than what the aircraft is designed for since it has been optimized for that mission. The fuel tanks, which are completely contained in the wings, are 90% full when the OFP-6M is to fly a full load at its designed range of 3000 nm.

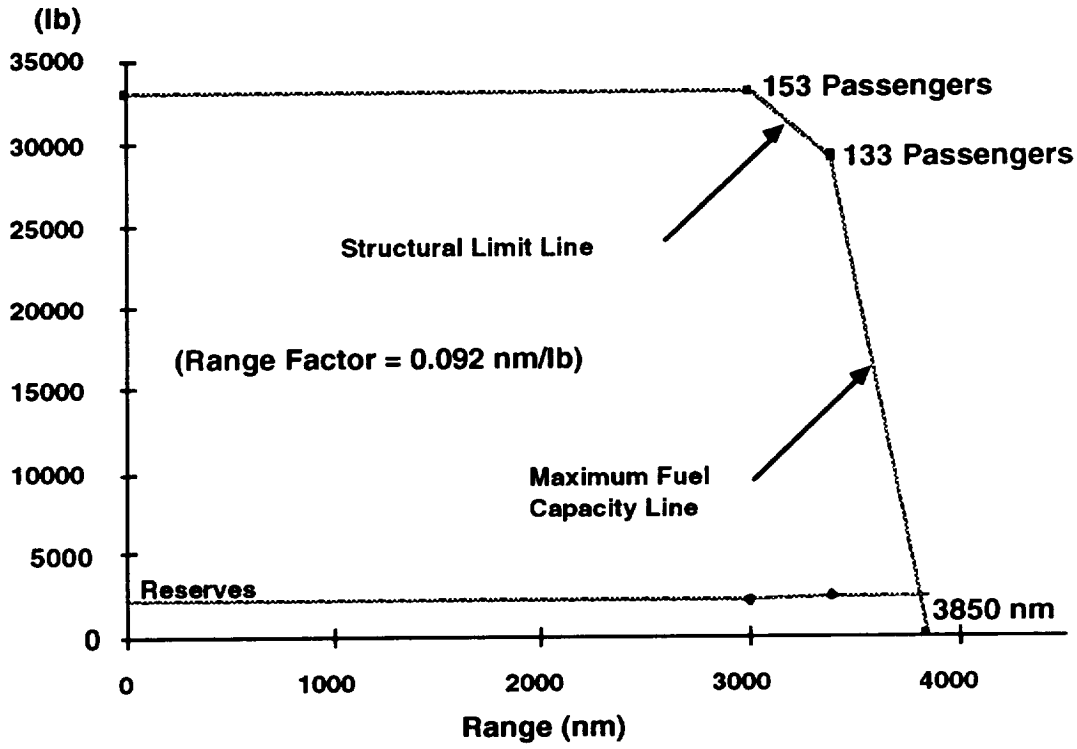

Figure 6.10 OFP-6M Payload-Range Diagram

7 Structures and Materials

7.1 V-n Diagram

The V-n diagrams are shown in Figures 7.1 and 7.2. Figure 7.1 shows that the OFP-6M is not gust sensitive when it is operating under cruise conditions. The OFP-6M is able to operate at a maximum load factor of 2.5 g's. The OFP-6M has a cruise speed of 250 KEAS, dive speed of 275 KEAS, and a stall speed 140 KEAS.

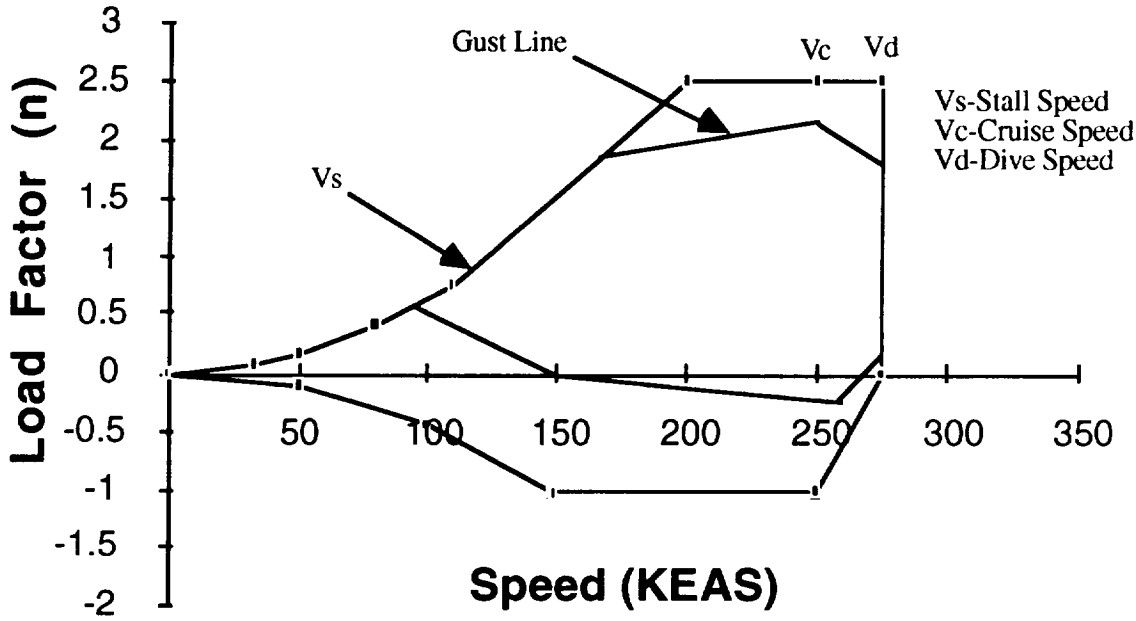

Figure 7.1 OFP-6M V-n diagram for Cruise

From Figure 7.2, the OFP-6M is gust sensitive under landing conditions. As seen on Figure 7.2, the gust line first becomes greater than the structural limit line at about 170

KEAS which is much faster than the landing speed. Thus, the OFP-6M is safe to operate at a load factor of 2.5 g's under landing conditions.

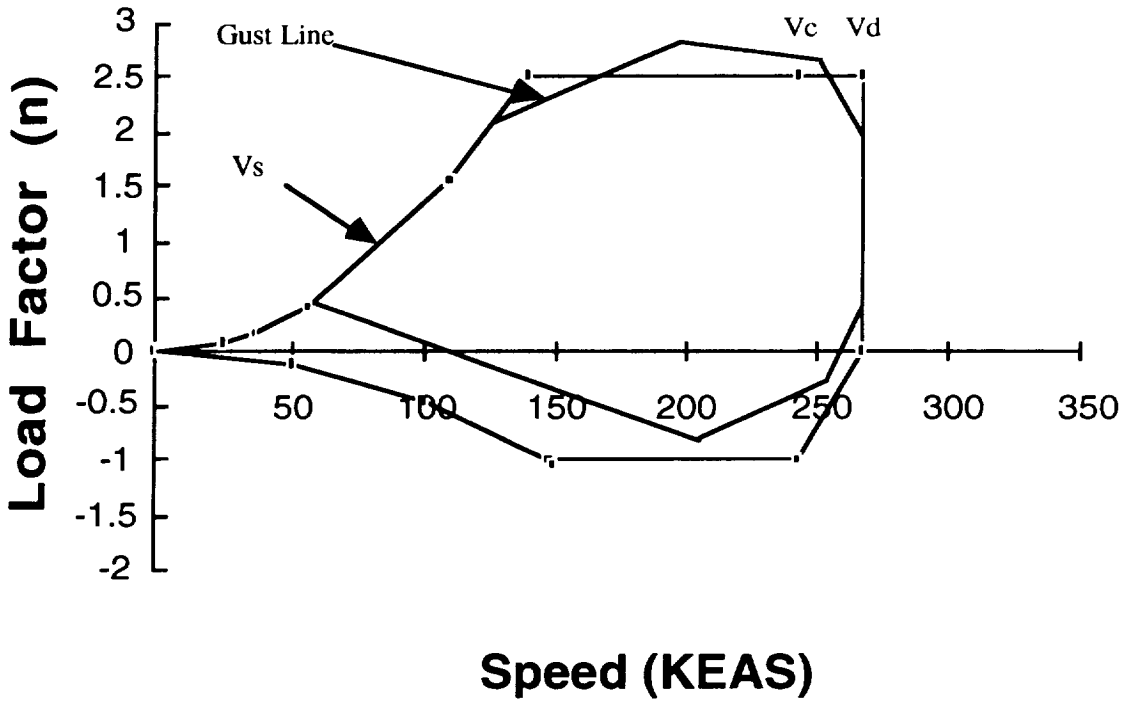

Figure 7.2 OFP-6M V-n Diagram for Landing

7.2 Material Selection

The materials used most in the aircraft are Graphite-Epoxy composites and 2024 aluminum. Graphite Epoxy is a matrix composite which has been used in the defense industry for two decades and becoming more popular on commercial aircraft. Aluminum has been used on aircraft since the 1930's. Aluminum such as T-2024 gives an aircraft the needed strength and stiffness with the benefit of low weight (Ref. 14).

The main wing, horizontal and vertical tail are made from composite materials. This was chosen to save weight. These structures have composite spars, ribs, and skins as shown in Figure 7.3. This was chosen to keep the continuity of the wing structure,

since there is no connection of composite and metals in the wing structure. Also, composite material is resistant to corrosion, fatigue, and does not lose its strength when it is subjected to high temperature.

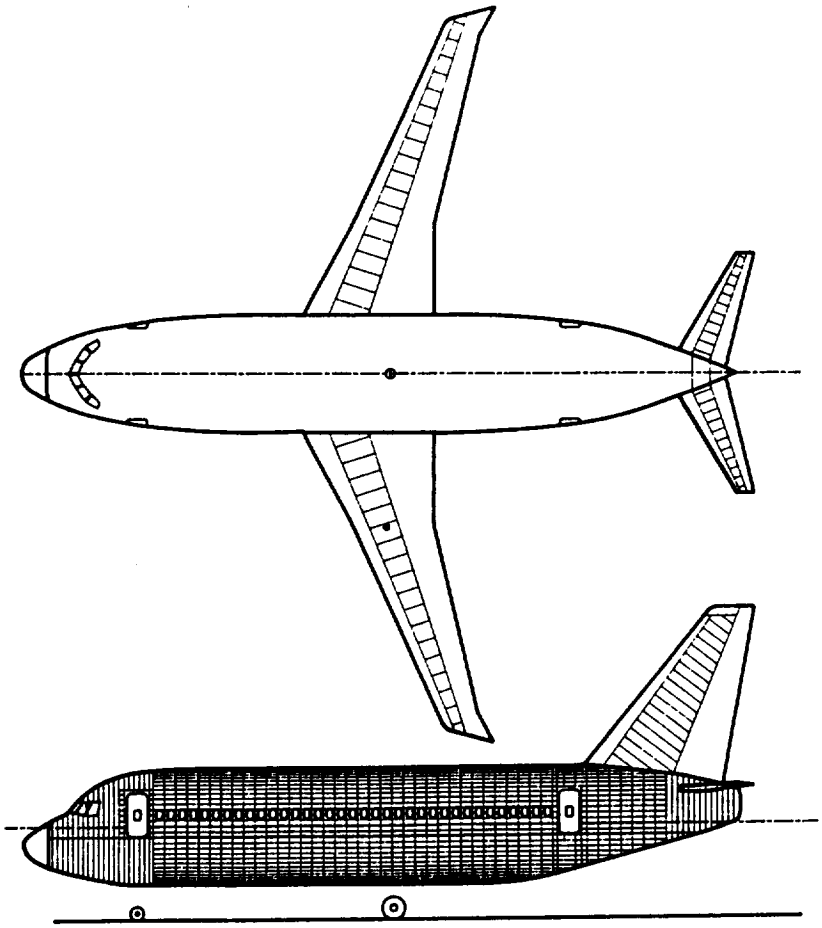

Figure 7.3 OFP-6M Structural Drawing

The flaps, control surfaces, landing gear doors, and access doors are made of composite materials since they are not subjected to forces and situations in which they can be damaged, and if they are damaged they are easily and quickly replaced.

The landing gear was designed like all other conventional landing gear. Steel was used for the landing gear because it is strong enough to carry the high stresses which are put on them during a landing sequence. Since the landing gear is large and needs to be strong, no other materials are capable and/or economical to use.

The radome dome at the front of the aircraft is made of fiberglass since fiberglass will let radio waves through. This part of the aircraft carries no structural loads, and fiberglass is easily repaired if damaged.

The fuselage utilizes aluminum for the stringers, ribs, and skin and uses composite materials for the floor boards.

7.3 Structure and Layout

The main wing was laid out using proven techniques and methods. There are two main spars going through the main wing which construct the main structure of the wing box. These spars are two composite C beams facing each other. The two beams were used to make the fuel capacity maximum, and C beams were used because making C beams out of composite is the most simple process to make a composite beam (Ref. 13). Also, the C beam gives the necessary stiffness to support the wing forces. The forces at the wing-fuselage connection under cruise conditions are in Table 7.1.

Table 7.1 OFP-6M Forces at Wing-Fuselage Connection for Cruise

Shear due to lift	56,500 lb
Shear due to drag	2,200 lb
Moment about X	1,024,800 ft-lb
Moment about Y	292,600 ft-lb
Moment about Z	17,100 ft-lb

In sizing the wing box a factor of 2.5 g forces and a safety factor of 1.1 were implemented. The horizontal and vertical tail uses two main spars with an additional spar for connection of the control surfaces. The horizontal tail is constructed similar to the main wing. A maneuvering pin is connected to the wing to trim the horizontal tail during flight. Figure 7.4 shows the OFP-6M wing box and dimensions.

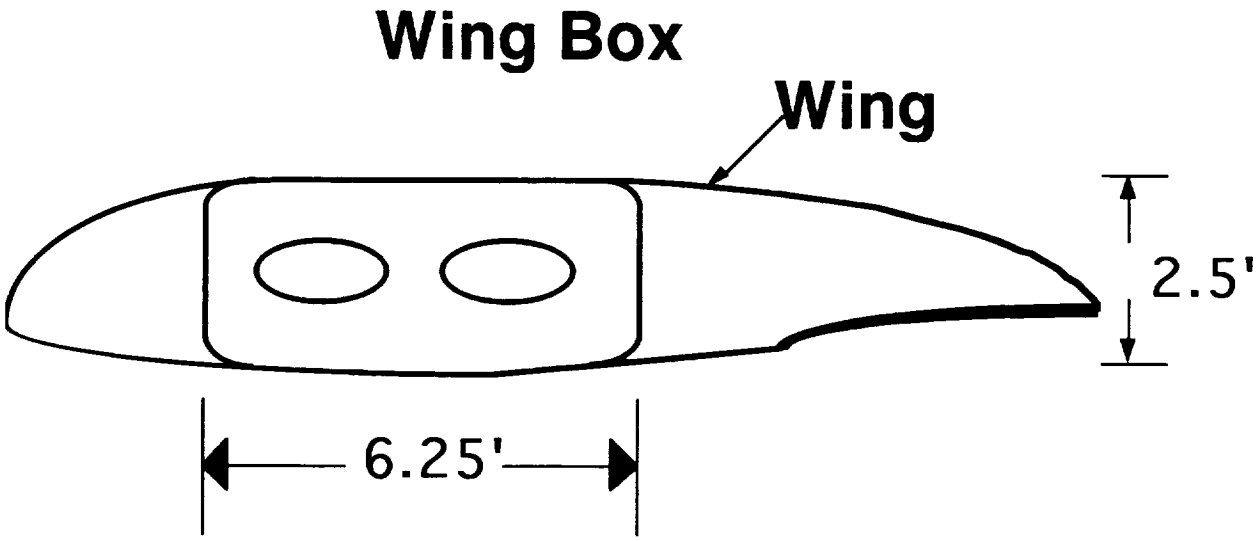

Figure 7.4 OFP-6M Wing Box

The fuselage is laid out with the main part of the fuselage having a stringer separation of 12 inches and a rib separation of 24 inches. These separations were taken by investigating other similar aircraft. The OFP-6M's fuselage was laid out to have a large diameter to optimize the fuselage area and volume of the plane. This large diameter gives an eight seat abreast seating and large amounts of cargo space in the cabin and underneath for stowage. This large diameter also enables the wing to be brought up from the bottom of the fuselage, which makes an easier connection of he wing box and no need for large dihedral. Finally, the large diameter gives easy stowage of the landing gear without bulges to completely cover the landing gear when retracted.

8 Weight and Balance

8.1 Component Weight Breakdown

The purpose of the weight breakdown was to identify major weight components that could most effectively reduce the weight of the aircraft through the use of composites, technology integration or other methods. To find a rough estimate of the major group weight breakdown empirical data was combined and then modified to reflect the OFP-6M configuration. Such a weight breakdown is shown in Figure 8.1.

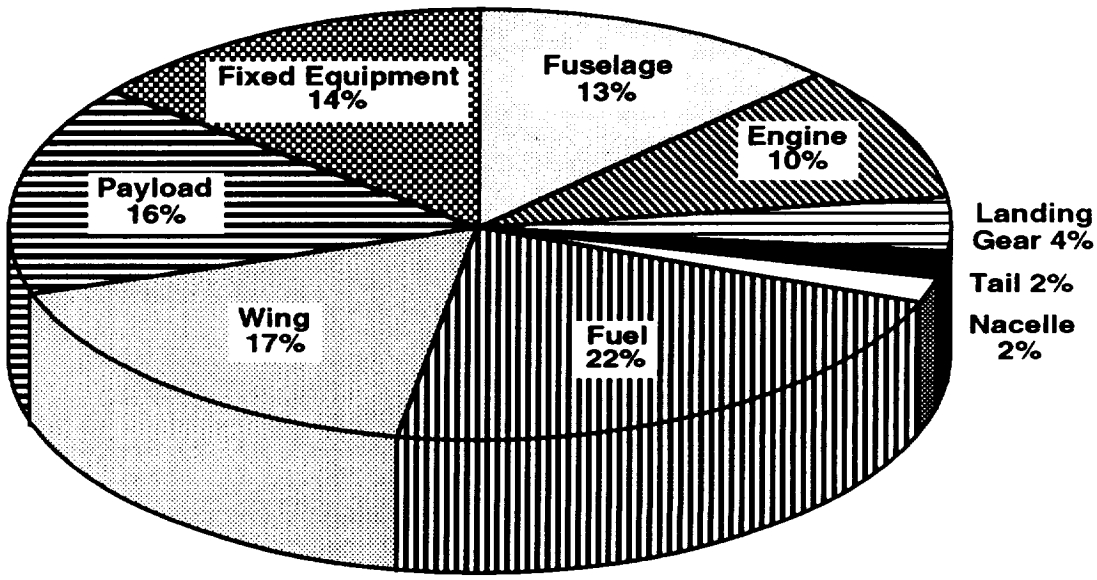

Figure 8.1 OFP-6M Weight Breakdown at Maximum Take-Off Weight

The results identified several major weight components to reduce. Because of the OFP-6M's 3000 nm range and 153 passenger capacity, fuel weight was the largest overall weight component. The best way to decrease the required fuel weight is by reducing the overall weight of the aircraft. Therefore, the other weight components were considered

first (Ref. 44). The second largest percent of weight is due to the wing which was reduced in weight by using composites for the wing box and other parts of the wing (Ref. 10). To further lower the weight of the wing, the wing loading was increased to decrease the amount of wing area (see Section 2.5).

The resulting major group weight breakdown at maximum take-off weight for the OFP-6M is shown in Figure 8.1. The use of composites in the floor beams, empennage, nacelles, etc. and the efficient use of current technology reduced the remaining weight of the OFP-6M resulting in a high payload percentage (Ref. 10).

8.2 Center of Gravity Analysis

8.2.1. Aerodynamic Center

The location of the Aerodynamic Center (AC) of the aircraft was calculated by geometric methods and is located at 38.4 ft aft of the datum (Ref. 44). The datum is located at the center of forward type B door. This method required that the AC for the wing, tail, and fuselage be found first. The AC of the supercritical wing and tail was assumed to be located at 0.4 of the c_{ave} line and the location of these cords were calculated using geometric methods from (Ref. 38). The AC of the fuselage was found by similar methods.

8.2.2. Center of Gravity

The location of the CG was found by first determining the CG for each component group of the aircraft. Component groups were formed by combining similar elements of the aircraft. Moment arms for each group were established from a datum. By summing moments and using approximated weight values the CG of the aircraft was found using a spread sheet.

The CG under a fully loaded condition was found to be at 45% Mean Aerodynamic Chord (MAC) or at 39 ft aft of the datum. The center of lift was located 5% MAC forward of the CG to provide a small amount of negative stability in the pitch mode. The CG range was found using the same spread sheet by removing component weights for the fuel, payload, cabin attendants, and flight crew in combinations (Ref. 35). The range of CG location is from 42% MAC to 46.5% MAC as shown in Figure 8.2. The most aft position is with full fuel and a flight deck crew but without passengers, cabin attendants, and baggage. The most forward position is with full crew, passengers and baggage but no fuel. The total CG range shift is only 4.5% MAC (0.53 ft). This is an extremely small CG shift for an aircraft of this size and type and is due to design elements such as a wide but short cabin and the concentration of the mass near the longitudinal center of the aircraft. The location of the main landing gear was checked to be 3.91 ft aft of the most aft CG location to confirm that the aircraft will not tip back on the tail in any loading condition. The trim drag will be minimal with the small, almost constant, negative, stability margin and minimal CG change.

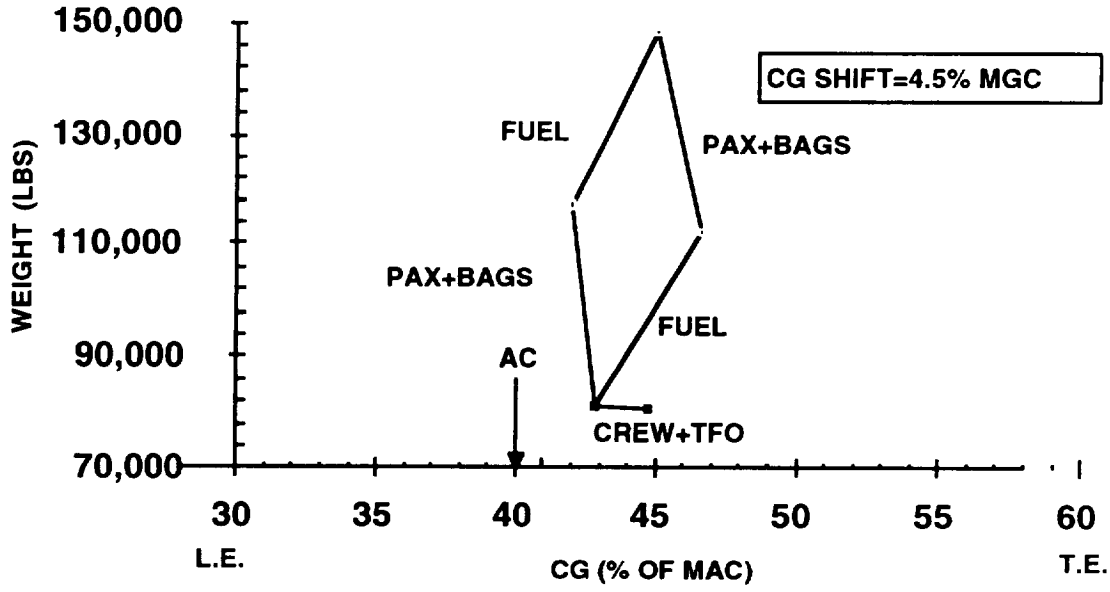

Figure 8.2 OFP-6M CG Travel

8.3 Moment of Inertia

The moments of inertia shown in Table 8.1 were calculated by breaking the aircraft into separate pieces, by utilizing the parallel axis theorem, and summing the individual moments of inertia for each piece.

Table 8.1 OFP-6M Results of Methods To Find Moments of Inertia

Method	Ixx (slug ft^2)	Iyy (slug ft^2)	Izz (slug ft^2)
First	790,800	2,300,000	3,040,000
Second	798,000	1,848,000	2,688,000

The OFP-6M is similar in shape to the Boeing 737-300. The moment of inertia's of the OFP-6M and the Boeing 737-300 are relatively similar in their order of magnitude. The large diameter and other geometry changes make the OFP-6M different to the Boeing 737-300. However these two planes are similar enough to compare and show that the moment of inertia's of the OFP-6M are reasonable.

9 Stability and Control

9.1 Stability

9.1.1. Longitudinal Stability

Figure 9.1 shows the longitudinal X-Plot for the OFP-6M. It was designed to be 5% statically unstable in the longitudinal plane to reduce the trim drag of the aircraft.

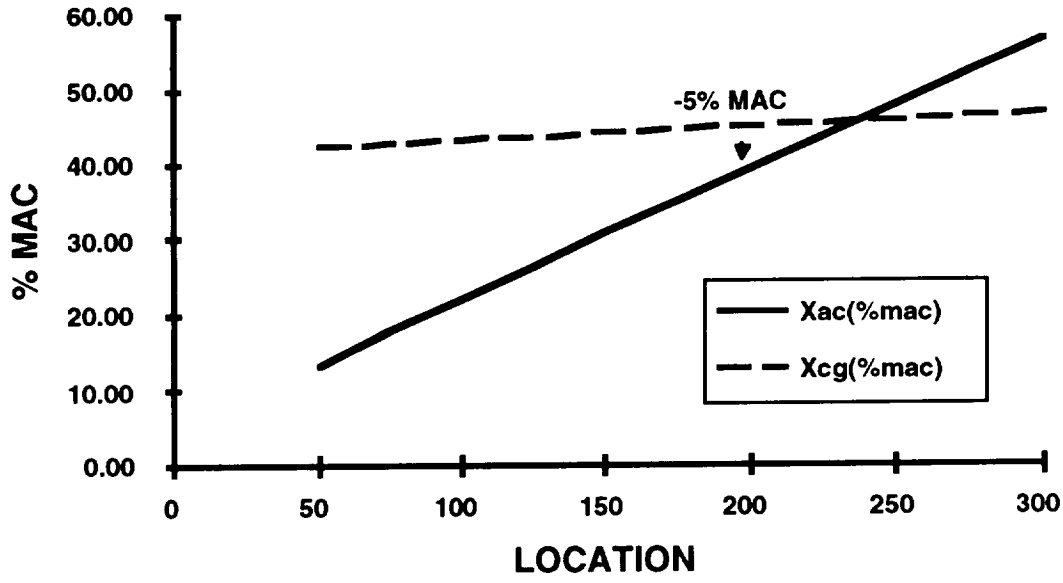

Figure 9.1 Longitudinal X-Plot for the OFP-6M

To accommodate the static instability, a SAS will be in use. Without the system in operation, the OFP-6M will be marginally controllable. This is because the OFP-6M is expected to be unstable in the phugoid mode which is well within the pilot's control bandwidth. However, it is also unstable in the short period mode which would produce an uncomfortable motion in any turbulence if SAS was not used. Calculated longitudinal stability derivatives are shown in Table 9.1. Though the SAS is essential for normal

control of the OFP-6M, the control system redundancies are such that the statistical probability of complete flight computer loss is nearly zero (see Section 9.2).

Table 9.1 Longitudinal Stability Derivatives for OFP-6M

C_{Du}	0.0000	$C_{D\alpha}$	0.3208
C_{Lu}	0.7543	$C_{L\alpha}$	7.2466
C_{mu}	0.1737	$C_{m\alpha}$	4.3920
C_{Dq}	0.0000	$C_{D\alpha}$.dot	0.0000
C_{Lq}	1.8526	$C_{L\alpha}$.dot	2.9133
C_{mq}	-30.0988	$C_{m\alpha}$.dot	-10.5548

9.1.2. Lateral Stability

The OFP-6M was designed with minimal lateral stability to reduce the size of the vertical stabilizer and hence skin friction drag of the empennage. The calculated lateral stability derivatives are shown in Table 9.2. The major constraint of the vertical stabilizer is to provide adequate structure for the relatively large and powerful rudder. The small vertical stabilizer (relative to the rudder) will provide a stable yet highly under damped response but will be compensated by the SAS. The wing dihedral was constrained by engine clearance requirements rather than by lateral stability considerations. However, it is within acceptable limits for normal and Dutch roll.

Table 9.2 Lateral Stability Derivatives for OFP-6M

C_{yp}	-0.3260	$C_{y\beta}$	-1.3980
C_{lp}	-0.0840	C_{lB}	-0.2276
C_{np}	-0.0920	$C_{n\beta}$	0.0474
C_{yr}	0.9250	$C_{y\beta.dot}$	0.0305
C_{lr}	0.4000	$C_{l\beta.dot}$	0.0055
C_{nr}	-0.4870	$C_{n\beta.dot}$	0.0163

9.2 Control System

The control system will be a FBL system with electrohydrostatic actuators. The fiber-optic wiring of the FBL system will incorporate triple routing redundancy to effectively minimize the probability of system failure due to one route being cut. Additionally, the control system will have quadruple redundancy in the flight computers so that complete system failure will be extremely improbable.

FBL was chosen for the OFP-6M for the following reasons. FBL has all the advantages of FBW. Compared to mechanical systems, FBW has reduced weight, reduced aging characteristics, no routing and rigging problems associated with mechanical systems, and more easily achievable redundancy. Additionally, FBW is more easily integrated to SAS and the automatic pilot system, more easily limits control deflections to a non-destructive value, limits aircraft operation into known modes, and reduces pilot work load especially at high demand tasks like the OEI condition. Compared to FBW, FBL has the additional advantages of even lighter weight, higher data rate for an all digital system, easier multipath control system routing and design, no cable fatigue like that of wire, and absolute immunity to electromagnetic interference.

FBW is now common in newer aircraft and data communication with fiber-optics and light in terrestrial applications has proven to be superior in reliability and cost to high data rate systems using wire. After consideration of current trends in FBL technology in aircraft, it is predicted that the production cost of FBL to be comparable, if not slightly lower, than FBW (Ref. 15).

Actual motion of the control surfaces is achieved by the electrohydrostatic actuators. The actuators operate off energy from the electrical system, thereby increasing its required output. However this disadvantage is off set by the benefits of the electrohydrostatic actuator. They not only have increased performance which is beneficial for the SAS, but also nearly eliminate the need for a complex and heavy hydraulic system. Additionally with the near elimination of the hydraulic system, the safety problems of high pressure hydraulic lines are nearly eliminated as well.

9.3 Empennage Sizing

The OFP-6M is a relatively short, wide aircraft. If the empennage of the OFP-6M were to be sized for stability considerations, it would require a relatively large horizontal tail. For the reduction of the horizontal tail and trim drag, the optimum finess ration for a stable aircraft is about 8:1. However, with a SAS in operation, the optimum fineness ratio without stability considerations is 6:1 (Ref. 34). Since the fineness ratio of the OFP-6M is below 8:1, it has a short moment arm. The reduction of tail size for this aircraft is critical for efficient operation. This reduction is achieved by sizing the empennage for minimum necessary control power and rotation without regards to stability. Stability is then achieved with SAS.

When X-plots were generated and examined, the OFP-6M was designed 5% unstable to reduce trim drag. Additionally the size of the empennage was reduced to the minimum necessary for control power. The reduction of tail size not only decreases the

weight of the aircraft, but would also decrease wetted area to reduce skin friction drag. Both these reductions would decrease the fuel consumption of the OFP-6M. Though addition of a sophisticated control system is necessary for an unstable aircraft, the reduction of fuel consumption was a justifiable trade. Because of the critical nature of the reduced empennage size and the minimal CG excursion of the OFP-6M, the empennage was not sized for stability. Therefore, the critical design parameters examined were rotation at take-off and maneuverability during the OEI condition. Table 9.2 gives the empennage characteristics for the OFP-6M.

Table 9.3 OFP-6M Empennage Characteristics

Horizontal Tail		Vertical Tail	
Area	200 ft^2	Area	319 ft^2
Airfoil Type	Supercritical	Airfoil Type	Conventional Symmetrical
sweep angle at 0.4 c	25°	sweep angle at 0.4c	30°
Aspect Ratio	6.1	Aspect Ratio	2.0
Taper Ratio	0.3	Taper Ratio	0.3
Span	34.9 ft	Span	23.0 ft
Average Chord	5.73 ft	Average Chord	13.8 ft
Elevator Area	76 ft^2	Rudder Area	131 ft^2

9.3.1. Horizontal Tail

The supercritical airfoil section of the wing was used for the horizontal tail. This airfoil section was chosen so that the required sweep of the tail would not be excessive at M = 0.8 (see Section 4.1). Double slotted elevators were used to increase the horizontal tail maximum lift coefficient to the necessary value of 2.5. With this lift coefficient, the

C-2.

area of the horizontal tail area was determined, using summation of moment equations, to be 200 square feet. Additionally, the elevator area was determined using statistical analysis to be 76 square feet (Ref. 34).

9.3.2. Vertical Tail

The vertical tail is a conventional symmetrical airfoil with a maximum lift coefficient of approximately 2.0. Using the summation of moments occurred during the OEI condition, the required vertical tail area was calculated to be 265 ft^2. The maneuverability of the aircraft at this condition was also necessary, so an additional 20% maneuverability was added by a 20% increase in the vertical tail area. The final tail area was then calculated as 319 ft^2. Additionally, the rudder area was determined, using statistical analysis to be 131 ft^2 (Ref. 34).

9.3.3. Trim Conditions

The primary trim control of the OFP-6M in the longitudinal direction is the horizontal stabilizer with a double slotted elevator. The trim diagram shown in Figure 9.2 indicates that at the cruise Cl value 0.58, the OFP-6M is in a trimable condition.

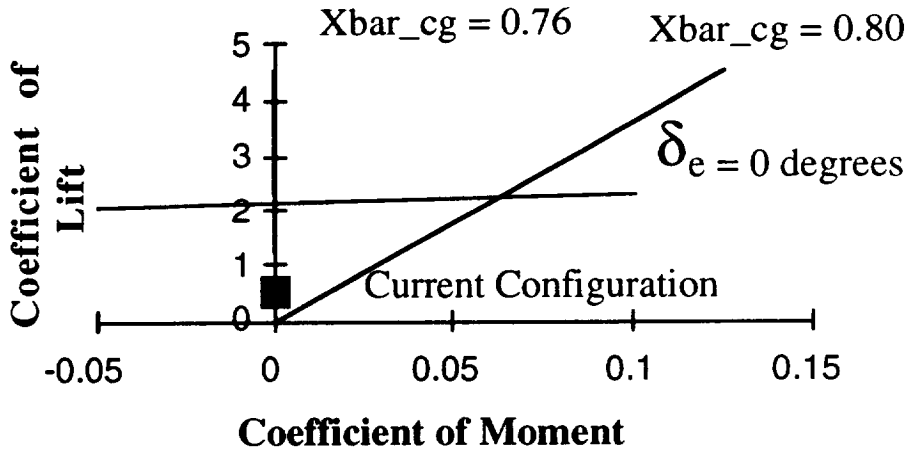

Figure 9.2 OFP-6M Trim Diagram for Cruise

10 Landing Gear

The OFP-6M's landing gear was designed to the criteria that the landing gear must be a simple system because cost is the driving factor. Furthermore, the aircraft must be accessible to as many airfields as possible, and the landing gear needs to stow neatly into the fuselage when retracted.

10.1 Gear Placement

These criteria lead to a conventional tricycle landing gear which is found on almost all commercial transport jets today. The main gear supports 95% of the total weight and the nose gear supports 5% of the total weight. This distribution was calculated at the most aft CG location, therefore 95% is the most weight the main gear will have to support. The 5% on the main gear gives enough weight on the nose gear for maneuvering on the airfield before takeoff.

The wide body and the shortness of the fuselage makes the turnover angle (Θ) never reach the 63 degree maximum with the placement of the landing gear anywhere along the wing. With the main landing gear placed at the edge of the fuselage, the turnover angle is only 55 degrees. However, this configuration makes the retraction and placement of the gear difficult. Therefore, the main landing gear were placed farther out on the wing. The final configuration of the landing gear results in a turnover angle of 45 degrees. A schematic of the turnover angle can be seen in Figure 10.1.

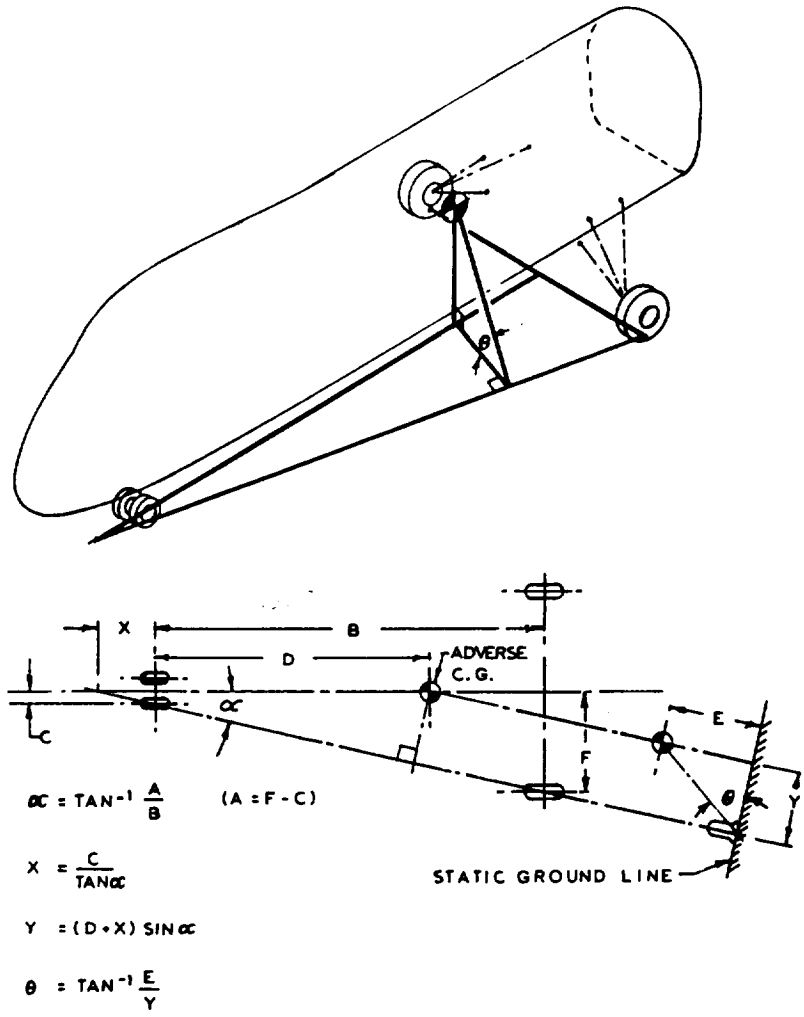

(Source: Ref. 9)

Figure 10.1 OFP-6M Turnover Angle Schematic

10.2 Retraction Sequence and Steering

The criteria that the landing gear must stow neatly into the fuselage drove the design of the four abreast, dual twin, landing gear concept. Fully extended, the landing gear has four wheels abreast on one strut. This concept gives a lower Load Classification Number (LCN) than the twin system and a comparable LCN to the twin tandem (Ref. 9). Also, the dual twin gives the OFP-6M a tight turning radius with negligible tire scrubbing (Ref. 45). The three types of landing gear are shown on Figure 10.2.

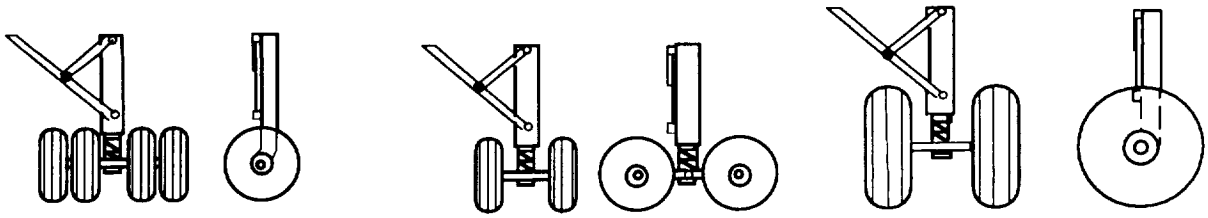

Figure 10.2 OFP-6M Landing Gear Concepts

The main, dual twin, landing gear goes through a 90 degree twist during retraction. With this retraction sequence, the landing gear stores neatly inside the fuselage with no additions to the fuselage to completely cover the landing gear. The retraction mechanism is basically the same, however the retraction bar is placed in front of the strut, instead of being on the side, and the strut is left free to rotate. When the gear is retracted, the retraction bar pulls up and rotates the gear the 90 degrees when it is stowed in the fuselage. This system does not require any extra or complex hardware to retract the landing gear. If the landing gear fails the weight of the main landing gear can be used to deploy it for landing. A schematic of a similar retraction sequence is shown on Figure 10.3.

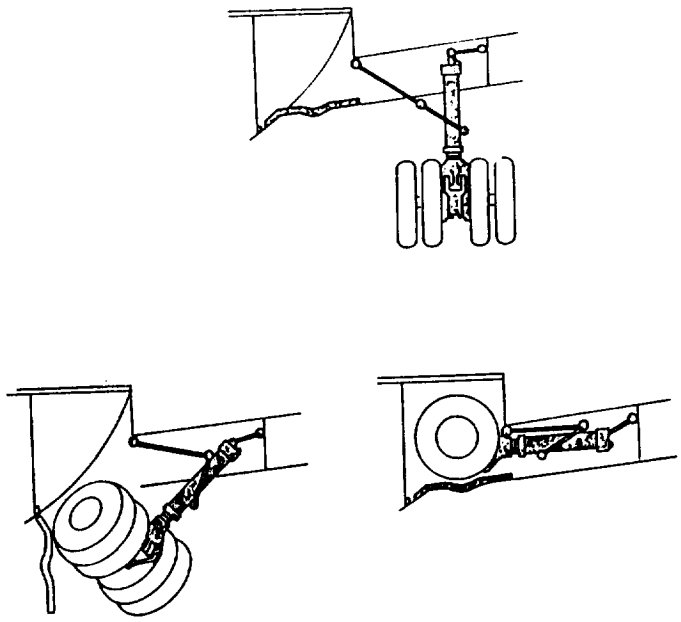

(Source: Ref. 45)

Figure 10.3 OFP-6M Main Landing Gear Retraction Sequence

The nose gear consists of dual wheels arranged on one strut. The strut retracts forward into the nose of the aircraft. If the landing gear fails the nose gear can fall and the wind drag of the nose gear will retract the nose gear into the proper position for landing. The nose gear consists of a rack and pinion steering system. This system is relatively simple and will give the aircraft a turn angel of 68 degrees and a minimum turn radius of 70 feet. The pilot can turn the nose gear by a simple, small steering wheel found beside his seat. The turn radius of the OFP-6M can be seen in Figure 10.4.

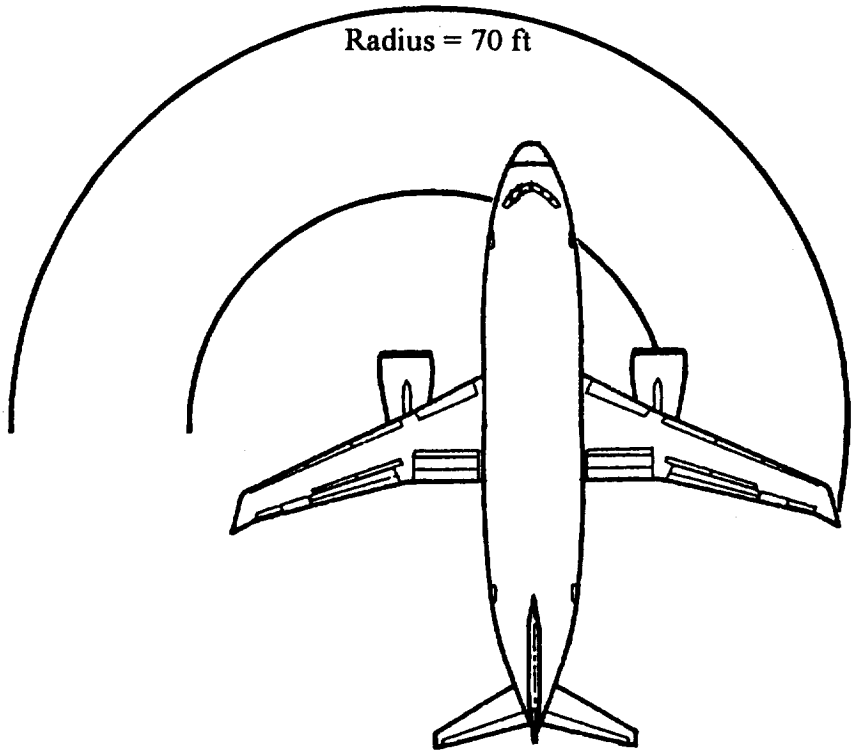

Figure 10.4 OFP-6M Turning Radius

10.3 Brakes

The brakes of the OFP-6M are carbon brakes. The advantages of carbon brakes are that they are lighter, absorb more energy for shorter stopping, temperature, corrosion, fatigue resistant, and last up to three times longer as steel brakes (Ref. 9). Weight is a main driving factor in the design of an aircraft. A savings in weight will result in a savings in fuel. Also, maintenance on landing gear results in lost flying time of the aircraft. Any reduction of maintenance time will result in more flying time for the aircraft. By looking at the trends of other aircraft companies and weighing the options, carbon brakes are the best choice for the OFP-6M. Finally, the design of the landing gear allows the OFP-6M to use only two brake clusters for each strut. A schematic of the

brake cluster us shown on Figure 10.5. This schematic is a comparable landing gear system from the Hawker Siddeley Trident.

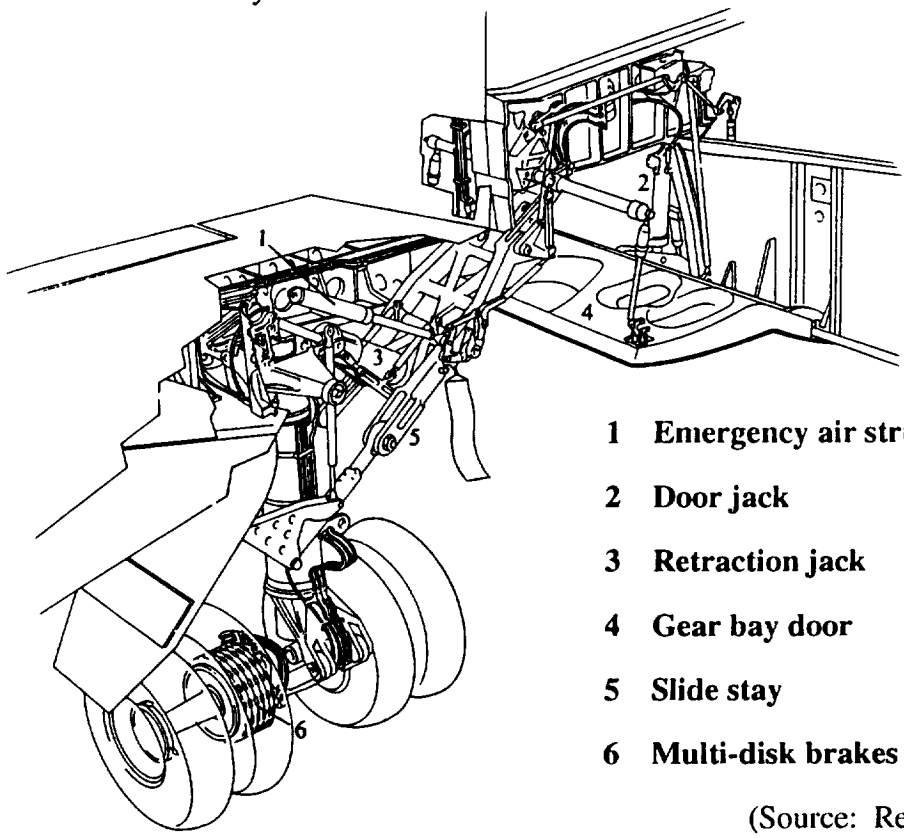

1 Emergency air strut

2 Door jack

3 Retraction jack

4 Gear bay door

5 Slide stay

6 Multi-disk brakes

(Source: Ref. 45)

Figure 10.5 OFP-6M Schematic of the Landing Gear

10.4 Tire Selection and Strut Design

The tires for the main and nose landing gear were chosen from available landing gear tire data (Ref. 37). The calculated static and dynamic loads on the aircraft yielded the following design criteria:

- **23,600 lb per tire for the main gear**
- **5,900 lb per tire for the nose gear**
- **220 mph max. take off speed**
- **Tire pressure around 150 psi**

The tires selected for the main gear are 40 in x 14 in type VII. These tires have a loading of 25,000 lb, inflation pressure of 155 psi, and a maximum speed of 225 mph. The tires for the nose gear are 24 in x 7 in type VII. These tires have a loading of 6,000 lb, inflation pressure of 155 psi, and a maximum speed of 225 mph. The Type VII tires were chosen because they have a narrow width which can handle high loads. The narrow width makes stowage of the landing gear after retraction easier.

The static and dynamic loads of the landing gear were calculated and the strut of the landing gear was sized according to FAR 25. The analysis of the landing gear required a shock absorber length of 15 inches and a diameter of 9 inches. The shock struts of the main and nose landing gear are to be oleo-pneumatic struts. An example of the stroke diagram of an oleo-pneumatic strut is shown on Figure 10.6.

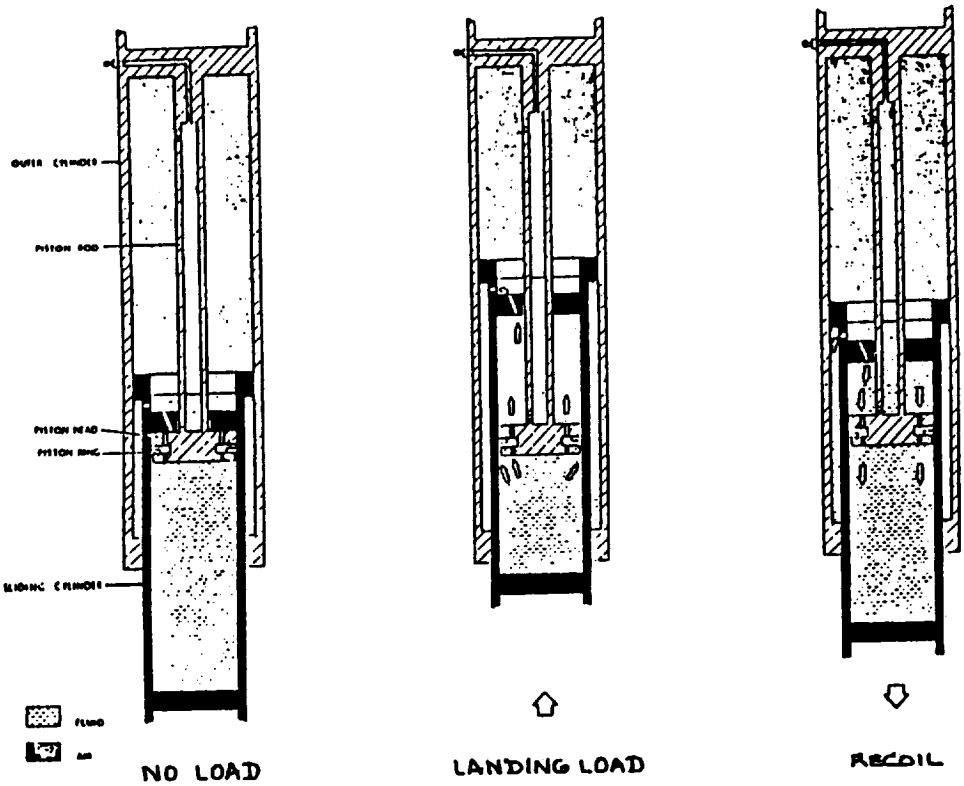

(Source: Ref. 37)

Figure 10.6 OFP-6M Stroke Diagram

10.5 Pavement Loading

Pavement loading is an important parameter to consider. The pavement loading determines which airfields the aircraft is permitted to land without creating damage to the airfield.

The pavement loading analysis was completed by using a computer program donated from the McDonnell Douglas company. The program gave the information for the landing gear used as shown in Table 10.1.

Table 10.1 OFP-6M California Bearing Ratio and Pavement Thickness

CBR	Pavement Thickness
10	16.0 in
15	11.6 in

This information yielded a maximum LCN of 42. The LCN determines which airfields the aircraft is allowed to land. The lower the LCN number the more airfields the aircraft can land. This value is calculated at maximum weight for the aircraft, therefore the aircraft will not operate at a LCN greater than 42. This value is less than the Boeing 737-200, thus is competitive in its size class (Ref. 6).

11 Systems

11.1 Fuel System

Because the purpose of the fuel system is to safely transport fuel, a highly combustible liquid, the design is of great importance to the safety of the aircraft. There is only one fuel tank in each wing and an optional center fuel tank in the fuselage wing box. This arrangement, similar in design to the Boeing 777, is designed for simplicity to prevent fuel management mistakes by the crew(Ref. 8). Since fuel management mistakes are the second largest cause of aircraft loss, simplicity in the fuel system is more important then the slight structural penalty. The more simple fuel system has less parts and less weight then a more complex fuel system. Using a trade study, it was found that the increased weight due to the structural penalty was offset by the reduced weight of the more simple fuel system with in the resolution of the calculations. Some load relief to the wing structure is provided by the engines. The fuel system of the OFP-6M is shown in Figure 11.1. Also the storage and transport of the fuel is a factor in the static stability of the aircraft. Since the effective CG shift, due to fuel, of the OFP-6M is minimal, no complex and mistake prone trim tank fuel management is needed to avoid stability problems. The fuel system on the OFP-6M is designed with a venting system adequate to avoid excessive pressure build up. The OFP-6M is designed with sufficient refueling and maintenance accessibility so that it will be easily maintained. All tanks can be filled from a single point refueling station on the under side of the right wing. The wing tanks can also be filled from over wing fill ports near each wing tip. This is needed for operation from more austere ground facilities. Wing and fuselage fuel dumps are provided for emergency use.

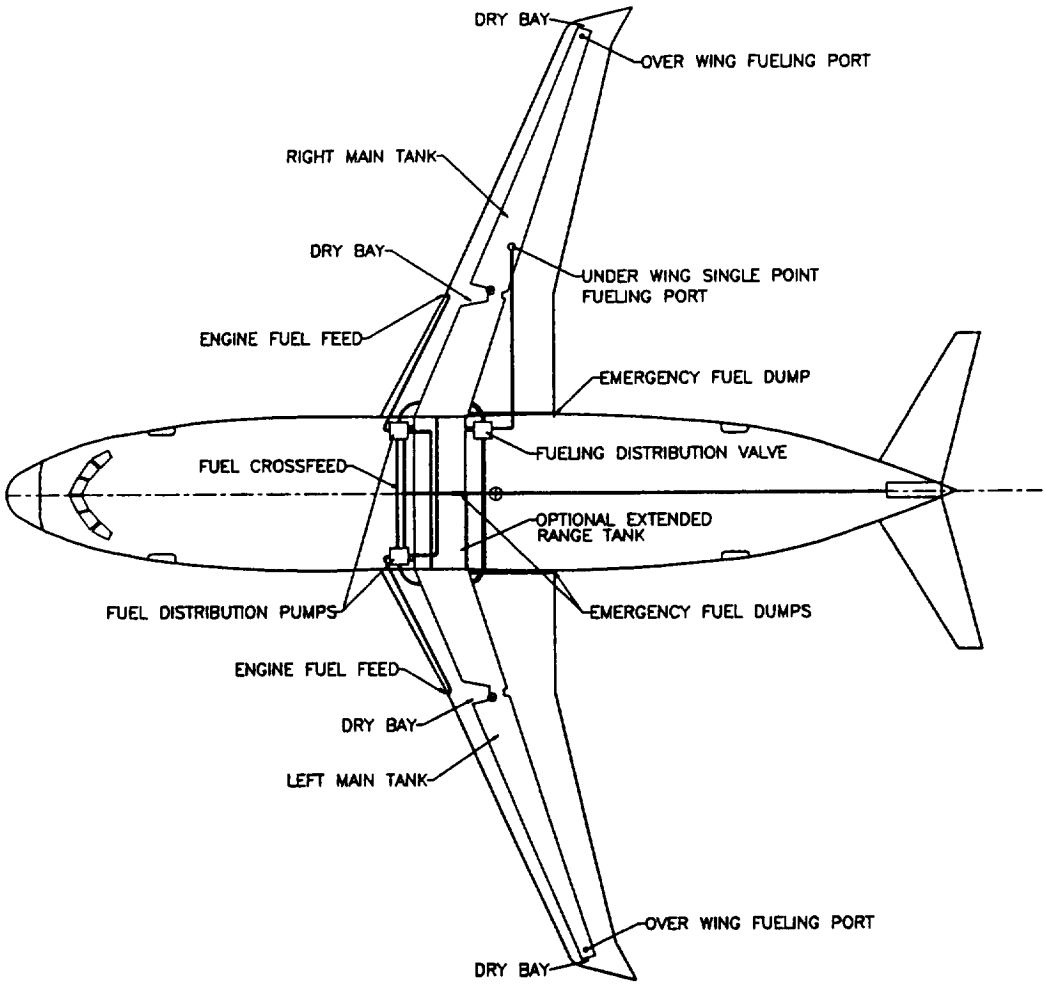

Figure 11.1 Schematic of OFP-6M Fueling System

11.2 Hydraulic System

Due to the extensive use of electrohydrostatic actuator and FBL technology in the OFP-6M, the hydraulic system will be eliminated. The FBL system will be connected to electrohydrostatic actuators near the control surfaces and landing gear. This reduces the weight and safety problems associated with high pressure hydraulic lines.

11.3 Control System

The control system of the OFP-6M will be a FBL system connected to electrohydrostatic actuators at the control surfaces (see Section 9.2).

11.4 Electrical System

The electrical system will be used for lighting, instruments and avionics system, and engine starting systems. As previously stated, the primary and secondary control systems will be controlled by a fiber-optic FBL system connected to electrohydrostatic actuators which will be powered by the electrical system. Additionally, the electrohydrostatic actuators will be used to activate the landing gear. Primary power generation will be supplied by engine driven generators that use magnaquench technology. Magnaquench motors and generators were developed by General Motors Inc. in the 1980's, are over 98% efficient, 60% the volume of, and less then half the weight of old technology motors and generators of the same capacity. Magnaquench technology is now used in numerous applications including aerospace and consumer applications. The system will use high voltage low current to allow the use of light weight wire and provide efficient power transfer. Accounting for all component efficiencies, the system is over 94% efficient. The trade studies done by Plan-It X show the addition to the electrical system needed by the elimination of the hydraulic system is lighter then the hydraulic system that it replaces. The electrohydrostatic landing gear retraction system will include hydraulic accumulators, pressurized before flight, sufficient to not only raise the gear, but also to lower it should the flight need to be aborted just after landing gear retraction. In case of malfunction, the secondary power system will consist of a battery system as well as a Ram Air Turbine.

11.5 Pneumatic System

The Pneumatic system of the OFP-6M is shown in Figure 11.2. The pneumatic system will be supplied by bleed air off the engine and the APU. It will power the packs as well as supplying the leading edge anti-ice devices and actuating thrust reversers. Also, the pneumatic system will be used to start the engines with bleed air off the APU, the other engine, or the APU with bleed air off the engines.

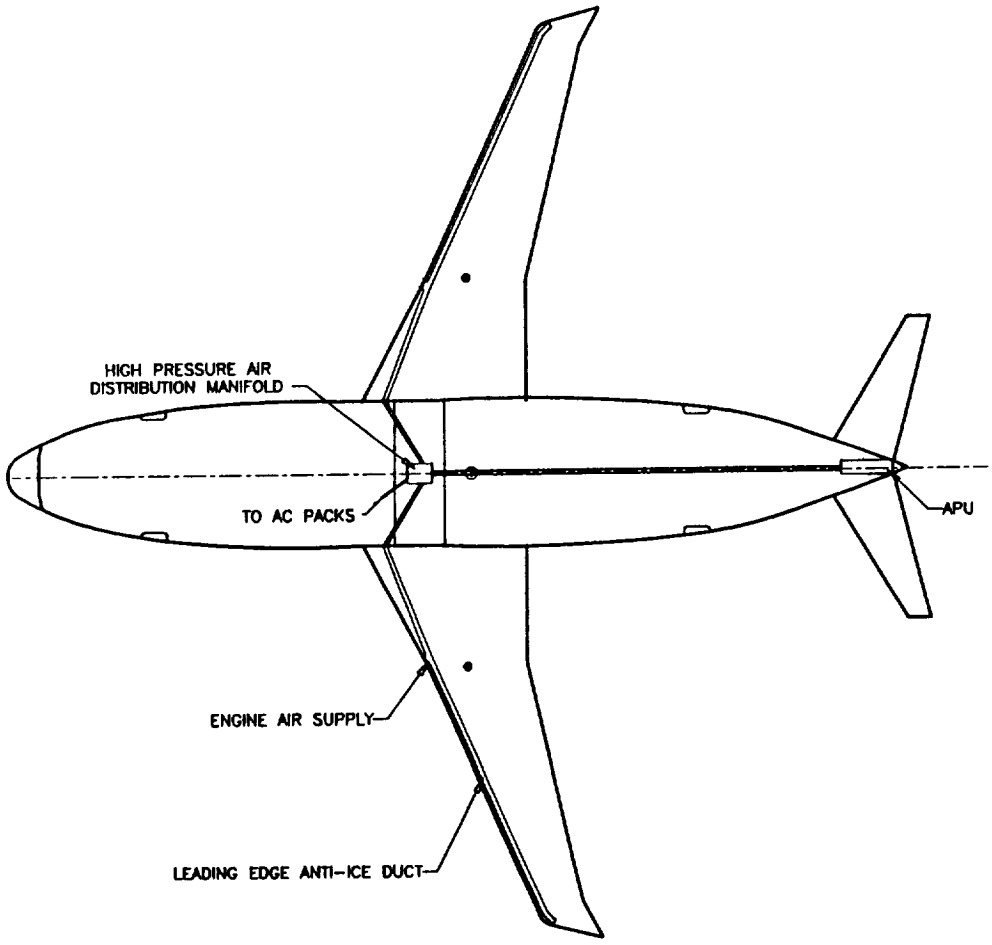

Figure 11.2 Schematic of OFP-6M Pneumatic System

12 Airport Operation and Maintenance

12.1 Ground Support and Gate Access

Figure 12.1 shows that the OFP-6M is accessible to all services as well as accessible to a loading gate or loading staircase.

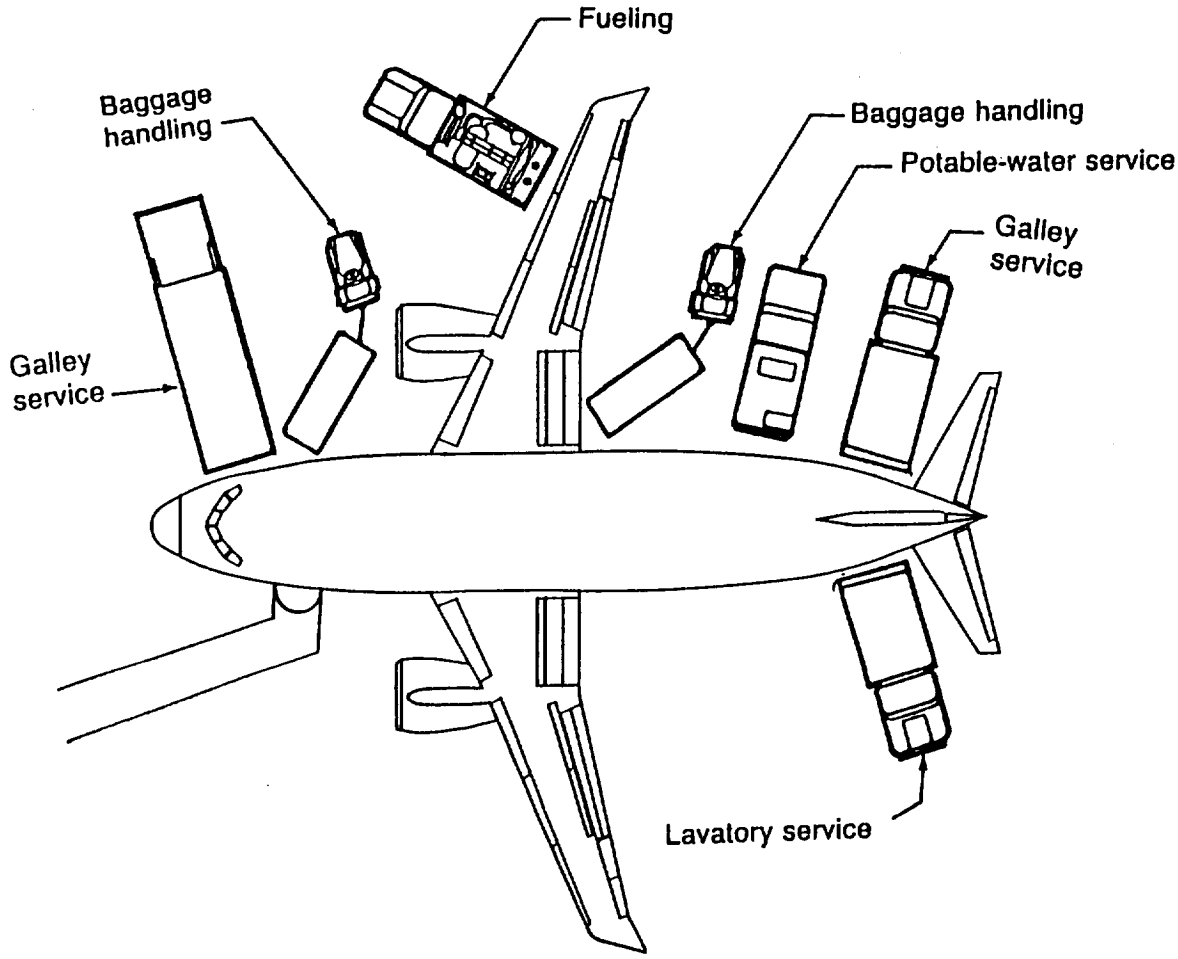

Figure 12.1 OFP-6M Service Diagram

13 Manufacturing

13.1 Manufacturing Philosophy

The driving factors on the OFP-6M are affordability as well as quality. Therefore Total Quality Management (TQM), Design For Manufacturing and Assembly (DFMA), and Integrated Product Development (IPD) will be used in all phases of design and production. It has been shown that waste can be minimized and production greatly increased by use of these methods. This can be shown by the example of McDonnell Douglas. By use of TQM and DFMA, Douglas reduced its debt by 1.1 billion dollars in 1993 and during this same period enjoyed its best return on investment since 1985 while being second in industry in sales (Ref. 19).

TQM is based on customer satisfaction and quality, rather than quantity. This is true whether it is the final customer or the next production step. The philosophy behind TQM depends on teamwork and the empowerment of all employees, stating that those best qualified to make production decisions, are those doing the production, thus eliminating middle management .

DFMA and IPD strive to reduce inventory cost as well as reducing the cost of manufacturing, maintenance, and support. Integrated product teams are employed to reduce number and complexity of parts so as to increase the support of the entire program. Use of high speed machining and low rate expandable tooling systems in manufacturing cells help to provide a rate transparent manufacturing capability. This will allow the aircraft cost to be independent of manufacturing rate and provide a considerable savings to the program.

Essentially, the OFP-6M will attempt to use the lessons learned by McDonnell Douglas and other companies using TQM, DFMA, and IPD to reduce the cost of

production. With effective use of these methods, waste on the OFP-6M will be greatly reduced and the program will be well streamlined so as to compete in the current market. This streamlining is vital to the success of the OFP-6M program. Today's market is extremely competitive and these modern methods are needed to advance to be on-weight, on-time, on-performance, and below cost.

13.2 Component Manufacture

In order to most efficiently manufacture components of the OFP-6M, current proven technology and state-of-the-art methods will be used. Components of continuous cross-section will be produced using extrusion. Large composite components like wing skins and flooring will be manufactured using automated and automated-assisted lay-up of pre-preg composite materials. All parts will be trimmed using automated hydro-jets to reduce toxic dust. Small components will be manufactured using injection molding of thermoset resins strengthened with carbon or other fibers as appropriate. This method, though having a slightly higher tooling cost, will produce parts with less defects thereby reducing required rework and providing better tolerance control. Cast metal components like landing gear components will be produced using matched die casting. Larger sheet metal components will be produced using standard techniques such as machining and hydro-forming.

Components are assembled in a system of manufacturing cells to increase rate transparent manufacturing capability. Bonding will be used to attach composite components to composite components and metal components to metal components. Metal to metal bonding technology has been used extensively in military aircraft and has been used extensively by Folker Aircraft. A minimal number of rivets will be used to attach composite to metal materials due to the dissimilar properties of the two components.

13.3 Wing Manufacture

The composite wing skin is fabricated in one piece for each wing section using semi-automated lay-up. The autoclave required is no larger than those used for the empennage on the Boeing 777, therefore one-piece manufacturing has been proven feasible. Composite spars will be created using automated lay-up manufactured U cross-section beams. The ribs and spars will be assembled, then systems added before the wing skin is installed. Maintainability is assured by ample access panels. The horizontal and vertical stabilizers will also be assembled in this fashion.

13.4 Fuselage Manufacture

The fuselage is manufactured in four sections using conventional methods with the exemption of metal to metal bonding rather than use of riveting. The use of advanced computer aided design techniques will cause the alignment of the fuselage to be essentially flawless and less adjustments are required on the final assembly. This technique has been proven by Boeing on the assembly on the 777. The misalignment of the fuselage of the Boeing 777 due to manufacturing is less than that caused by differential heating from the sun (Ref. 8). The nose, center section including the wing, and tail sections of the fuselage will then be joined on final assembly.

13.5 Final Assembly

The empennage, wings, and fuselage sections will be shipped on rails to the final assembly line where a system of cranes will allow the parts to be joined as shown in

Figure 13.1. Avionics and engines can then be installed and tested. The exposed composite sections of the aircraft are spray metal coated with a micro-thin layer of aluminum to provide lightning and ultra-violet light protection. Finally, the aircraft is washed and painted, with water based paints that are UV cured, to customer specifications in the environmentally secure color augmentation facility.

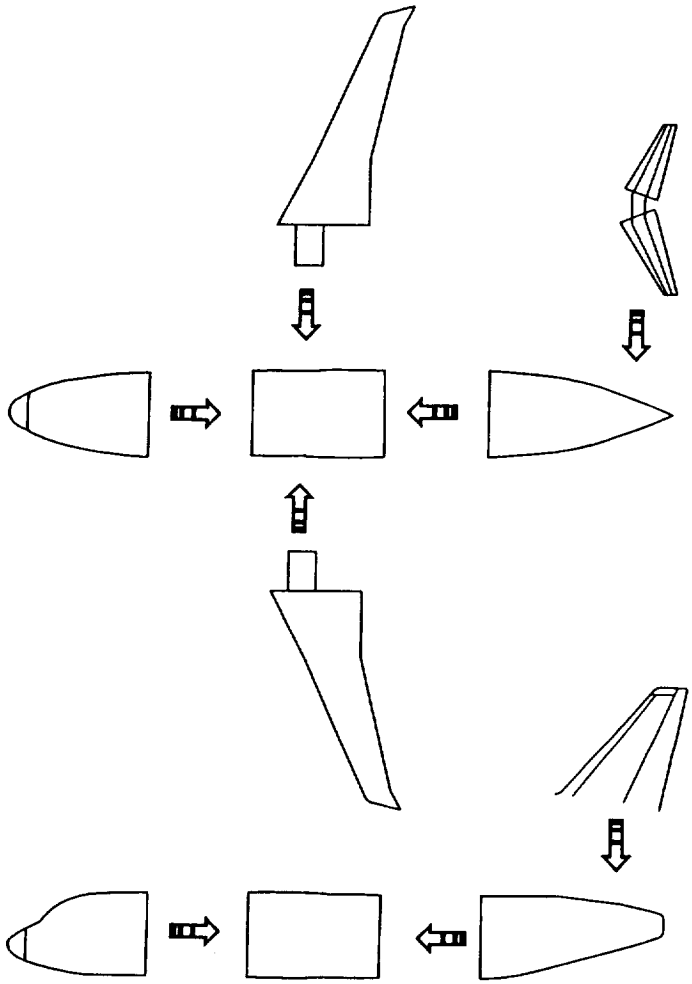

Figure 13.1 OFP-6M Manufacturing Diagram

14 Cost

The basic philosophy followed when designing the OFP-6M was to make the best, most competitive product possible, while still keeping the cost to a minimum. This was done by comparing aspects of the airplane to those being used now, analyzing future trends, then making educated decisions on which equipment to use or how to design for a certain aspect of the airplane. There are two opposing philosophies at work in this design: having a modern competitive aircraft which will not be outdated in five years, and keeping cost to a minimum.

Production cost was analyzed for a fleet of 1000 to have a total manufacturing cost of $21.9 billion with manufacturing man hours at $2.7 billion, materials at $1.9 billion, and tooling cost at $188 million (Ref. 40). These costs were determined by using old methods which assume values and do not take into account new methods of design. Using DFMA these costs have been reduced 5-10% (Ref. 19). Designing the plane to have the least amount of parts reduces complexity and manufacture time. It takes less tools to produce the aircraft and also reduces weight and the amount of material to produce the plane. By simplifying the design and making the aircraft with the least amount of complexity and number of parts possible, all three major areas of production cost can be reduced. Less quality control time and repair time is required because fewer parts are needed to inspect, break, etc.

Further major costs of acquisition of a fleet of 1000 aircraft are shown in the Table 14.1.

Table 14.1 Major Acquisition Costs for OFP-6M

all numbers in 1994 dollars	Engines & Avionics	Cost of Finance	Manufacturing Profit	Total Acquisition
Cost ($ billion)	12.4	2.2	2.2	24.1

Though engine and avionics cost is difficult to reduce as it is paid out to vendors, the cost of finance and manufacturing profit are strict percentages and will react to the other cost factors. Therefore, as other costs are reduced by modern design techniques, these costs will also be reduced. Figure 14.1 shows DOC versus range for the OFP-6M. This shows that as the range is increased the DOC decreases.

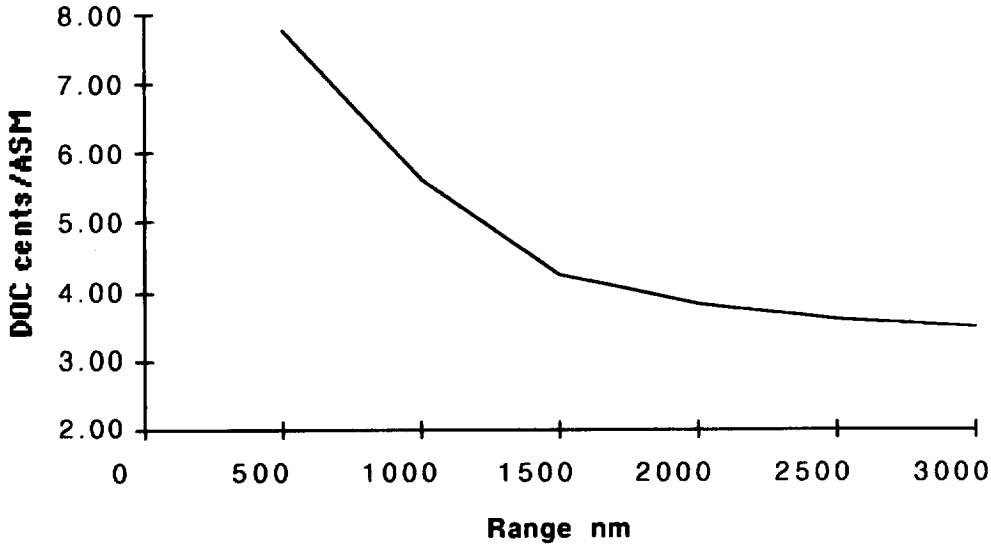

Figure 14.1 OFP-6M Direct Operating Cost Versus Range

As a result of the costs determined above, direct and indirect operating costs were determined and are shown in Table 14.2.

Table 14.2 OFP-6M Range Versus Operating Costs

Range (nm)	DOC (cents/ASM)	IOC (cents/ASM)	TOC (cents/nm)
500	7.77	1.94	9.71
1000	5.62	1.41	7.03
1500	4.25	1.06	5.31
2000	3.83	.96	4.79
2500	3.58	.90	4.48
3000	3.49	.87	4.36

As shown in Figure 14.2 the OFP-6M has a lower DOC when compared to its direct competition of the 737-300 and 757-200. The DOC is the bottom line for airlines in today's economy. To be competitive, the OFP-6M has reduced DOC costs to that below its competition.

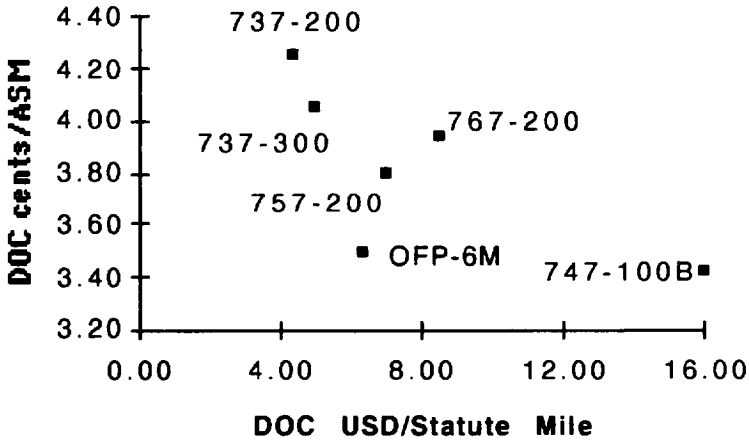

Figure 14.2 OFP-6M DOC Comparisons to Competitive Aircraft

DOC was broken down even further for better cost analysis as shown in Figure 14.3. As can be seen, maintenance is the largest part of DOC. By designing for

manufacturing applications, the number of parts is reduced. This in turn can reduce maintenance and maintenance DOC up to 15%, reducing total DOC accordingly (Ref. 18). By installing maintenance sensors on highly maintained systems, maintenance DOC can be furthur reduced by up to 10%.

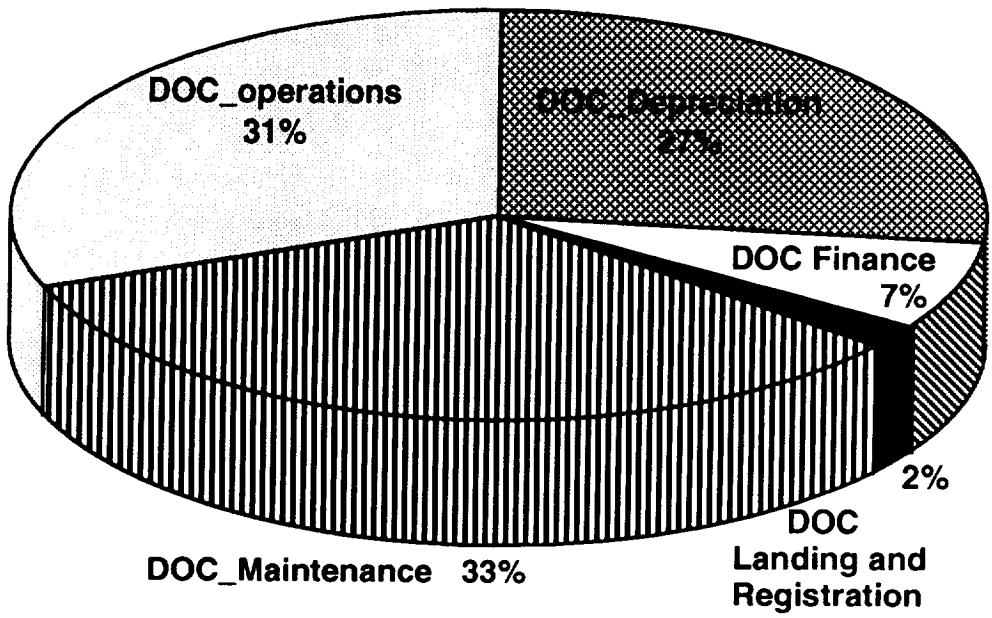

Figure 14.3 DOC Cost Breakdown for the OFP-6M

The aircraft market price was calculated to be $29.5 million. The price of the OFP-6M compares favorably to today's market, with the Boeing 737 between $31 and $45 million, depending on configuration (Ref. 26). This determined a life cycle cost of $273 billion, and a research and development cost of $375 million.

15 Conclusions and Recommendations

15.1 Advantages of the OFP-6M Design

The advantages of the OFP-6M is that it is simple and reliable. Its main purpose is to provide comfort, reliability and low operating cost. Among the advantages of the OFP-6M design are:

- **Twin aisle for quick turn around time.**
- **Extensive storage and closet space.**
- **Large overhead compartments.**
- **Location of engines allows for easy maintenance.**
- **Large cargo space.**
- **Lavatories and galleys placed apart from each other.**
- **Minimal CG shift.**
- **Composite structures lighter and more efficient.**
- **Supercritical wing thickness and low drag rise.**
- **High BPR turbofan engines with low a SFC.**
- **Interior Feeling of Roominess.**

15.2 Disadvantages of the OFP-6M design

- **Engine placement increase chances of FOD.**
- **High material cost (composites).**
- **Unused interior space in first class and rear of aircraft.**

The goals of the OFP-6M transport are to provide an original but sensible, and practical solution to the RFP, by combining important, essential preliminary design factors with growing technology. As technology advances, the OFP-6M can advance along with it. These new technologies are reducing operating costs and are the driving factor of old and new aircraft. Manufacturing efficiency, new materials, and advanced control systems will be some of the emerging technologies that will be considered the OFP-6M. By implementing an alternative design approach to the conventional commercial transport jet, the OFP-6M will achieve customer satisfaction through efficiency and reliability.

16 References

(1) Abbott, Ira and Albert Von Doenhoff, Theory of Wing Sections. New York: Dover Publications, 1959.

(2) Air Transportation Association, "Consequences of Deregulation of the Scheduled Air Transport Industry: An Analytical Approach, April 1975.

(3) Aviation Week and Space Technology (January 18, 1993)

(4) Boeing Commercial Aircraft Group, 737 Systems

(5) Boeing Commercial Aircraft Group, 747 Systems

(6) Boeing Commercial Aircraft Group, 757 Systems

(7) Boeing Commercial Aircraft Group, 767 Systems

(8) Boeing Commercial Aircraft Group, 777 Systems Folder

(9) Currey, Norman S.: Aircraft Landing Gear Design: Principles and Practices, 1988

(10) Fink, Donald E. "Composites may Cut Costs", Aviation Week, Vol. 140 No. 4, January 24,1994. (pp. 53)

(11) Gouhin, Patrick. "1993/1994 AIAA/Lockheed Undergraduate Team Aircraft Competition Engine Data Package" (Memorandum to Design Advisors & Prospective Design Competitors). August 31, 1993

(12) Harris, Charles D., "Aerodynamic Characteristics of Two NASA Supercritical Airfoils With Different Maximum Thicknesses", NASA Technical Memorandum X-2532, NASA Langley Research Center, Hampton, Va., April 1972

(13) Hill, Philip and Peterson, Carl: Thermodynamics of Propulsion (p. 242)

(14) Hoskin, Brian C. and Baker Alan A.: Composite Materials for Aircraft Structures

(15) Hughes, David. "Raytheon/Beech Pursue Low-Cost Fly-By-Light", Aviation Week, Vol 140, NO. 18, May 2, 1994.

(16) Hughes, James W. "Jet Propulsion: Now and the Future." (Slides from presentation by Pratt & Whitney to Aeronautical Engineering Department, California Polytechnic State University at San Luis Obispo, 1992)

(17) Lan, Chuan-Tau and Jan Roskam. Aircraft Aerodynamics and Performance, Roskam Aviation and Engineering Corp., 1988.

(18) McDonnell Douglas, Preliminary Design Review. Long Beach, California: February 4, 1994.

(19) McDonnell-Douglas Corporation, 90 Days: First Quarter, 1994. (video tape)

(20) Mecham, Michael. "Recession Woes Spark New JAL Cost-Cutting", Aviation Week, Vol. 140 No. 4, January 24,1994. (pp. 34-5)

(21) Niu, Michael C.U.: Airframe Structural Design, 1988.

(22) Phillips, Edward H. "Airline Outlook", Aviation Week, Vol. 140 No. 16, April 18,1994. (p.15)

(23) Phillips, Edward H. "Northwest Posts Profit: Losses for AMR, USAIR", Aviation Week, Vol. 140 No. 17, April 25, 1994. (p.31)

(24) Phillips, Edward H. "366TH Adopts New Concepts, Systems", Aviation Week, Vol. 140, No. 17, April 25, 1994. (p.38)

(25) Phillips, Edward H. "Simpler 737 Flap Design", Aviation Week, Vol. 140 No. 16, April 18,1994. (p.38)

(26) Proctor, Paul. "Airline Outlook", Aviation Week, Vol. 140 No. 4, January 24,1994. (p.29)

(27) Proctor, Paul. "Airline Outlook", Aviation Week, Vol. 140 No. 16, February 7,1994. (p.15)

(28) Proctor, Paul. "Airline Outlook", Aviation Week, Vol. 140 No., April 11, 1994. (p.15)

(29) Proctor, Paul. "Airline Outlook", Aviation Week, Vol. 140 No., March 14,1994. (p.21)

(30) Proctor, Paul. "Airline Outlook", Aviation Week, Vol. 140, March 7,1994. (p.15)

(31) Raymer, Daniel P., Aircraft Design: A Conceptual Approach, American Institute of Aeronautics and Astronautics, Inc., Washington, DC, 1992

(32) Rolls-Royce, The Jet Engine, Rolls-Royce plc, 1986.

(33) Roskam, Dr. John, Aircraft Design Part I, Roskam Aviation and Engineering Corp., 1986.

(34) Roskam, Dr. John, Aircraft Design Part II, Roskam Aviation and Engineering Corp., 1986.

(35) Roskam, Dr. John, Aircraft Design Part III, Roskam Aviation and Engineering Corp., 1986.

(36) Roskam, Dr. John, Aircraft Design Part IV, Roskam Aviation and Engineering Corp., 1986.

(37) Roskam, Dr. John, Aircraft Design Part V, Roskam Aviation and Engineering Corp., 1986.

(38) Roskam, Dr. John, Aircraft Design Part VI, Roskam Aviation and Engineering Corp., 1986.

(39) Roskam, Dr. John, Aircraft Design Part VII, Roskam Aviation and Engineering Corp., 1986.

(40) Roskam, Dr. John, Aircraft Design Part VIII, Roskam Aviation and Engineering Corp., 1986.

(41) Scholtes, Peter R., The Team Handbook, Joiner Associates Inc., Madison, WI, 1993.

(42) Shevell, Richard: Fundamentals of Flight, second edition, Prentice Hall, 1989

(43) Sratford, Alan H. Air Transportation in the Supersonic Era, The McMillan Press LTD, 2nd Edition, 1973.

(44) Stilton, Darrol, The Design of the Aeroplane. London, England: Oxford BSV Professional Books, 1983.

(45) Tryckare, Tre: The Lore of Flight, 1970, 1994.

(46) Woods, Wilton. "Goodbye Hub & Spoke", Fortune, Vol. 128 No. 15, December 13, 1993. (p.160-61)

(47) Zambert, Mark. Jane's All the World's Aircraft 1990-91, Jane's Information Group Limited, Surrey, United Kingdom, 1990.